AGU PUBLICATIONS

Reviews of Geophysics

REVIEW ARTICLE

10.1002/2014RG000452

Key Points:
- Assess the state of knowledge on Yellowstone's magma-hydrothermal system
- Emphasize the substantial advances that emerged in the past 25 years
- Most advances stem from the application of modern technologies

Correspondence to:
S. Hurwitz,
shaulh@usgs.gov

Citation:
Hurwitz, S., and J. B. Lowenstern (2014), Dynamics of the Yellowstone hydrothermal system, *Rev. Geophys.*, *51*, doi:10.1002/2014RG000452.

Received 19 MAR 2014
Accepted 3 JUN 2014
Accepted article online 9 JUN 2014

Dynamics of the Yellowstone hydrothermal system

Shaul Hurwitz[1] and Jacob B. Lowenstern[1]

[1]U.S. Geological Survey, Menlo Park, California, USA

Abstract The Yellowstone Plateau Volcanic Field is characterized by extensive seismicity, episodes of uplift and subsidence, and a hydrothermal system that comprises more than 10,000 thermal features, including geysers, fumaroles, mud pots, thermal springs, and hydrothermal explosion craters. The diverse chemical and isotopic compositions of waters and gases derive from mantle, crustal, and meteoric sources and extensive water-gas-rock interaction at variable pressures and temperatures. The thermal features are host to all domains of life that utilize diverse inorganic sources of energy for metabolism. The unique and exceptional features of the hydrothermal system have attracted numerous researchers to Yellowstone beginning with the Washburn and Hayden expeditions in the 1870s. Since a seminal review published a quarter of a century ago, research in many fields has greatly advanced our understanding of the many coupled processes operating in and on the hydrothermal system. Specific advances include more refined geophysical images of the magmatic system, better constraints on the time scale of magmatic processes, characterization of fluid sources and water-rock interactions, quantitative estimates of heat and magmatic volatile fluxes, discovering and quantifying the role of thermophile microorganisms in the geochemical cycle, defining the chronology of hydrothermal explosions and their relation to glacial cycles, defining possible links between hydrothermal activity, deformation, and seismicity; quantifying geyser dynamics; and the discovery of extensive hydrothermal activity in Yellowstone Lake. Discussion of these many advances forms the basis of this review.

"This whole region was, in comparatively modern geologic times, the scene of the most wonderful volcanic activity of any portion of our country. The hot springs and the geysers represent the late stages–the vents or escape pipes-of these remarkable volcanic manifestations of the internal forces. All these springs are adorned with decorations more beautiful than human art ever conceived, and which have required thousands of years for the cunning hand of nature to form" [*Hayden*, 1883, p. 70]. Ferdinand V. Hayden led the 1871 geological survey of northwestern Wyoming, leading to the establishment of Yellowstone as the first U.S. National Park in 1872.

1. Introduction

The Yellowstone Plateau Volcanic Field (YPVF) is responsible for three cataclysmic volcanic eruptions over the past 2.1 million years [*Christiansen*, 2001] as the most recent manifestation of a mantle hot spot that over the past 17 million years has produced a string of large calderas along the Snake River Plain [*Pierce and Morgan*, 1992; *Smith and Braile*, 1994; *Pierce and Morgan*, 2009]. The youngest cataclysmic eruption at 0.64 Ma resulted in the formation of the Yellowstone Caldera (Figure 1) and was followed by several eruptive episodes of large-volume rhyolite flows. Although the most recent eruption was ~70,000 years ago, the Yellowstone Caldera is one of Earth's most "restless" calderas [*Newhall and Dzurisin*, 1988; *Lowenstern et al.*, 2006; *Smith et al.*, 2009] characterized by extensive seismicity, episodes of uplift and subsidence, and a very large and dynamic hydrothermal system.

The diversity of documented phenomena in Yellowstone's hydrothermal system is unparalleled. The system comprises the largest concentration of geysers and hydrothermal explosion craters on Earth, more than 10,000 thermal features, including fumaroles, mud pots, and frying pans, and varicolored thermal pools. Thermal waters have a pH range from 1.5 to 10.0, diverse chemistry, and contain gases from mantle, crustal, and meteoric sources. The fluids discharged at the surface deposit silica sinter, travertine, native sulfur, and other minerals. The springs host biota from all three domains of life (Bacteria, Archaea, and Eukaryote), which use diverse inorganic sources of energy for metabolism. Hydrothermal activity is modulated and perturbed by processes that operate over time scales ranging from seconds (e.g., earthquakes), to days (e.g., air pressure and temperature variations), to seasonal (e.g., precipitation, snow melt, lake level), to decadal, centennial, millennial (e.g., caldera inflation and deflation and ice sheet advance and retreat), and even longer (volcanic cycles).

©2014. American Geophysical Union. All Rights Reserved.

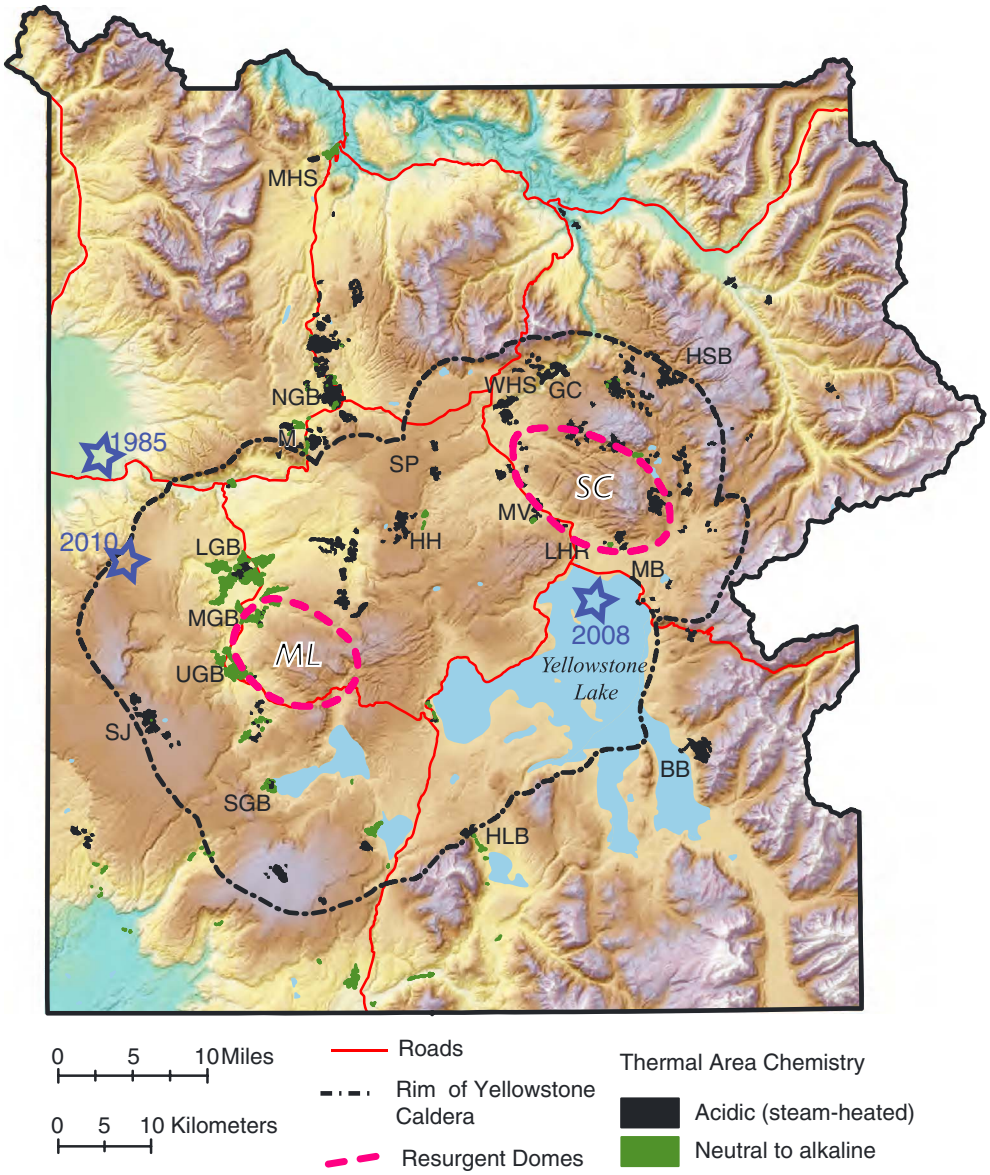

Figure 1. Shaded-relief image of Yellowstone National Park showing acid sulfate (black) and neutral to alkaline (green) thermal features, Yellowstone Caldera boundaries, and the Mallard Lake (ML) and Sour Creek (SC) resurgent domes [*Christiansen et al.*, 2007]. Labeled thermal areas are MHS – Mammoth Hot Springs, NGB – Norris Geyser Basin, LGB – Lower Geyser Basin, MGB – Midway Geyser Basin, UGB – Upper Geyser Basin, SGB – Shoshone Geyser Basin, HLB – Heart Lake Geyser Basin, M – Monument Geyser Basin, BB – Brimstone Basin, MB – Mary Bay explosion crater, LHR – LeHardy Rapids, MV – Mud Volcano, GC – Grand Canyon of the Yellowstone River, WHS – Washburn Hot Springs, HSB – Hot Spring Basin, SJ – Smoke Jumper Hot Springs, HH – Highland Hot Springs, and SP – Solfatara Plateau. The blue stars show the locations of the three large earthquake swarms shown in Figure 2.

Much of the research on hydrothermal activity in the YPVF is motivated by the need to assess hazards, to preserve unique natural features, and to understand the origin and propagation of life in extreme environments. In contrast to other large Quaternary silicic calderas (e.g., Taupo in New Zealand and Long Valley in Eastern California), Yellowstone National Park is protected from geothermal energy or mineral exploration and development and therefore provides a unique opportunity to conduct research on an undisturbed hydrothermal system and to characterize natural causes of variability that operate at widely varying spatial and temporal scales. However, characterizing and quantifying myriad processes in the hydrothermal system is daunting because of the large extent and the tremendous number and diversity of thermal features and because access is limited when the region is snow and/or ice covered throughout much of the year.

©2014. American Geophysical Union. All Rights Reserved.

Some of the major questions that have guided research in recent decades follow: How does the composition and emission rate of magmatic volatiles and heat measured at the ground surface inform us about the state of magma at depth? How do earthquake swarms and episodic inflation and deflation cycles of the Yellowstone Caldera relate to hydrothermal versus magmatic activity? How do periodic forces that operate at scales ranging from seconds to millennia affect thermal activity? What are the major controls on the functional relationship among geochemical processes and the microbial inhabitants of thermal springs? What are the forces controlling eruptive and explosive behavior? Research aimed at addressing these questions resulted in many new discoveries and provided an improved understanding of many controlling processes.

In this review we assess the state of knowledge about Yellowstone's magmatic-hydrothermal system and emphasize the substantial advances that have emerged in the past quarter of a century since a similar review by *Fournier* [1989]. These recent advances mainly stem from the development of modern technologies, densification of monitoring networks, accumulation of large databases, discovery of hydrothermal vents in Yellowstone Lake, evidence relating thermophile microorganisms to the geochemical cycle, and additional research intensity due to establishment of the Yellowstone Center for Resources in 1993 and the Yellowstone Volcano Observatory in 2001. This progress has built upon more than 140 years of research since the 1870 Washburn expedition, the 1871 Hayden expedition, and the establishment of Yellowstone National Park in 1872. We hope that this review will help establish a basis for future research directions.

2. Volcanic History and State of the Magmatic System

The YPVF was formed during three eruptive cycles over the past 2.1 million years [*Christiansen*, 2001]. The volcanic system emerged from a landscape of Precambrian, Paleozoic, and Mesozoic rocks, overlain in parts by Tertiary volcanic and sedimentary rocks of the Absaroka Ranges. The Pleistocene eruptive rocks consist dominantly of rhyolites and include numerous lava flows and voluminous units of ash flow tuffs from the climactic eruptions. The first eruption at 2.059 ± 0.004 Ma [*Lanphere et al*., 2002] produced the >2450 km^3 Huckleberry Ridge Tuff. The second eruption at 1.285 ± 0.004 Ma [*Lanphere et al*., 2002], produced the >280 km^3 Mesa Falls Tuff and the resulting Henrys Fork caldera, and the last eruption 0.639 ± 0.002 Ma [*Lanphere et al*., 2002] produced the 1000 km^3 Lava Creek Tuff and the associated Yellowstone Caldera [*Christiansen*, 2001]. During each of these cycles, basaltic lavas erupted around the margins of the active rhyolitic source area but not within it.

The Yellowstone Caldera is an elliptical depression that covers an area of ~80×50 km (Figure 1) and is filled with 600–1000 km^3 of post-0.64 Ma rhyolitic lava [*Christiansen et al*., 2007]. Following caldera formation, uplift within the caldera formed the Mallard Lake and Sour Creek resurgent domes [*Christiansen*, 2001]. Subsequent post-caldera eruptions occurred during two major episodes and collectively formed the Plateau Rhyolite. The first episode commenced either at 600 ± 20 ka [*Morgan and Shanks*, 2005] or 516 ± 7 ka [*Gansecki et al*., 1996] and continued to 257 ± 13 ka [*Christiansen et al*., 2007] to form the Upper Basin Member. The second episode formed the Central Plateau Member and started at about 170 ka with effusive eruptions that produced >600 cubic kilometers of rhyolitic lava and ended 72 ± 4 ka [*Christiansen et al*., 2007]. These rhyolite flows nearly filled the Yellowstone Caldera from eruptive vents along two linear northwest trending zones. At least two significant explosive eruptions are concurrent with the effusive eruptions of the Central Plateau Member, one depositing the tuff of Bluff Point during the formation of the ~10 km diameter West Thumb caldera in the western part of Yellowstone Lake, and the other depositing the tuff of Cold Mountain Creek [*Christiansen*, 2001; *Christiansen et al*., 2007]. Basaltic lavas erupted intermittently following the eruption of the Lava Creek Tuff on the northeast, north, west, and south margins of the plateau.

Geophysical studies have proposed that an upper crustal magma reservoir with a partially crystallized melt of silicic composition, often described as a "crystal mush," underlies the Yellowstone Caldera. This inference is based on three-dimensional tomographic inversion of local earthquakes [*Miller and Smith*, 1999; *Husen et al*., 2004; *Chu et al*., 2010; *Farrell et al*., 2014] or ambient noise [*Lü et al*., 2013], the depth of the seismogenic zone beneath the caldera [*Smith and Braile*, 1994; *Waite and Smith*, 2004; *Husen et al*., 2004; *Farrell et al*., 2009, 2014], an electrically conductive layer beneath the caldera [*Kelbert et al*., 2012], inversion of ground-surface displacement measurements [*Pelton and Smith*, 1979; *Dzurisin and Yamashita*, 1987; *Dzurisin et al*., 1990; *Wicks et al*., 1998; *Dzurisin et al*., 1999; *Wicks et al*., 2006; *Chang et al*., 2007, 2010; *Dzurisin et al*., 2012], elevated heat flux [*Morgan et al*., 1977; *Hurwitz et al*., 2012a], and models of stress transfer within the caldera [*Luttrell et al*., 2013].

©2014. American Geophysical Union. All Rights Reserved.

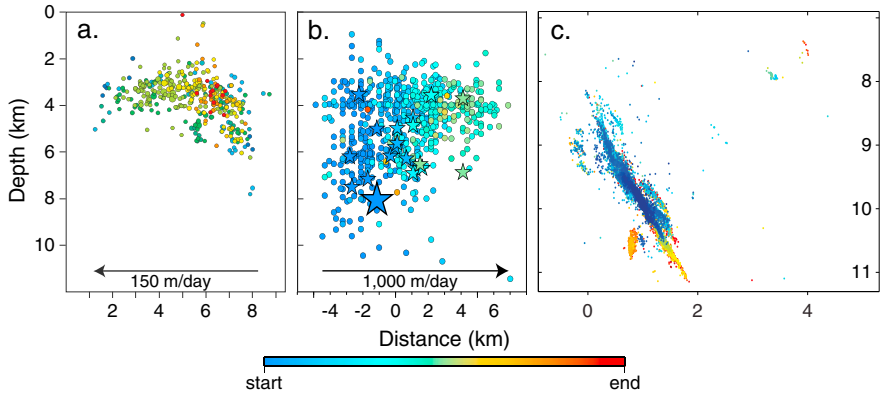

Figure 2. Space-time progression of three large earthquake swarms labeled in Figure 3: 1 – the October 1985 northwest caldera swarm [*Waite and Smith*, 2002], 2 – the 2008–2009 Yellowstone Lake swarm [*Farrell et al.*, 2010], and 3 – the 2010 Madison Plateau swarm [*Shelly et al.*, 2013]. The color scale represents (a) 34 days, (b) 12 days, and (c) 12 days, respectively.

The huge flux of magma-derived volatiles suggests that the upper crustal silicic magma is underlain by a basaltic system [*Lowenstern and Hurwitz*, 2008], and seismic images obtained from data acquired by the USArray seismic network (http://www.usarray.org/) show substantial low-velocity anomalies in the upper mantle and lower crust beneath the Yellowstone Caldera [*Obrebski et al.*, 2011; *Wagner et al.*, 2012]. All of these results contrast with interpretations of electromagnetic data suggesting little or no melt in the lower crust and upper mantle directly beneath the caldera [*Kelbert et al.*, 2012].

3. Seismicity and Deformation

The YPVF is characterized by thousands of earthquakes annually; they are typically small ($M < 3$), and within or immediately north and northwest of the Yellowstone Caldera. In contrast, hydrothermal activity in the Mammoth Hot Springs area is not associated with abundant seismicity. Within the caldera, most earthquakes are shallower than ~6 km, but deeper events occur between Norris Geyser Basin and the epicenter of the M −7.3 Hebgen Lake, Montana earthquake [*Waite and Smith*, 2004; *Farrell et al.*, 2009]. A majority of the small earthquakes occur in swarms, meaning that they are clustered in space and time [*Waite and Smith*, 2002; *Farrell et al.*, 2009, 2010; *Shelly et al.*, 2013]. These swarms can be characterized by systematic temporal migration of seismicity (Figure 2). For example, during the 2008–2009 earthquake swarm beneath northern Yellowstone Lake, epicenters migrated northward at a rate of ~1 km · d^{-1}, and the maximum focal depths decreased from 12 to 2 km [*Farrell et al.*, 2010]. Nearly all large swarms appear coincident with transition from inflation to deflation (or vice versa) of the Yellowstone Caldera [*Smith et al.*, 2009] (Figure 3).

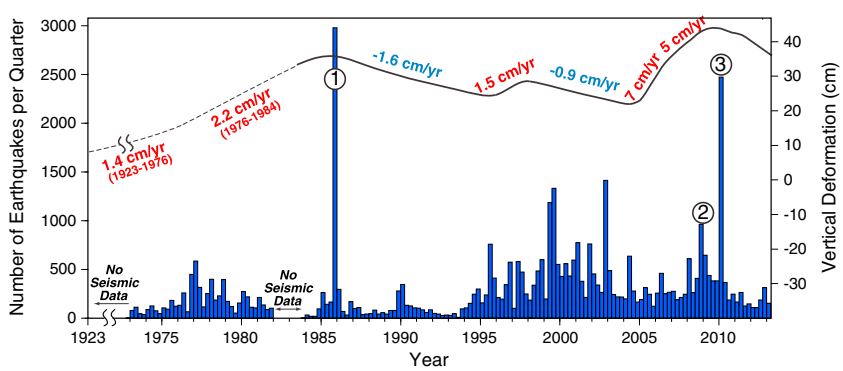

Figure 3. Time series of Yellowstone Caldera uplift and subsidence patterns along with quarterly catalog earthquake counts. The numbers in the circles relate to seismic swarms shown in Figure 2. The 1985 and 2010 swarms were associated with the transition from uplift to subsidence of the caldera. Modified from *Smith et al.* [2009] and *Shelly et al.* [2013].

©2014. American Geophysical Union. All Rights Reserved.

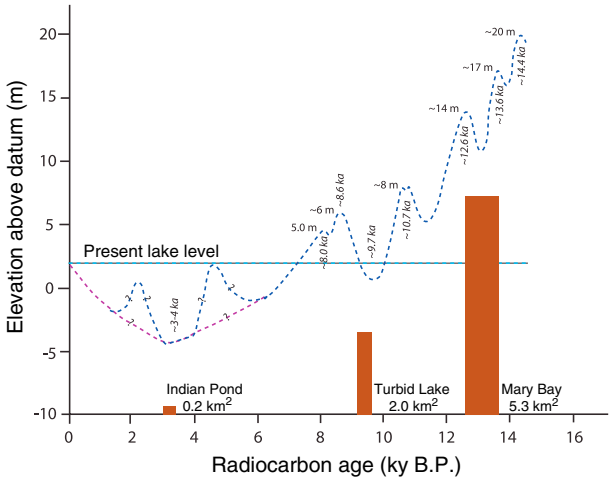

Figure 4. Yellowstone lake levels during the past 15 ka (blue dashed curve) reconstructed from shoreline terraces, relative to a gage on the northern shore of the lake. Datum is at LeHardy Rapids, the erosional base level on the Yellowstone River, 4.5 km north of Yellowstone Lake outlet (Figure 1). The brown rectangles represent some of the hydrothermal explosion craters in and around Yellowstone Lake. The width of the rectangle represents calibrated radiocarbon age + 2σ and the height is relatively scaled by the area of the crater. The decline in elevation from 14.4 to 3–4 ka mainly represents erosion of the lake outlet base level. The shorter lake level increases and decreases represent uplift and subsidence of the Yellowstone Caldera. The magenta curve between ~6.5 ka and the present is an alternative lake level record that is allowed by the data. Modified from *Pierce et al.* [2002] and *Christiansen et al.* [2007].

Ground-surface elevations have been measured since 1923, initially with leveling techniques and since the 1990s with Global Positioning System (GPS) methods [*Meertens and Smith*, 1991; *Puskas et al.*, 2007; *Chang et al.*, 2007] and Interferometric Synthetic Aperture Radar (InSAR) [*Wicks et al.*, 1998, 2006; *Aly and Cochran*, 2011]. These measurements have revealed that the Yellowstone Caldera has experienced multiple episodes of caldera-wide deformation, with uplift and subsidence rates averaging 1–2 $cm \cdot yr^{-1}$ centered on the Mallard Lake and Sour Creek resurgent domes and the northern boundary of the caldera (Figure 1) [*Pelton and Smith*, 1979; *Dzurisin et al.*, 1990; *Wicks et al.*, 1998; *Dzurisin et al.*, 1990, 1999; *Wicks et al.*, 2006; *Chang et al.*, 2007, 2010]. InSAR and GPS data have revealed heterogeneous deformation within the Yellowstone Caldera and large vertical displacements, relative to the caldera, of a region just north of the caldera rim near Norris Geyser Basin, the "north rim uplift anomaly" [*Wicks et al.*, 2006; *Chang et al.*, 2007]. Within the caldera, differential uplift and subsidence of the Sour Creek and the Mallard Lake domes has been documented [*Wicks et al.*, 2006].

Models for these deformation episodes typically invoke volume change of a discrete source, or multiple sources in a homogeneous, isotropic, and elastic half-space at depths of 6 to 10 km assumed to represent a magma chamber [*Dzurisin et al.*, 1990; *Wicks et al.*, 2006; *Chang et al.*, 2007; *Vasco et al.*, 2007]. Although these models have provided mathematical solutions relating surface uplift to volume change of the source at depth, they cannot differentiate between the possible deforming fluids (magma or hydrothermal fluid), and explanations or quantitative solutions for episodes of subsidence are somewhat less convincing.

In addition to the geodetic measurements of caldera inflation and deflation that are available only for approximately 90 years, tilt in dated Yellowstone Lake terraces provides evidence that large amplitude (meters) and long-wavelength cycles of caldera inflation and deflation have been persistent for the past 14,000 years (Figure 4) [*Locke and Meyer*, 1994; *Pierce et al.*, 2002].

4. Episodic Heat and Mass Transport From Magma to the Hydrothermal System

Nearly all the heat and much of the noncondensable gas discharged at Yellowstone are derived from the underlying magmatic system and transported through the hydrothermal system (Figure 5). In the absence of deep drill holes, information on heat and mass transfer into and through the hydrothermal system is available only indirectly from geophysical and geochemical observations, data from deep drilling elsewhere, exhumed ore deposits, and laboratory experiments. In several geothermal exploration wells where temperatures exceed 370°C (e.g., in Lardarello in Italy, Kakkonda in Japan, and Krafla in Iceland), a narrow zone of low-permeability rocks forms by deposition of silicate and other minerals [*Fournier*, 1991; *Ikeuchi et al.*, 1998; *Schiffman et al.*, 2012]. Sharp fluid-pressure gradients have been measured across this zone: above are brittle rocks where meteoric-derived hydrothermal fluids circulate at hydrostatic to sublithostatic pressures; below is a hotter region with lithostatic fluid pressures in ductile (plastic) rocks [*Fournier*, 1991, 1999; *Cox*, 2005]. Hypersaline brine and gas exsolved from magma accumulate at lithostatic pressure in ductile rocks at

©2014. American Geophysical Union. All Rights Reserved.

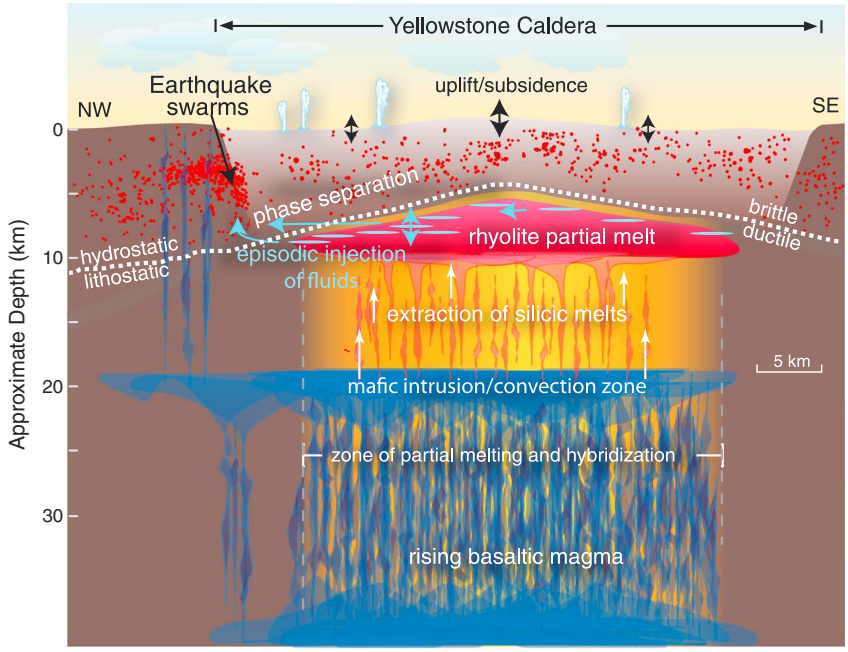

Figure 5. A schematic cross section of the magmatic and hydrothermal systems underlying the Yellowstone Caldera, showing magmatic volatiles exsolved during crystallization of the silicic magma and/or from basalt intrusions or convection and the hypothesized relationship with earthquake swarms in the caldera margins. The exsolved aqueous fluids accumulate at lithostatic pressures in the ductile regime and under high strain rates are episodically injected into the brittle regime, where fluid pressures are generally much lower. The transient increase in fluid pressure in the brittle regime then triggers earthquake swarms, while the movement of fluids facilitates caldera subsidence. Figure modified from *Lowenstern and Hurwitz* [2008] and *Shelly et al*. [2013].

near-magmatic temperatures in relatively thin, horizontal lenses (Figure 5) [*Bailey*, 1990; *Fournier*, 1999]. The temperatures and pressures at which the ductile/brittle transition takes place in these wells are similar to temperatures and pressures where mineral assemblages in silicic rocks undergo a transition from ductile to brittle deformation in tectonically active regions with high-temperature gradients [*Evans et al*., 1990; *Hirth and Tullis*, 1994; *Dingwell*, 1997; *Simpson*, 2001] and strain rates in the range 10^{-12} to 10^{-13} s^{-1} [*Fournier*, 1991]. In this temperature range, the solubility of silicate minerals decreases markedly as pressure decreases, enhancing mineral precipitation in fractures [*Fournier and Potter*, 1982; *Fournier*, 1985].

The low-permeability zone is episodically breached in response to a temporary and local strain-rate increase [*Fournier*, 1991, 1999; *Cox*, 2005]. At high strain rates, the ductile material undergoes shear (brittle) failure in response to small stress perturbations [e.g., *Dingwell*, 1997; *Mader et al*., 2013], and hypersaline brine and gas of likely magmatic origin are expelled into the brittle crust. The resulting increase in fluid pressure and temperature within the brittle crust induces faulting and brecciation that allow for enhanced transport of magmatic volatiles and heat [*Fournier*, 1999]. Within the hydrothermal system, however, elevated temperatures and enhanced reactivity of aqueous fluids tend to decrease permeability. To maintain permeabilities sufficient for advective transport of heat and volatiles, ongoing seismicity and deformation are required.

In the past quarter of a century, several studies have documented processes that provide circumstantial support for models that link (1) episodic fluid migration across the brittle-ductile transition zone, (2) heat and volatile transport into and across the hydrothermal system, (3) seismic swarms, and (4) inflation and deflation of the Yellowstone Caldera. *Dzurisin and Yamashita* [1987] first proposed that magmatic fluids might be controlling deformation of the Yellowstone Caldera "Uplift may be caused by basaltic intrusions near the base of the reservoir or accumulation of magmatic fluids during cooling and crystallization within the reservoir" and "Subsidence might be a response to regional tectonic extension or release of trapped magmatic fluids." Later, *Dzurisin et al*. [1990] proposed that "Subsidence occurs during episodic hydrofracturing and injection of pore fluid from the deep lithostatic-pressure zone into a shallow hydrostatic-pressure zone." Thus, hypotheses

©2014. American Geophysical Union. All Rights Reserved.

linking episodes of caldera inflation and deflation to episodic fluid migration were proposed shortly after an inflation-deflation transition was observed. The feasibility of these hypotheses was later verified by numerical models linking hydrothermal injection into the base of the brittle crust with hydrothermal flow, poroelastic deformation, and caldera inflation and deflation [*Chiodini et al*., 2003; *Hurwitz et al*., 2007a; *Todesco*, 2009; *Hutnak et al*., 2009; *Rinaldi et al*., 2010]. Nevertheless, most recent deformation models invoke volume changes of a discrete source or sources as the impetus for caldera inflation and/or deflation, but these models cannot distinguish between a hydrothermal or magmatic fluid causing the volumetric change [*Wicks et al*., 2006; *Chang et al*., 2007; *Vasco et al*., 2007; *Aly and Cochran*, 2011].

Three large earthquake swarms have occurred in proximity to the Yellowstone Caldera boundary since 1985 (Figure 3). The transition from inflation to deflation following two of the earthquake swarms suggests that in addition to episodic injection of magmatic volatiles into the hydrothermal system, which could result in overall pressure increase and inflation, episodic breaching of the deep (and brittle) hydrothermal system might also be the mechanism for pressure release. The focal mechanisms of earthquakes in these swarms, their temporal migration pattern and their depths, were interpreted to result from hydrothermal fluid migration and pressure release from the caldera [*Waite and Smith*, 2002; *Farrell et al*., 2009, 2010; *Shelly et al*., 2013]. The largest recorded earthquake swarm lasted for more than 3 months beginning in October 1985 and included more than 3000 earthquakes with $M < 5$ [*Waite and Smith*, 2002; *Farrell et al*., 2009]. During the first month the swarm front migrated laterally away from the caldera at an average rate of 150 m d^{-1} (Figure 2a). Coincident with the onset of the swarm, the caldera transitioned from inflation to deflation (Figure 3). The temporal pattern of earthquake swarms and the change in caldera deformation pattern were explained by migration of hydrothermal fluids radially outward from the Yellowstone Caldera following rupture of a sealed hydrothermal system within the caldera [*Waite and Smith*, 2002]. The December–January 2008–2009 earthquake swarm consisted of 811 earthquakes with $M < 4.1$. The swarm front migrated laterally along a N-S vertical plane of hypocenters at a rate of 1 km d^{-1} and vertically from maximum focal depths of 12 km to 2 km (Figure 2b) beneath the northern part of Yellowstone Lake [*Farrell et al*., 2010]. It was proposed that the swarm was induced by magmatic fluid migration or propagation of a poroelastic stress pulse along a preexisting fracture zone [*Farrell et al*., 2010]. The January 2010 Madison Plateau swarm (Figure 2c) near the northwest boundary of the Yellowstone Caldera was thought to be triggered by the rupture of a zone of confined high-pressure aqueous fluids into a preexisting crustal fault system, prompting release of accumulated stress [*Shelly et al*., 2013]. The earthquake centroids migrated with time outward from the initial source. The injection of fluid from high- to low-pressure domains may have been accommodated by hybrid shear and dilatational failure, as is commonly observed in exhumed hydrothermally affected fault zones [e.g., *Hill*, 1977; *Sibson*, 1987, 1996]. *Shelly et al*. [2013] showed that the spatial-temporal migration of the earthquake activity front in the three major swarms can be well fit by a diffusion equation $r = \sqrt{4\pi Dt}$, where r is distance from the initial source, D is hydraulic diffusivity, and t is time.

Radiocarbon concentrations in individual growth rings in a tree core from Mud Volcano (Figure 1) showed a sharp ~25% drop in ^{14}C, interpreted as due to a fivefold increase in CO_2 emission during the year after a seismic swarm in 1978 [*Evans et al*., 2010]. These authors concluded that a large pulse of CO_2 traversed Yellowstone's hydrothermal system in a relatively short time (<1 year) and ultimately triggered the swarm seismicity [*Evans et al*., 2010].

Examples linking temporal variations of magmatic volatile discharge with episodes of caldera inflation and deflation were also documented at the Campi Flegrei Caldera in southern Italy. Since measurements began in 1983, increases in some fumarole gas ratios (CO_2/H_2O, CO_2/CH_4, and CO_2/H_2S) were coincident with caldera inflation and earthquake swarms resulting from repeat injections of magmatic gases into the hydrothermal system [*Chiodini et al*., 2003, 2012a; *Caliro et al*., 2014].

Chloride discharge measurements through the major rivers of the YPVF have been carried out since 1983 (Figure 6). One of the goals of this effort was to establish a temporal correlation between chloride discharge and inflation and deflation cycles of the Yellowstone Caldera that could indicate possible leakages of magmatic chloride into the hydrothermal system [*Dzurisin et al*., 1990; *Fournier*, 2004]. *Fournier* [1989] estimated that addition of about 0.2–0.4% magmatic brine could account for the concentration of chloride in the deepest circulating thermal water in the YPVF, and therefore, a small increase in magmatic brine input to the hydrothermal system would likely cause a significant change in the chloride discharge. However, no

©2014. American Geophysical Union. All Rights Reserved.

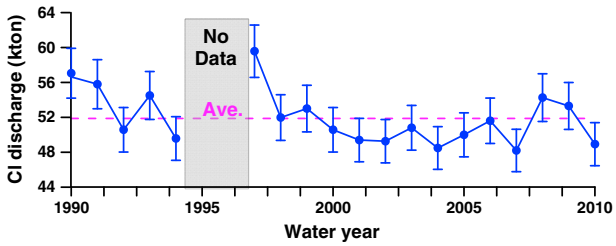

Figure 6. Chloride discharge from the Yellowstone, Madison, Snake, and Fall Rivers between 1990 and 2010. Details on the calculations and methods are in *Friedman and Norton* [2007], and *Hurwitz et al.* [2007b, 2007c]. The error bars represent an estimated 5% uncertainty, and the shaded area represents 2 years (1995 and 1996) for which data are not available. The horizontal dashed magenta line represents the average discharge for the 20 year period.

correlation has been found to date in the temporal trends of chloride discharge and deformation (Figures 3 and 6) [*Fournier*, 2004; *Hurwitz et al*., 2007b]. Based on the heterogeneous distribution of chloride among the drainage basins in the YPVF and the assumption of a single, uniform parent thermal fluid, *Hurwitz et al*. [2007b] proposed that large-scale (tens of kilometers) lateral redistribution of Cl^- might take decades or longer, as thermal water flows toward its discharge sites (e.g., the geyser basins along the drainages of the Firehole and Gibbon Rivers). With this extended time lag, correlations on annual or decadal time scales should not be expected. Further, chloride discharge variations are mainly dominated by the annual hydrologic cycle [*Hurwitz et al*., 2007b, 2010], and any variation due to magmatic Cl injection rate would likely be small in comparison.

All of the major thermal areas including those within Yellowstone Lake and the geyser basins along the Firehole and Gibbon River drainage basins are associated with negative magnetic anomalies, reflecting hydrothermal alteration that has destroyed the magnetic susceptibility of minerals in the rhyolites [*Finn and Morgan*, 2002; *Bouligand et al*., 2014]. However, most of the magnetic lows extend beyond the active thermal areas, implying either that subsurface alteration is more widespread or that postglacial hydrothermal activity migrated with time.

5. Chemistry of the Hydrothermal System

A series of accomplishments have marked the past 25 years of research into Yellowstone's hydrothermal system; included among them are the accumulation of large data sets of water and gas chemistry, the application of new geochemical tracers, continuous measurements of river water chemistry, discovery of thermal vents and extensive hydrothermal activity on the floor of Yellowstone Lake, radiometric dating of hydrothermal deposits, and discoveries relating thermophile microorganisms to the geochemical cycle.

5.1. Thermal Water Chemistry

A prominent geochemical model invokes a 340–370°C fluid, rich in dissolved CO_2 and H_2S and with ~400 ppm Cl^- as the "parent" fluid for all the thermal waters discharged in the YPVF [*Truesdell and Fournier*, 1976; *Fournier*, 1989]. The parent is modified by boiling and removal of steam, by mixing with cold and dilute groundwater at depth and near the surface, and by water-rock interaction, before discharge at thermal springs.

Water stable isotopes ($\delta^{18}O$ and δD) showed early on that the thermal waters originate almost entirely as rain and snow that percolate to depth and then return to the surface; any magmatic component is $<$ ~10% [*Craig et al*., 1956; *Truesdell et al*., 1977]. More recent studies have confirmed that the δD-$\delta^{18}O$ values of precipitation and cold surface waters in the YPVF fall close to the Global Meteoric Water Line [*Parry and Bowman*, 1990; *Kharaka et al*., 2002; *Rye and Truesdell*, 2007; *Gardner et al*., 2011; *Bergfeld et al*., 2011; *Hurwitz et al*., 2012b]. Whereas the δD range of thermal waters brackets the range of values for local cold surface waters in the Norris, Lower, and Upper Geyser Basins, *Truesdell et al*. [1977] noticed that the δD values of thermal waters from drill holes in the Lower and Norris Geyser Basins are more negative than those of thermal spring waters and of local meteoric waters. This difference led *Truesdell et al*. [1977] to propose models whereby δD of thermal waters are modified by mixing with cold locally derived water in shallow reservoirs, followed by boiling as the mixtures rise to the surface.

Based on models in which all the steam remains mixed with the liquid and separates near a single temperature (single stage) or in which steam is separated from the liquid as it is formed (continuous),

©2014. American Geophysical Union. All Rights Reserved.

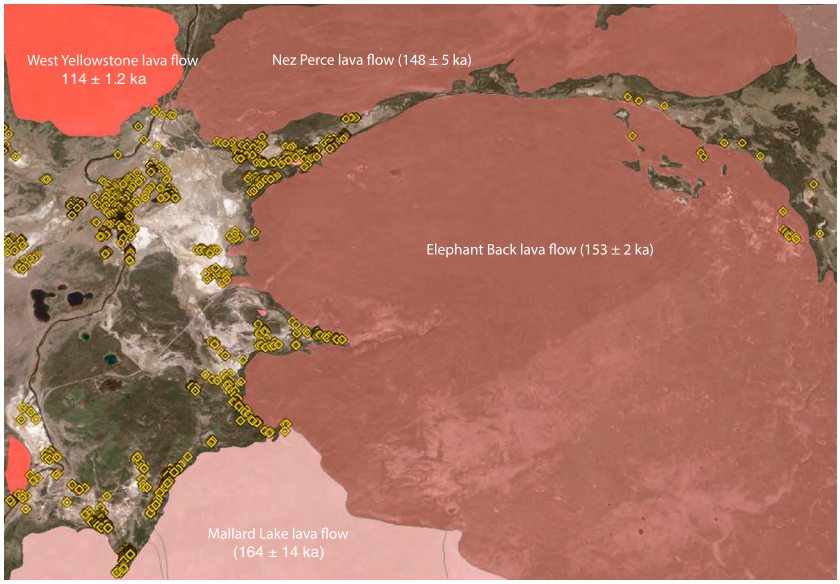

Figure 7. Air photo of eastern part of Lower Geyser Basin with overlay of mapped and dated lavas [*Christiansen*, 2001; *Christiansen et al*., 2007]. The yellow diamonds represent the YNP thermal features inventory (Yellowstone Center for Resources thermal inventory database available at http://www.rcn.montana.edu/). Numerous thermal features are found at the margins of the Elephant Back, Mallard Lake, and Nez Perce lava flows, within glacial and younger sediments. Discharged waters may migrate at the base of these lavas [*Morgan and Shanks*, 2005], and prior to emplacement of the lava flows, the distribution of thermal features was likely much different.

Truesdell et al. [1977] proposed that mixing a parent fluid (360°C, 310 ppm Cl^-, and δD of –149‰) with cold and dilute meteoric water can account for the diverse range of isotopic compositions of thermal water in the geyser basins of the YPVF. More recently, *Balistrieri et al*. [2007] demonstrated that the δD values of sublacustrine vent waters in Yellowstone Lake can also originate from the same parent fluid. However, the calculated δD value of the parent fluid (–149‰) is lighter than all meteoric water in the Yellowstone Caldera, leaving its recharge area a mystery. Lighter meteoric water is found only in the Gallatin and northern Absaroka Ranges in the northwest part of the YPVF with δD as light as −178‰ [*Kharaka et al*., 2002; *Rye and Truesdell*, 2007]. However, because the recharge area for this isotopically light recharge water is too small to balance the present outflow of deep thermal water from the YPVF, *Rye and Truesdell* [2007] suggested that some meteoric water recharge possibly occurred during a cooler time in the Pleistocene or during the Little Ice Age in the midfourteenth to midnineteenth centuries. The designation of source recharge areas and the models used for calculating water age depend on many simplifying assumptions and therefore remain highly uncertain.

The parent fluid ascends to the surface through a series of successively shallower and cooler reservoirs separated by zones of localized low permeability [*Dobson et al*., 2003], where water-gas-rock chemical reactions and equilibration occur in response to changing temperatures and pressures. In some parts of the system aqueous fluids undergo decompressional boiling and degassing, and in other parts they cool by conduction to the wall rocks [*Truesdell and Fournier*, 1976; *Fournier*, 1989]. Mixing of thermal waters containing high concentrations of dissolved Cl^-, Na^+, Li^+, and SiO_2 with shallow, near-surface meteoric waters that are relatively rich in Ca^{2+} and Mg^{2+} further modifies the composition of discharged thermal water [*Hurwitz et al*., 2010].

Topography exerts a major control on phase distribution (e.g., liquid and steam) and the associated chemical composition of discharged waters. Thermal waters are typically classified based on their pH as either alkaline-chloride, with typical pH values of 7–10, or acid sulfate with pH values between 5 and 1. Some thermal waters are a mixture of these two compositions [e.g., *Allen and Day*, 1935; *Fournier*, 1989; *Nordstrom et al*., 2009]. Most of the alkaline-chloride thermal springs are concentrated along the edge of thick (150–300 m) post-caldera rhyolite flows (Figure 7), or in low-elevation basins between adjacent rhyolite flows [*Morgan et al*., 2009]. In contrast to the fracture-rich tuff deposits [*Jaworowski et al*., 2006], most young rhyolitic lava

©2014. American Geophysical Union. All Rights Reserved.

flows are largely unfractured and have low-permeability interiors, whereas basal flow breccias are more permeable and thus may direct lateral hydrothermal flow to discharge along the contact between the flow margin and low-permeability basin fill [*Morgan et al*., 2009]. Many thermal areas existing prior to eruption of these young lavas would have been buried beneath tens to hundreds of meters of rhyolite, such that the thermal waters would migrate laterally to issue at the lava margin.

Alkaline-chloride thermal waters discharge in the geyser basins along the Firehole and Gibbon River drainages on the western side of the Yellowstone Caldera, and in Yellowstone Lake [*Shanks et al*., 2005; *Balistrieri et al*., 2007], the Grand Canyon of the Yellowstone in the eastern part of the Yellowstone Caldera, and along the Norris-Mammoth corridor north of the caldera (the area between Norris Geyser Basin (NGB) and Mammoth Hot Springs (MHS) in Figure 1) [*Sorey and Colvard*, 1997]. In these areas, the water table is at or near the ground surface, allowing discharge of mainly liquid water. Boiling in these areas occurs near or at the ground surface. Alkaline-chloride waters are characterized by relatively high concentrations of Cl^-, SiO_2, Na^+ Li^+, and B, low concentrations of Ca^{2+} and Mg^{2+} [*Fournier*, 1989; *Hurwitz et al*., 2012b].

Acid sulfate thermal features are prevalent in high-elevation areas in the eastern part of the Yellowstone Caldera (where the seismically imaged partially molten magma is shallowest [*Miller and Smith*, 1999; *Husen et al*., 2004; *Farrell et al*., 2014]), along the Norris-Mammoth Corridor, and at the tops of major lava flows (e.g., Smoke Jumper and Highland Hot Springs) (Figure 1). Beneath these vapor-dominated areas, the hydrothermal water table is assumed to be deep, and steam and less soluble gases (CO_2, H_2S, H_2, CH_4, and He) are exsolved from the boiling alkaline waters, thereby carrying heat and gases to the ground surface through fumaroles, mud pots, and acid boiling pools [*Allen and Day*, 1935; *White et al*., 1971]. Some of the acid sulfate springs and seeps in the eastern part of the caldera also contain high concentrations of hydrocarbons, probably originating from shallow sedimentary rocks [*Love and Good*, 1970; *Clifton et al*., 1990; *Lorenson et al*., 1991; *Werner et al*., 2008; *Bergfeld et al*., 2011, 2012].

Within Shoshone [*Hearn et al*., 1990] and Heart Lake [*Lowenstern et al*., 2012] Geyser Basins located adjacent to the Yellowstone Caldera boundary (Figure 1), alkaline-chloride springs discharge at low elevation, whereas gas discharge and acid sulfate thermal features are at higher elevations. In Norris Geyser Basin, a seasonal transition from alkaline chloride to acid sulfate was attributed to water-level changes and shifting of the depth of boiling that affects mixing of the two water types in the shallow subsurface [*Fournier et al*., 2002].

In contrast, the chemical composition of water at Mammoth Hot Springs (Figure 1) is carbonate rich and saturated in calcium carbonate (travertine). The pH of the discharged waters is typically about 6 but increases rapidly as CO_2 is degassed [*Sorey and Colvard*, 1997; *Kharaka et al*., 2000]. Compared with alkaline-chloride waters, thermal waters at Mammoth Hot Springs are relatively rich in Ca^{2+}, Mg^{2+}, HCO_3^-, and SO_4^{2-}.

The volume of thermal water discharge in the YPVF is much smaller than the volume of precipitation recharge. Snowmelt hydrograph analysis implies that ≥ 70% of the water flowing in the major rivers consists of modern precipitation [*Gardner et al*., 2010b], and *Hurwitz et al*. [2012b] showed that tritium concentrations in the Firehole River above and below the Upper Geyser Basin are similar even though the geyser basin discharges thermal water with no detectable tritium.

The interaction between the shallow, cold meteoric water and the deep thermal waters is minimal. Tritium (half-life of 12.32 ± 0.02 years) was used in the 1970s to trace the recharge of recent precipitation into Yellowstone hot spring waters [*Pearson and Truesdell*, 1978]. Deep thermal water contained tritium concentrations below the detection limit. More recently, tritium measurements with lower detection limits and higher precision again revealed concentrations below detection limit in several geysers in the Upper Geyser Basin [*Hurwitz et al*., 2012b] and in thermal springs at the Norris Geyser Basin [*Gardner et al*., 2011]. Chlorinated fluorocarbon (CFC) concentrations in thermal waters also suggest minimal proportions of modern precipitation in thermal water discharge [*Gardner et al*., 2011]. The tritium and CFC data suggest that where mixing of meteoric and thermal waters takes place, it is limited to the surface, or the shallow subsurface. The limited interaction between ascending thermal water and surface waters was also demonstrated at smaller scales. Silica precipitation and the formation of low-permeability, armored channels at Rabbit Creek in the Lower Geyser Basin significantly reduce exchange between stream water and shallow thermal groundwater [*Vitale et al*., 2008]. Using an electromagnetic imaging method, it was shown that the

©2014. American Geophysical Union. All Rights Reserved.

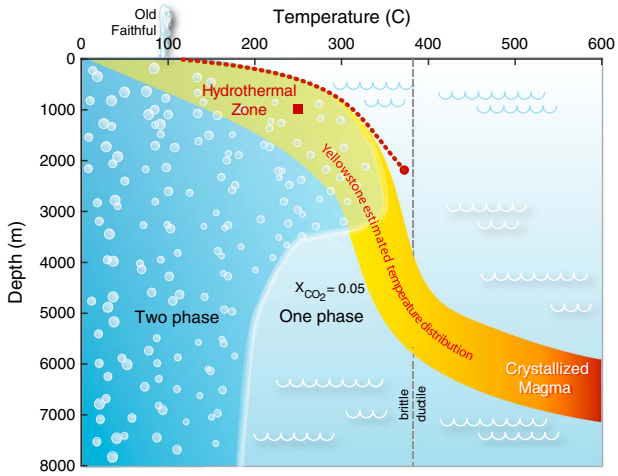

Figure 8. Diagram modeling the phase distribution in the Yellowstone hydrothermal system. The assumed pressure follows a hydrostatic gradient. The estimated temperature distribution reflects near-solidus (i.e., > ~ 700°C) conditions at depths around 8 km and temperatures close to the pure H_2O liquid-vapor curve (dotted red line) near the surface. A transitional zone bridges the two depth ranges. The two-phase field represents conditions at which a 5 mol% CO_2 to 95% H_2O will unmix to form a water-dominated liquid and a CO_2-H_2O vapor. Much of the upper few kilometers is predicted to be vapor saturated. The one-phase field is a steam-CO_2 supercritical phase stable at higher temperatures. Modified from *Lowenstern and Hurwitz* [2008].

conduits that feed siliceous hot springs are largely isolated from shallow groundwater and that most mixing between the ascending thermal waters and meteoric waters occurs after hot-spring discharge infiltrates the subsurface [*Gibson and Hinman*, 2013].

Despite the large variations in hydrothermal activity at many different time scales (daily, seasonal, and decadal), the large chemical databases acquired over the past two decades [e.g., *Parry and Bowman*, 1990; *Ball et al.*, 1998, 2002, 2007, 2010; *McCleskey et al.*, 2005; *Gemery-Hill et al.*, 2007] imply that the compositions of thermal waters in the YPVF have not changed considerably since the earliest studies of *Gooch and Whitfield* [1888] and *Allen and Day* [1935]. For example, despite the very different analytical methods used, the concentrations of Cl^-, Na^+, and SiO_2 in Old Faithful Geyser waters have not changed between the measurements made in the 1880s [*Gooch and Whitfield*, 1888] and 2007 [*Hurwitz et al.*, 2012b], implying that the volumes of thermal reservoirs where groundwater and rocks thermally equilibrate are large compared to the volumes of other possible sources of water and that mixing between shallow meteoric water and deep thermal waters is negligible.

5.2. Transport and Speciation of Magmatic Volatiles in the Hydrothermal System

The transport of volatiles between magma and the ground surface depends mainly on the solubility of the volatile species in water and on their reactivity with rocks. Episodic fluid flow from the high-pressure ductile region to the hydrostatically pressured brittle crust and continuing ascent of the fluid will result in phase separation (Figure 8). The more soluble or reactive volatiles (HCl, HF, and HBr) readily dissolve in crustal waters and will react with rock, exchanging K, Na, and Ca for hydrogen ion. The anions are ultimately transported (as Cl^-, F^-, and Br^-) to the relatively low-elevation areas in the Firehole River and Gibbon River geyser basins where they are discharged as salts [*Hurwitz et al.*, 2007b]. The lateral transport of these Cl^--rich, thermal waters may take decades or longer; therefore, even significant changes in river Cl^- flux may not relate to concurrent events of magmatic unrest [*Hurwitz et al.*, 2007b].

Though reaction of magmatic HCl and SO_2 with Yellowstone crustal rocks may occur at near-magmatic temperatures, most of the reaction of CO_2 occurs at lower temperature. *Fournier* [1989] noted that waters inferred to equilibrate at temperatures >270°C had $Cl^- >> HCO_3^-$, whereas waters equilibrated at lower temperatures had $Cl^-/HCO_3^- \approx 1$. Two types of waters in the geyser basins were defined on the basis of HCO_3^-/Cl^- [*Fournier et al.*, 1976; *Fournier*, 1989]. Black Sand type waters have high HCO_3^- concentrations compared with Geyser Hill type waters because they have undergone less decompressional boiling during ascent. More dissolved CO_2 remains in these waters as carbonic acid (H_2CO_3) which, as temperatures decline, reacts with the wall rock, resulting in higher HCO_3^- concentrations. In Norris Geyser Basin, where the estimated temperatures of the shallow reservoirs are possibly higher than 300°C [*Fournier et al.*, 2002], waters have undergone considerable boiling and therefore have low HCO_3^- concentrations. Laboratory experiments reacting rhyolite with CO_2 at 200° and 350°C confirmed that conversion of albite to clay plus quartz was much faster at 200° and that Na^+ concentrations in the reacted fluids were ~27 times higher than in the higher-temperature experiments [*Bischoff and Rosenbauer*, 1996]. These authors concluded that consumption of carbonic acid and creation of HCO_3^- is maximized between 150° and 200°C.

©2014. American Geophysical Union. All Rights Reserved.

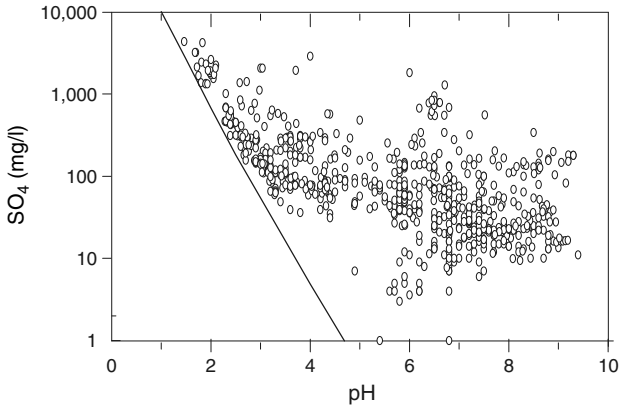

Figure 9. The concentration of sulfate as a function of pH for Yellowstone waters (circles). Solid line shows relationship between pH and sulfate concentration for pure H_2SO_4 at 25°C. The highest SO_4^{2-} concentrations result from evaporative concentration at elevated temperatures. Low SO_4^{2-} concentrations for thermal waters decrease as the Cl^- concentration increases from boiling which probably reflects anhydrite solubility equilibrium. After *Nordstrom et al.* [2009].

Notwithstanding this prevalent subsurface reaction, the discharge of HCO_3^- in YPVF rivers [*Hurwitz et al.*, 2007a, 2007b, 2007c] is only 1–2% as large as the discharge of CO_2 gas [*Werner and Brantley*, 2003]. Mass balance and isotopic constraints require that the great preponderance of CO_2 and HCO_3^- emerging from Yellowstone contains "dead" carbon from magmatic and metamorphic sources [*Werner and Brantley*, 2003; *Evans et al.*, 2006; *Lowenstern and Hurwitz*, 2008].

Chlorine is considered to be one of the more conservative components of magma-hydrothermal systems [e.g., *Ellis and Mahon*, 1977; *Giggenbach*, 1997] and is therefore used as a tracer for heat released by the magma (section 6.2). Because of its high solubility in liquid water, sodium chloride will partition into the liquid phase and avoid entering any vapor phase created through boiling. For this reason, Cl is either below or near the analytical detection limit in fumaroles or gas from acid pools in the YPVF [*Bergfeld et al.*, 2011]. A reconnaissance study of chlorine stable isotopes of waters from four thermal areas found δ^{37}Cl values ranging between −0.13 and +0.42, with no systematic spatial variation or correlation with other chemical parameters [*Zhang et al.*, 2004]. This small fractionation implies that high-temperature kinetic fractionation is insignificant [*Sharp et al.*, 2010] and is consistent with studies showing that large δ^{37}Cl differences in the mantle and crust are rare [*Sharp et al.*, 2007].

Gas emissions at Yellowstone do not contain appreciable SO_2 [*Bergfeld et al.*, 2011; *Chiodini et al.*, 2012b], because it is highly soluble in groundwater [*Symonds et al.*, 2001], and at temperatures below ~400°C, hydrogen sulfide (H_2S) is formed by disproportionation reactions:

$$4SO_{2(g)} + 4H_2O_{(aq)} \rightarrow 3H_2SO_{4(aq)} + H_2S_{(aq)}$$

Shallower in the hydrothermal system, sulfur speciation is complex because it is a key redox element that supports different microbial populations through a series of energetically favorable reactions. Oxidation of $H_2S_{(g)}$ ascending through fumaroles, to form crystals of elemental sulfur (S°) deposited at the ground surface and/or SO_4^{2-} dissolved in water, is complicated by the formation of several intermediate sulfoxyanions whose stability depends on oxidizing agents, catalysts, and water temperature, composition and pH [*Xu et al.*, 1998, 2000; *Knickerbocker et al.*, 2000; *Nordstrom et al.*, 2005, 2009; *Macur et al.*, 2013]. Elemental sulfur is also formed by the disproportionation of thiosulfate in acid waters and can hydrolyze and partially oxidize by disproportionation at temperatures above ~100°C. However, at temperatures $<$ ~ 100°C, elemental sulfur is only oxidized rapidly by microbial catalysis [*Xu et al.*, 1998; *Nordstrom et al.*, 2009]. At pH values below about 3, H^+ is the dominant cation, and H^+ and SO_4^{2-} concentrations increase substantially approximating equilibrium dissociation of pure H_2SO_4 (Figure 9) [*Nordstrom et al.*, 2009].

The surface of Cinder Pool in Norris Geyser Basin pool is partially covered with millimeter-size, black, hollow sulfur spherules, while at the bottom of the pool at a depth of 18 m, sulfur forms molten layers at temperatures above its melting point of 114°C [*Xu et al.*, 2000]. The floating sulfur spherules are formed by gas discharge from the molten sulfur. When the sulfur-coated gas bubbles rise up through the overlying boiling water, the sulfur solidifies and traps the gas that makes the spherules buoyant. Eventually, the trapped gas escapes through small holes that form in the spherules [*Xu et al.*, 2000].

Fluoride concentrations of ≤50 mg/L are found in thermal waters with pH $>$6 and temperatures $>$50°C. At lower pH, dissolved fluoride strongly complexes with H^+ and Al^{3+} [*Deng et al.*, 2011]. Like many intraplate rhyolites [*Carroll and Webster*, 1994], Yellowstone has relatively low Cl/F (~0.5 by mass), as can be observed in

©2014. American Geophysical Union. All Rights Reserved.

Table 1. Volatile Discharge Through Yellowstone Rivers and Soils, and Abundance in Lavas

	Riverine Discharge[a] ($t\,d^{-1}$)	Diffuse Soil Discharge [b] ($t\,d^{-1}$)	Rhyolitic Melt Inclusions[c] (ppm)
CO_2	546	7,000–33,000	<400
S	56	58–275	<100
Cl	139	--	1,100
F	18	--	2,000

[a]Average annual discharge from the Yellowstone, Madison, Snake, and Fall Rivers for 2002–2010. Discharge of CO_2 and S recalculated from HCO_3^- and SO_4^{2-}.
[b]See section 6.1 for details. Soil flux of S is based on an average molar CO_2/H_2S of 166 (CO_2/S mass ratio of 120) measured in gas, excluding ratios greater than 10,000 [*Bergfeld et al.*, 2011].
[c]Quartz-hosted silicate melt inclusions from post-caldera rhyolites. From *Lowenstern and Hurwitz* [2008].

both glass inclusions trapped in quartz crystals (Table 1) [*Lowenstern and Hurwitz*, 2008] and erupted rhyolitic glass [*Christiansen*, 2001]. Notably, the Cl/F are much higher in thermal waters (~8) [*Hurwitz et al.*, 2007b] implying either preferential degassing of chlorine compared to fluorine from silicic magmas [*Carroll and Webster*, 1994], an additional shallow source enriched in chlorine that contributes to the waters, or a large sink of fluorine in the shallow crust.

Fluorite (CaF_2) is the most common fluorine-rich accessory mineral, and hydrothermal fluorite-bearing veins are abundant in magma-hydrothermal settings [e.g., *Ellis and Mahon*, 1964; *Richardson and Holland*, 1979a]. Fluorite is precipitated either as a consequence of changes in temperature and pressure along the hydrothermal flow path or due to the interaction of hydrothermal solutions with wall rocks [*Nordstrom and Jenne*, 1977; *Richardson and Holland*, 1979a]. Laboratory experiments at temperatures of 25°C to 260°C demonstrated that increasing NaCl or KCl in solutions increases fluorite solubility substantially. For NaCl concentrations ranging from 0.1 to 1.0 M, solubility is maximized at ~ 100°C and then decreases with increasing temperature to ~350°C. Fluorite solubility increases continuously between 25°C and 400°C when $M_{NaCl} > 2$ M [*Richardson and Holland*, 1979b]. In fact, abundant fluorite was found in cores from several research holes (<330 m) drilled in Yellowstone's geyser basins during the 1960s [e.g., *Honda and Muffler*, 1970; *White et al.*, 1975; *Keith and Muffler*, 1978; *Keith et al.*, 1978]. Simple mass balance calculations suggest that (1) if chlorine input and outputs from the hydrothermal system are in steady state, (2) the Cl/F input to the hydrothermal system is similar to that in rhyolitic melt (0.55), (3) the average mass of F-discharged from the hydrothermal system is 18 $t \cdot d^{-1}$ (Table 1), and (4) the only sink for F^- is fluorite, then $1.76 \cdot 10^5$ t of fluorite are deposited annually. If this deposition rate were constant since the formation of the Yellowstone Caldera, the volume of fluorite (density of 3200 $kg\,m^{-3}$) deposited would be 35 km^3. If this volume were spread equally over the entire 2900 km^2 of the Yellowstone Caldera, its thickness would be approximately 12 m. This large volume suggests that substantial fluorite deposition occurs within the hydrothermal system.

5.3. River Water Chemistry

Because of the tremendous number and wide distribution of thermal features at the YPVF, it is difficult to collect a time series that reflects the discharge and chemistry of the hydrothermal system. Instead, several studies have used Yellowstone rivers as a proxy for hydrothermal output. Though diluted by precipitation, river chemistry and flow rates can be used to calculate hydrothermal discharge [*Hurwitz et al.*, 2007b, 2010; *McCleskey et al.*, 2010a, 2010b]. There are large-scale temporal and spatial patterns of hydrothermal discharge (Figures 6, 10, and 11). Water chemistry during the high runoff period between late April and mid-June differs significantly from water composition during the base flow. Normalized by Cl, the abundances of HCO_3^-, SO_4^{2-}, Ca^{2+}, and Mg^{2+} increase during the high runoff period. The ratio increase is significantly greater in rivers with a high runoff component (Yellowstone and Lamar Rivers) compared with the Firehole and Gibbon Rivers where the increase in discharge following snowmelt is much smaller [*Hurwitz et al.*, 2010; *Gardner et al.*, 2010b]. The increase in ion ratios represents higher proportions of waters derived from near-surface, low-temperature weathering of rhyolitic rocks [*Hurwitz et al.*, 2010]. Waters from the Firehole and Gibbon Rivers are extremely enriched in Na^+ compared with a global compilation of river compositions [*Gaillardet et al.*, 1999], resulting from high-temperature water-rock interaction in the drainage basins. This enrichment is typical for alkaline-neutral-chloride waters in volcanic systems worldwide [*Giggenbach*, 1988].

©2014. American Geophysical Union. All Rights Reserved.

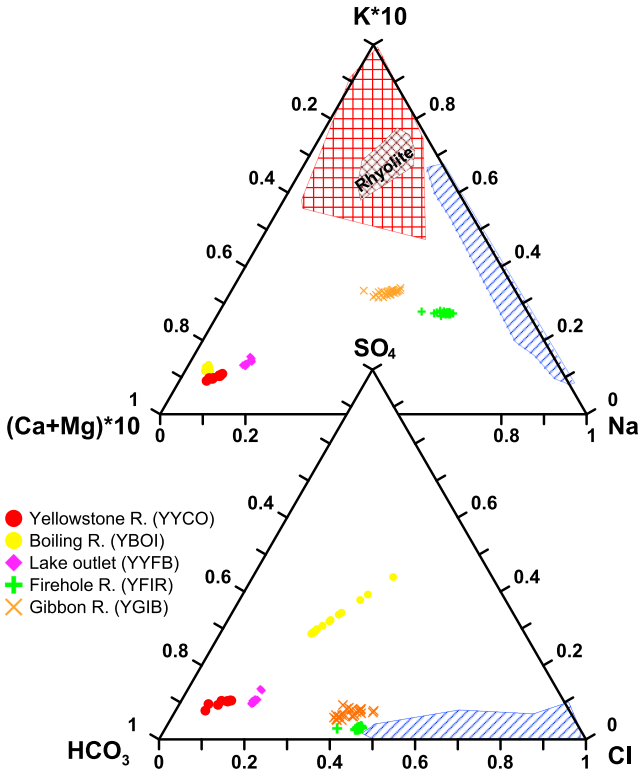

Figure 10. Ternary plots showing molar ratios of major cations and anions in YPVF rivers. The hatched blue areas represent compositions of alkaline-chloride waters, the red-hatched areas represent compositions of acid sulfate waters, and the brown-hatched area represents the composition of an average rhyolite. Modified from *Hurwitz et al.* [2010].

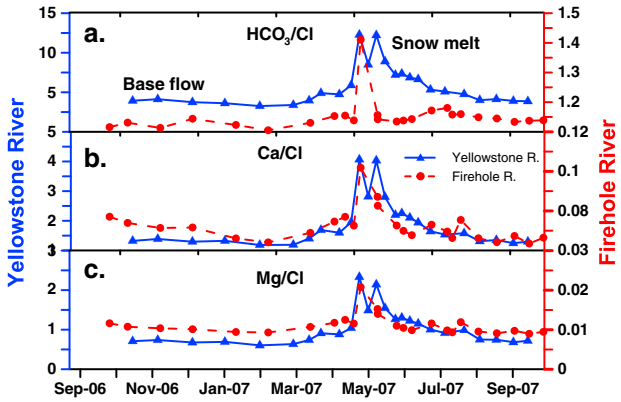

Figure 11. Seasonal variations in molar ratios of select ions to chloride in the Yellowstone and Firehole Rivers. During base flow, the ratios are dominated by hydrothermal input, and following snowmelt, the ion to chloride ratio increase mainly reflects a contribution from hydrolysis of surface rocks. Note the different scales for the ratios in the two rivers; the ratios in the Firehole River that drains the Upper, Midway, and Lower Geyser Basins (Figure 1) are dominated by hydrothermal inputs, whereas the ratios in the Yellowstone River which drains 68% of the YPVF area, including Yellowstone Lake, most of the acid sulfate thermal basins, the Lamar Valley, and Mammoth Hot Springs, are largely dominated by the "cold water" component. Modified from *Hurwitz et al.* [2010].

The relatively high molar Na^+/HCO_3^- (~1.9) in waters that drain thermal areas of YPVF implies that about 50% of the Na^+ in the Firehole and Gibbon Rivers is derived from sources other than interaction of silicate rocks with carbonic acid. The remaining 50% of the Na^+ is balanced by Cl^-, which reflects a NaCl component formed deep in the hydrothermal system or from magma degassing. The large compositional variability of water in the Yellowstone and Gardner Rivers is mainly due to seasonal effects. The composition trends from a HCO_3^--rich end-member during spring runoff to a more Cl^-- and SO_4^{2-}-enriched (thermal) composition during base flow conditions. More recently, *McCleskey et al.* [2012] demonstrated that major rain events leach efflorescent salts in the geyser basins, implying that increase in solute flux during high spring discharge may also be due to flushing of near-surface precipitates that accumulate during the summer and fall and are released only during spring runoff or major rain events.

5.4. Trace Element Systematics

Boron and lithium concentrations in magma-hydrothermal systems hosted in silicic rocks are typically high compared with other settings and are often used to quantify conditions of high-temperature water-rock interaction [e.g., *Leeman and Sisson*, 1996; *Reyes and Trompetter*, 2012]. A reconnaissance study by *Shaw and Sturchio* [1992] showed large boron and lithium concentration variations with progressive alteration of a rhyolitic flow from Yellowstone. In Yellowstone's thermal waters, Li^+/B vary substantially between and within thermal basins (Figure 12). This variation seems to correlate with reservoir temperature that is inferred independently by geothermometry and mineral-solution equilibria calculations. Norris Geyser Basin has the highest reservoir temperature (200–325°C) among Yellowstone's geyser basins [*Fournier et al.*, 1992] and the lowest molar Li/B (0.9 ± 0.1). Thermal waters discharging from Yellowstone Lake vents have reservoir temperatures of ~220°C

©2014. American Geophysical Union. All Rights Reserved.

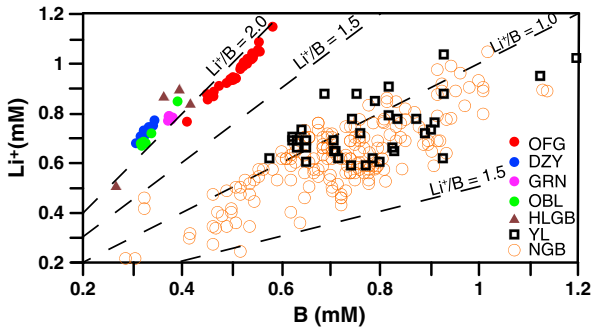

Figure 12. Boron and lithium concentrations of geyser waters from the Upper Geyser Basin (OFG – Old Faithful Geyser, DZY – Daisy Geyser, GRN – Grand Geyser, and OBL – Oblong Geyser), four high-temperature alkaline-Cl waters from Heart Lake Geyser Basin (HLGB) (data from *Lowenstern et al.* [2012]), thermal vents in Yellowstone Lake (YL) (the data from *Gemery-Hill et al.* [2007] were multiplied by 100 because of low concentrations), and from Norris Geyser Basin (NGB) (data from *Thompson and Demonge* [1996] and *Ball et al.* [2007]. Samples with concentrations lower than 0.2 mM of Li or B were removed). The increasing Li/B from Norris Geyser Basin (0.9 ± 0.1) and Yellowstone Lake (1.0 ± 0.2) to Old Faithful (1.9 ± 0.0), Daisy Geyser (2.2 ± 0.0), and Heart Lake Geyser Basin (2.2 ± 0.2) correlates with decreasing reservoir equilibrium temperatures.

[*Shanks et al.*, 2005] and have similar ratios (1.0 ± 0.2). Within the Upper Geyser Basin, Geyser Hill-type waters (Old Faithful) emerge from a slightly hotter reservoir (~210°C) and have lower ratios (1.9 ± 0.0) compared with Black Sand-type (Daisy) waters (~190°C; 2.2 ± 0.0) [*Fournier*, 1989; *Hurwitz et al.*, 2012b]. The temperature and ratio in Heart Lake thermal waters (~205°C; 2.2 ± 0.2) are similar to those of thermal waters from the Upper Geyser Basin. In both basins, waters discharged at the surface equilibrated at temperatures ranging from ~170°C to 200°C before being discharged at the springs and/or geysers. This suggests that in Yellowstone's hydrothermal system the temperature-dependent concentrations of Li and B might provide information on reservoir equilibrium temperatures. At higher temperatures, Li is extracted from thermal waters and incorporated into alteration minerals. As waters progressively cool, the affinity of boron for mineral phases increases as reflected by increasing Li^+/B with decreasing temperature. Similar lithium and boron systematics are observed in the hydrothermal system of the Taupo Volcanic Zone on the northern island of New Zealand [*Reyes and Trompetter*, 2012].

Reconnaissance studies of boron and lithium isotopes were carried out on a relatively small number of water and rock samples. The δ^{11}B values of alkaline-chloride thermal waters are close to the values of unaltered rhyolite (−5.2‰), whereas lower δ^{11}B values of thermal waters from Mammoth Hot Springs (−8.0‰) reflect either boron leached from sedimentary rocks or from hydrothermally altered rhyolite [*Palmer and Sturchio*, 1990]. However, more recent studies measured δ^{11}B values ranging from −8.5‰ to −7.4‰ in rhyolite [*Savov et al.*, 2009], possibly reflecting temperature-dependent fractionation or various degrees of alteration. Thermal waters have δ^7Li values ranging from +1.0 to +6.5‰, compared with δ^7Li ranging between −3.6 and +7.5‰ in rhyolite, generally increasing with increasing hydrothermal alteration [*Sturchio and Chan*, 2003].

Washburn Hot Springs in the northeast part of the Yellowstone Caldera contain high concentrations of ammonium (NH_4), up to 46 mmol [*Allen and Day*, 1935; *Fournier*, 1989; *Holloway et al.*, 2011]. High ammonium concentrations (although an order of magnitude less than in Washburn Hot Springs) were also measured in other thermal areas in the eastern part of the caldera. Ammonium concentrations were much lower in thermal springs along the Firehole and Gibbon Rivers [*McCleskey et al.*, 2010a, 2010b; *Holloway et al.*, 2011]. The high ammonium concentrations at Washburn Hot Springs and other thermal springs in the east part of the caldera correlate spatially with underlying organic-rich sedimentary rocks. It was also shown that reduction of nitrogen (N_2) to ammonia (NH_3) at temperatures up to 89°C and pH as low as 1.9 can be mediated by microbial activity [*Hamilton et al.*, 2011].

Elevated concentrations of rare earth elements (REE) are present in both alkaline-neutral chloride and acid sulfate thermal waters and are correlated with major element chemistry and pH. Relative to the host rhyolite the REE patterns of thermal waters are variably depleted in Heavy and Light Rare Earth and Elements (HREEs and LREEs) and usually have a pronounced positive europium anomaly [*Lewis et al.*, 1997]. Speciation calculations of the thermal waters suggest that the main control over REE speciation is the relative abundances of potential complexing agents; however, pH and absolute abundances are also important [*Lewis et al.*, 1998].

Concentrations of typical ore metals that form aqueous cations, such as lead (Pb), copper (Cu), zinc (Zn), cadmium (Cd), cobalt (Co), and nickel (Ni) are often at or below analytical detection limits, whereas concentrations of metals and metalloids that form oxyanions such as arsenic (As), antimony (Sb), vanadium (V),

©2014. American Geophysical Union. All Rights Reserved.

tungsten (W), and molybdenum (Mo) are notably elevated [*Ball et al*., 2002, 2007, 2010; *McCleskey et al*., 2005; *Gemery-Hill et al*., 2007; *Nordstrom et al*., 2009]. Arsenic is commonly present in thermal waters at much higher concentrations than any other trace metal or metalloid [*Nordstorm and McCleskey*, 2012] with the highest concentration found of 14.6 mg/L although typical concentrations are 0.5 to 3.0 mg/L, 2 orders of magnitude greater than the Environmental Protection Agency standard for drinking water (http://water.epa.gov/lawsregs/rulesregs/sdwa/currentregulations.cfm). Speciation of some metals and metalloids is extremely complex because of the variable dependence on volatility [*Planer-Friedrich and Merkel*, 2006; *Planer-Friedrich et al*., 2006; *Hall et al*., 2006; *Planer-Friedrich et al*., 2006; *Sherman et al*., 2009], oxidation states [*Nordstrom et al*., 2005], pH [*Nordstrom et al*., 2005; *Planer-Friedrich et al*., 2007], and chemosynthetic biotic activity and bioaccumulation [e.g., *Donahoe-Christiansen et al*., 2004; *Inskeep et al*., 2004; *King et al*., 2006; *Inskeep et al*., 2007; *Lalonde et al*., 2007; *Hamamura et al*., 2009]. Some of the metals are transported by rivers to large distances from the YPVF [*Nimick et al*., 1998; *Chaffee et al*., 2007; *Nimick et al*., 2013].

Relatively high concentrations of gold (Au) (up to 1615 ppb in Beryl Spring sinter) were found in siliceous sinters by *Fournier et al*. [1994]. These authors showed that variations in Au concentrations among sinters cannot reflect differences in dissolution of Au from the rocks. Rather, Au concentrations are correlated with the concentration of H_2S and total dissolved sulfide, because a decrease in H_2S concentration destabilizes dissolved gold bisulfide complexes in thermal reservoir waters *Fournier et al*. [1994]. Thus, some or all of the Au that comes out of solution when an initial gold bisulfide complex breaks down as a result of H_2S escape may be swept up to the surface as colloidal particles. Where colloidal silica also forms as a result of this boiling, free Au apparently becomes attached to the colloidal silica and deposits with the silica.

5.5. The Chemical and Isotopic Composition of Gases

Our understanding of gas geochemistry at Yellowstone has advanced greatly because, prior to the past 10 years, few complete gas composition data from the YPVF had been published. With the exception of a thorough study of noble gases [*Kennedy et al*., 1985], most studies published a handful of analyses from discrete geographic areas [*Hearn et al*., 1990; *Werner and Brantley*, 2003] or details and specifics on one aspect of gas geochemistry [*Lorenson et al*., 1991]. *Bergfeld et al*. [2011] provided a complete review of all existing gas data, plus over 130 new analyses of gas from thermal features collected between 2003 and 2009.

For fumaroles at the YPVF, steam may compose anywhere from 90% up to 99.99% of the gas depending on the location within the park. After subtracting H_2O, CO_2 typically makes up $>$90% of the dry gas, with H_2S, CH_4, H_2 and N_2 each making up anywhere between 0.1 and 5% of the remaining gas.

Kennedy et al. [1985] demonstrated that noble gases at Yellowstone are derived from a mixture of atmospheric, magmatic, and crustal sources. Atmospheric gases are introduced through the meteoric-derived groundwater that dominates the H_2O budget of the hydrothermal system. Magmatic gas is most evident at Mud Volcano, where $^3He/^4He$ is indicative of a mantle hot spot (R/*Ra* ~17). Crustal gases are more abundant in the eastern part of the park (e.g., Hot Spring Basin), where organic gases are present in greater abundance, and both crustal He and Ar are evident [*Clifton et al*., 1990; *Lorenson et al*., 1991; *Kennedy et al*., 1985; *Werner et al*., 2008; *Bergfeld et al*., 2011]. Contributions of crustal, meteoric, and magmatic gases vary geographically as shown both by gas compositions (Figure 13) as well as noble gases [*Bergfeld et al*., 2011].

The temperature of the reservoir (equilibration temperature) can be estimated with various gas geothermometers. *Werner et al*. [2008] used gas geothermometers to estimate temperatures between 230° to 330°C at Hot Spring Basin. *Bergfeld et al*. [2012] looked at the oxygen isotopic shift in groundwaters fluxed with cold CO_2 at Brimstone Basin. A simple mass-balance model revealed that subsurface geothermal temperatures in the area must have been warm (93 ± 19°C) even though there is no identifiable thermal signature in the area. Used in isolation, most gas geothermometers assume that all gas separates directly from a deep equilibrated liquid. However, as shown by *Chiodini and Marini* [1998], and as applied at Yellowstone by *Chiodini et al*. [2012b], gas ratios reflect both the temperature of chemical equilibration in the liquid and the temperature of separation from the liquid during adiabatic boiling. *Chiodini et al*. [2012b] further showed that reequilibration of gases in the vapor phase must be considered. After accounting for such effects, they found that the highest temperature reservoirs, near Mud Volcano and Beryl Springs, had the most magmatic He-isotope signature; whereas fluids from the Heart Lake Geyser Basin equilibrated in reservoirs at lower temperatures and had much more crustal He isotopic signatures. Thus, we can detect

©2014. American Geophysical Union. All Rights Reserved.

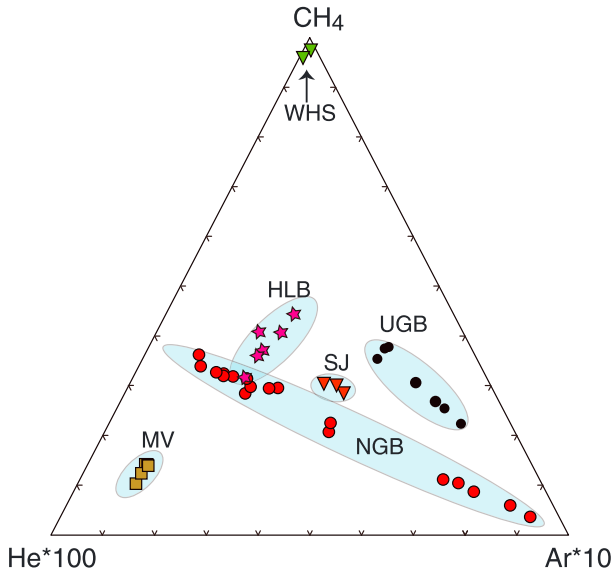

Figure 13. Ternary diagram showing gas compositions from fumaroles and frying pans. The compositions define discrete geographic areas with unique CH_4/He ratios. Gases from most areas are mixtures of magmatic and crustal components, variably diluted by atmospheric gases from meteoric waters (Ar end-member). WHS – Washburn Hot Springs, HLB – Heart Lake Geyser Basin, SJ – Smoke Jumper Hot Springs, UGB – Upper Geyser Basin, NGB – Norris Geyser Basin, and MV – Mud Volcano. Modified from *Bergfeld et al.* [2011].

high-temperature, magmatic hydrothermal end-members and lower temperature sources that reflect greater amounts of crustal input [*Chiodini et al.*, 2012a, 2012b; *Lowenstern et al.*, 2014].

Input of crustal gas is also revealed through observation of the ratios of hydrocarbon gases such as CH_4/C_2H_6 (C1/C2). *Bergfeld et al.* [2011] showed that thermal areas ranged widely in CH_4/C_2H_6, consistent with derivation of hydrocarbons at different temperatures or from different source rocks. The C1/C2 of some samples conform to that expected for thermogenic release of gas from sedimentary rocks [*Lorenson et al.*, 1991; *Bergfeld et al.*, 2011] and are geographically correlated with areas that contain known hydrocarbon seeps [*Love and Good*, 1970; *Clifton et al.*, 1990]. Abiotic production of many hydrocarbons is an inevitable result of metastable equilibrium in kerogen-bearing rocks at typical crustal oxidation states and temperatures between 150 and 300°C [*Shock et al.*, 2013].

A major change in perception of gas dynamics at Yellowstone occurred in the wake of *Werner and Brantley* [2003], who first quantified the high emissions of CO_2 from the YPVF (section 6.1). This high rate seems to require that subsurface hydrothermal reservoirs are gas-saturated in the upper few kilometers (Figure 8) [*Lowenstern and Hurwitz*, 2008] and that gas chemistry must be interpreted as an open system where deep magmatic and metamorphic gases continuously pass through superjacent meteoric-derived waters. *Lowenstern et al.* [2014] recognized that such open system gas flux includes abundant crust-derived ^{4}He that must have accumulated by radiogenic breakdown of uranium and thorium in the Archaean crustal rocks that form the basement beneath Yellowstone. Mantle-derived CO_2 sweeps into the crust and combined with the high temperatures and renewed tectonism associated with the hot spot, frees abundant crustal ^{4}He and CH_4 [*Lowenstern et al.*, 2014]. Open system behavior of gas was first observed at Yellowstone by *Allen and Day* [1935] who found that acid sulfate waters were typically stagnant but hosted abundant gas throughput, implying a source of continual gas replenishment from below. Addition of crustal gas could have a quantitative effect on estimates of groundwater ages based on noble gas abundances [*Gardner et al.*, 2010a; *Yokochi et al.*, 2013, 2014].

5.6. Hydrothermal Deposits

Most thermal springs at Yellowstone actively deposit minerals at high rates through diverse biotic and abiotic processes. Alkaline-chloride-rich waters that discharge in the geyser basins and in Yellowstone Lake can become supersaturated with silica, resulting in the deposition of siliceous sinters. Thermal waters discharging at Mammoth Hot Springs deposit travertine following loss of CO_2 gas near the near surface.

Use of the airborne visible and infrared imaging spectrometer (AVIRIS) [*Hellman and Ramsey*, 2004; *Livo et al.*, 2007] and the Advanced Spaceborne Thermal Emission and Reflection Radiometer (ASTER) [*Hellman and Ramsey*, 2004] allowed identification of several thermal areas where hydrothermal deposits are closely correlated with structural trends, suggesting focused fluid upflow through faults and fractures. In the Norris Geyser Basin overprinting of alteration minerals also suggests chemical changes with time and/or lateral migration of upflow zones within the basin that might indicate shifts in fault activity.

Precipitation of siliceous sinter is the result of abiotic and biotic processes [*Jones and Renaut*, 2011]. As thermal waters cool following discharge at the surface or in pools, the solubility of silica (SiO_2) decreases

©2014. American Geophysical Union. All Rights Reserved.

[*Fournier*, 1981; *Fournier and Potter*, 1982], leading to precipitation of the mineral opal-A and deposition of sinters that form cones, domal mounds, and terraces with a stair-step morphology. Repeated wetting and evaporation of surfaces, often to dryness, and capillary effects can control the deposition, morphology, and microstructure of most high-temperature subaerial sinter. Biotic effects on precipitation appear to be small even though microbial filaments are abundant on and within high-temperature sinter [*Walter et al*., 1972; *Blank et al*., 2002]. However, biotic effects on precipitation rates, texture, and pigmentation become progressively more significant, and the microbial communities variability increases as the water flows away from its vent and cools [*Braunstein and Lowe*, 2001; *Guidry and Chafetz*, 2002; *Lowe and Braunstein*, 2003; *Guidry and Chafetz*, 2003; *Havig et al*., 2011]. The color of the microbial mats is best evident in Grand Prismatic Spring in the Midway Geyser Basin (Figure 1), where the rainbow colors on the edges of the pool were the inspiration for the spring's name given by members of the 1871 Hayden expedition.

Hinman and Lindstrom [1996] described seasonal silica deposition rate variations at Octopus Spring in the Lower Geyser Basin. They attributed the higher deposition rates during the sub-zero air temperatures in the winter to decreased solubility with temperature. Subsequently, *Channing and Butler* [2007] made a similar observation at the Norris and the Upper Geyser Basins and attributed the high winter deposition rates to cryogenic opal-A precipitation in brine pockets, channels, and veins. The unconsolidated cryogenic opal-A sediments accumulate in and below ice until the spring thaw when it is either remobilized, or becomes adhered, in situ, by dehydration and cementation. Millimeter-scale lamination in sinter represents annual layering and regular seasonal fluctuations in silica sedimentation [*Lowe and Braunstein*, 2003].

Approximately 12–18 siliceous spires were discovered in the northern basins of Yellowstone Lake in the 1990s. These conical structures are composed of silicified filamentous bacteria, diatom tests, and amorphous silica, are found in water depths of 15 m, and are up to 8 m in height and 10 m wide at the base [*Klump et al*., 1995; *Cuhel et al*., 2002; *Morgan et al*., 2007; *Shanks et al*., 2007]. Similar subaerial spires are found at Monument Geyser Basin (Figure 1), where highly acidic gas is emitted and the water table is now assumed to be at a depth of ~250 m. The coincidence of acid springs and sinter deposits suggests that these spires were formed in the past, at a time when the water table was much higher and near the ground surface [*Morgan et al*., 2007].

There are only a few published radiometric dates of sinter deposits in Yellowstone. *Marler* [1956] described the growth of Old Faithful Geyser as episodic with alternating periods of growth and erosion. Based on a ^{14}C age of 730 ± 200 years for silicified wood embedded in the Old Faithful geyserite, *Marler* [1956] wrote "the logical inference is that Old Faithful Geyser began to erupt only about two centuries ago." More recently, several ^{14}C dates were obtained from sinter deposits at Castle Geyser, in the Upper Geyser Basin [*Foley*, 2006]. The shield upon which the geyser is built yields two ^{14}C dates of 8,787 ± 60 and 10,472 ± 70 years B.P., and three ^{14}C dates from the cone range between 1,038 ± 35 and 926 ± 35 years B.P. The large gap of dates between shield formation and the cone is consistent with the hypothesis of *Marler* [1956] that build up of geysers is highly episodic with alternating phases of construction and destruction, but the ^{14}C dates suggest that the constructive phase of the geyser is much longer. Uranium-series disequilibrium dates of two samples from a siliceous spire in northern Yellowstone Lake yield ages of about 11,000 years (determined by Neil Sturchio, University of Illinois at Chicago, published in *Morgan et al*. [2007]). The oldest age for Castle geyser and the age of the Yellowstone Lake spire suggest considerable postglacial deposition of silica sinters, consistent with the hypotheses of *Bargar and Fournier* [1988] and *Fournier* [1989] that the retreat of glacial ice sheets resulted in increased boiling in the hydrothermal system, which in turn enriched and supersaturated the residual liquids with silica, leading to high rates of siliceous sinter deposition.

Thermal waters discharging at the large travertine terraces of Mammoth Hot Springs in the northern part of the YPVF (Figure 1) emerge from a sequence of Mesozoic sedimentary rocks that includes limestone, dolomite, and gypsum-bearing shales [*Pierce et al*., 1991] where reservoir temperatures are 100–120°C [*Fournier*, 1989]. Uranium-series age determinations revealed a close correlation between travertine deposition rates (~1.0 cm · yr^{-1} in the past 7700 ± 440 years) and the chronology of the late Pleistocene Pinedale Glaciation [*Sturchio*, 1990; *Sturchio et al*., 1994].

Decompression during ascent to the surface causes degassing of CO_2 from the water, and the pH increases from ~6 at the vent to >8 or higher following the reaction

$$HCO_3^-{}_{(aq)} + H^+{}_{(aq)} \rightarrow CO_{2(g)}\uparrow + H_2O$$

©2014. American Geophysical Union. All Rights Reserved.

The extensive degassing of CO_2 overwhelms biotic controls on travertine deposition [*Leeman et al*., 1977; *Fouke et al*., 2000; *Chafetz and Guidry*, 2003; *Fouke*, 2011]. The increasing pH triggers calcite and aragonite saturation, and subsequent precipitation of aragonite following the reaction

$$Ca^{2+}{}_{(aq)} + 2HCO_3{}^{-}{}_{(aq)} \rightarrow CaCO_{3(s)} + CO_{2(g)}\uparrow + H_2O$$

Sturchio [1990] concluded based on radium isotope analysis that a complete diagenetic transformation from aragonite to calcite occurs within approximately 9 years.

5.7. Microbial Activity and the Geochemical Cycle

The discoveries of exotic forms of all three domains of life (Eukarya, Bacteria, and Archaea) in Yellowstone's thermal features have attracted numerous researchers since the early reviews on thermophiles by *Brock* [1978, 1985]. The emergence of sophisticated molecular and genetic sequencing methods over the past 25 years has accelerated research on the metabolic pathways and adaptation of microorganisms to the diverse and extreme environments in Yellowstone's hydrothermal system. Some of these studies showed that the metabolism of thermophile microorganisms is unique to the chemical composition of thermal waters and/or dissolved gases [e.g., *Barns et al*., 1994; *Reysenbach et al*., 2000; *Rice et al*., 2001; *Walker et al*., 2005; *Meyer-Dombard et al*., 2005]. Some metabolic reactions that are favorable sources of chemical energy at one set of geochemical conditions fail to provide energy at other conditions [e.g., *Nordstrom et al*., 2005; *Inskeep et al*., 2005; *Takacs-Vesbach et al*., 2008; *Shock et al*., 2010; *Hamilton et al*., 2011; *Cox et al*., 2011].

In alkaline thermal waters with temperatures >75°C, primary productivity occurs when energy for metabolism is obtained from the oxidation of inorganic compounds (chemolithoautotrophy) [*Boyd et al*., 2009; *Cox et al*., 2011; *Hamilton et al*., 2012]. At these high temperatures, hydrogen (H_2) is the main source of energy for primary production [*Blank et al*., 2002; *Spear et al*., 2005]. However, at pH < 6.5, the transition to chlorophyll-based, phototrophic metabolism occurs at temperatures lower than 75°C, and at pH ~ 2, there is no evidence for photosynthesis at > 45°C. Because of the much larger range of energy sources and metabolic diversity, chemotrophic communities have a greater genetic diversity compared with phototrophs [*D'Imperio et al*., 2008; *Shock et al*., 2010].

The discovery of significant thermophile biotic diversity in Yellowstone Lake vents since the early 2000s has opened a new window into Yellowstone's hydrothermal system [*Lovalvo et al*., 2010; *Clingenpeel et al*., 2011; *Yang et al*., 2011; *Kan et al*., 2011]. The thermal vents harbor spatially distinct chemosynthetic bacterial communities, which depend on water temperature and electron donor supply (H_2S and NH_3). Microbial chemosynthesis using hydrogen and methane as energy sources for metabolism was shown to be significant at high temperatures in several vents [*Clingenpeel et al*., 2011].

6. Rates of Heat and Mass Transport at the Ground Surface

The transport of heat and mass within the hydrothermal system entails multiphase and multicomponent fluid flow in rocks with highly transient and heterogeneous permeabilities [e.g., *Ingebritsen and Manning*, 2010; *Manga et al*., 2012] and physical, chemical, and biological processes that are strongly coupled (Figure 14). Significant advances have been made in the past 25 years including measurements of magmatic volatile discharge through rivers (e.g., Cl^-, F^-, $HCO_3{}^-$ and $SO_4{}^{2-}$) and soils (H_2S and CO_2), characterization of temporal patterns for some volatiles, improved understanding of heat-transport mechanisms, and application of satellite-based methods to quantify heat flux.

6.1. Mass Transport

Continuous sampling of the large rivers draining the YPVF (Figure 1) has been carried out since 1983 to provide estimates of total Cl^- discharge [*Norton and Friedman*, 1985; *Friedman and Norton*, 1990; *Ingebritsen et al*., 2001; *Friedman and Norton*, 2007], which in turn provides quantitative estimates of the total heat flow based on the Cl-enthalpy method [*Ellis and Mahon*, 1977; *Fournier*, 1979]. More recently, methods relating electric conductivity to chloride concentrations were introduced to track riverine Cl^- discharge at subhour rates [*Clor et al*., 2012; *McCleskey et al*., 2012]. Starting in 2002 the riverine discharge of $HCO_3{}^-$, $SO_4{}^{2-}$, and F^- were quantified as well [*Hurwitz et al*., 2007b, 2007c]. Additional goals of this monitoring program were to assess possible changes in heat and mass output that correlate with temporal patterns of caldera deformation and large earthquakes [*Fournier*, 2004].

©2014. American Geophysical Union. All Rights Reserved.

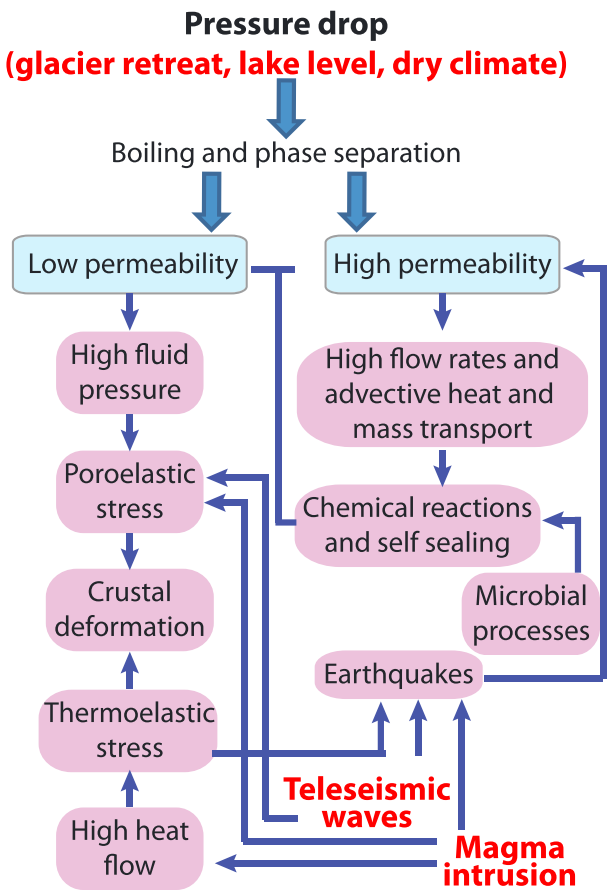

Figure 14. Schematic showing the coupled processes operating in magma hydrothermal systems in response to decompression, local and remote earthquakes, and magma intrusion.

Solute discharge is relatively constant during most of the year (base flow), but it increases during the spring runoff (Figure 6) implying that recharge of snow melt and ice thaw enhance thermal discharge. Mass discharge of the major volatiles in all rivers is in the following order, CO_2 (as HCO_3^-) > Cl^- > S (as SO_4^{2-}) > F^- (Table 1). However, each river is characterized by a unique chemical composition (Figure 10). For example, Cl/SO_4 is much higher in the Firehole River than the Yellowstone River. Such variations in chemistry and solute flux (discharge per area) among the river drainages may result from large-scale phase separation, lateral transport by thermal groundwater, and interaction with varying rock assemblages [*Hurwitz et al.*, 2007b]. Thus, any attempt to quantify the output of magmatic volatiles needs to account for discharge from all river drainages.

Volatiles emerge at the ground surface in gaseous form, both by diffuse degassing through soils and directly from bubbling pools and fumaroles. The distribution of diffuse soil emissions of CO_2 in the thermal areas of Yellowstone is heterogeneous at several spatial scales [*Werner et al.*, 2000; *Werner and Brantley*, 2003]. Fluxes of CO_2 through soils near terrains in which silica sinter and travertine ($CaCO_3$) form are low compared to those in the acid sulfate areas of the YPVF. We infer that the alkaline-neutral, high-chloride waters discharged from sinter-forming terrains are comparatively degassed (also see *Allen and Day* [1935]) after migrating laterally through and beneath the lava flows that surround the low-elevation geyser basins. When such waters boil, they also provide abundant gas (mainly CO_2, H_2, and H_2S) to the overlying acid sulfate areas [*Lowenstern et al.*, 2012].

Measurements of diffuse CO_2 flux through soils began in the late 1990s in the Mud Volcano area [*Werner et al.*, 2000] and were followed by measurements in several other thermal areas [*Werner and Brantley*, 2003]. Whereas the mean CO_2 flux in the Upper Geyser Basin (Figure 1) was 27 g m^{-2} d^{-1}, the flux in several acid sulfate areas was orders of magnitude higher [*Werner and Brantley*, 2003]. The diffuse CO_2 flux from the 35 km^2 of thermally altered acid sulfate areas was calculated to be 97.5% of the total diffuse flux from the YPVF, whereas flux from alkaline-chloride areas and from the travertine terraces at Mammoth Hot Springs account for 2% and <0.5%, respectively. To extrapolate the diffuse CO_2 flux from the several thermal basins where it was measured to all active thermal areas in Yellowstone, *Werner and Brantley* [2003] used the arithmetic average of all the measurements and calculated a total emission rate of 45 ± 16 kt d^{-1} from the YPVF. Based on carbon and helium isotope values, *Werner and Brantley* [2003] estimated that 30–50% of the CO_2 output from the YPVF is derived from pre-Quaternary sedimentary/metamorphic basement rocks, with the remainder being degassed from magma.

Since the study of *Werner and Brantley* [2003] was published, CO_2 flux measurements were made in the acid sulfate areas of Hot Spring Basin [*Werner et al.*, 2008], Brimstone Basin [*Bergfeld et al.*, 2012], Norris Geyser Basin, and Solfatara Plateau, and additional measurements were made at Mud Volcano (C. A. Werner, U.S. Geological Survey, written communication, 2014) (Figure 1). With the exception of small acid sulfate areas

©2014. American Geophysical Union. All Rights Reserved.

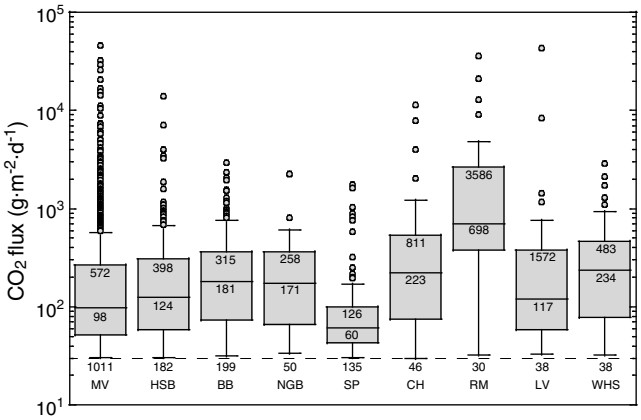

Figure 15. The distributions of CO_2 fluxes in thermal areas of Yellowstone using the gas accumulation chamber technique. The boxes represent the 25th and 75th percentiles of the data, and the horizontal lines in the boxes represent the median values. The horizontal bars (whiskers) bound the range of data, and the circles represent measurements that are considered outliers. The number above the area designator indicates the number of measurements. The statistics only include individual measurements that were greater than the background level of 30 g m^2 d^{-1}, represented by the dashed horizontal line. The numbers above and below the median line in the boxes are the average and median values, respectively. Data from Crater Hills (CH), Roaring Mountain (RM), Lamar Valley (LV), and Washburn Hot Springs (WHS) are from *Werner and Brantley* [2003]. Data from Hot Spring Basin (HSB) are from *Werner et al*. [2008] and data from Brimstone Basin (BB) are from *Bergfeld et al*. [2012]. The box representing Mud Volcano includes data previously published by *Werner and Brantley* [2003] and classified separately in their Figure 6 as GU97, GU98, GO97, GO98, and unpublished data collected in 2008 and 2010. Data from Norris Geyser Basin (NGB), Solfatara Plateau (SP), and additional, unpublished data from Mud Volcano are provided by Cynthia A. Werner (U.S. Geological Survey, written communication, 2014).

peripheral to the alkaline waters of geyser basins (e.g., Heart Lake) [*Lowenstern et al*., 2012], the diffuse fluxes at most acid sulfate basins are high and similar to those previously published by *Werner and Brantley* [2003] (Figure 15).

Using the same extrapolation method used by *Werner and Brantley* [2003] for the measurements they published and the new measurements results in a total emission rate of 20 ± 2 kt d^{-1} from the 35 km^2 of thermally altered, acid sulfate areas of the YPVF. This estimate is dominated by the large number of measurements made at Mud Volcano (Figure 15). If we average the mean flux from the nine thermal areas plotted in Figure 15, the total emission rate is 32 ± 1 kt d^{-1}. If we exclude from the calculations the average fluxes from Roaring Mountain and the Lamar Valley where fluxes are very high, but relatively few measurements were made (Figure 15), the total emission rate amounts to 15 ± 8 kt d^{-1}. This wide range of calculated emission rates emphasizes the sensitivity to the assumptions incorporated in the extrapolations. For example, the number of measurements made at Mud Volcano is more than 25 times the number of measurements made at Roaring Mountain, the Lamar Valley, or Washburn Hot Springs, but averages from all these areas have the same weight in the extrapolation method used by *Werner and Brantley* [2003]. Until more measurements are made in those poorly sampled regions, extrapolations will be subject to large degrees of uncertainty. Additionally, the calculated total emission rates do not account for CO_2 discharged from fumaroles and bubbling pools and do not account for seasonal (all measurements were made between June and September) and other temporal variability. At Mud Volcano, *Werner and Brantley* [2003] estimated that 30–60% of CO_2 emissions emerge directly from vents. Considering all the assumptions and extrapolations used to derive the total CO_2 emissions from the YPVF, we suggest that current estimates based on measurements with the gas accumulation chamber are imprecise but likely within the range of 10 to 60 kt d^{-1}.

6.2. Heat Transport

Even though Yellowstone's magmatic system is one of the most focused heat sources on Earth, processes that control heat transport between magma and the surface and the total heat output and its time variation, are poorly constrained. Quantifying heat output from the YPVF is a daunting task because of the large extent of thermal areas, the heterogeneous heat flux at many spatial and temporal scales, and because groundwater flow removes heat and chloride (a proxy for heat) from some areas and concentrates it in others.

The shallow subsurface transport of heat is spatially heterogeneous and to a first order, controlled by topography. Most of the thermal water in the park emerges at low elevations along the Firehole and Gibbon River drainages on the western side of the Yellowstone Caldera as alkaline-chloride thermal waters. The tangible heat associated with that water alone is >0.5 GW [*Hurwitz et al*., 2012a]. However, additional heat is associated with the acid sulfate terrain found at higher elevations, where abundant vapor emerges and acid

©2014. American Geophysical Union. All Rights Reserved.

sulfate ground is often near the boiling point of H_2O. The high enthalpy of steam (2663 kJ kg^{-1} at 92°C, the average boiling temperature in Yellowstone) relative to liquid water (enthalpy of 385 kJ kg^{-1} at 92°C) implies that a significant amount of heat is discharged in the ~35 km^2 of thermally active acid sulfate areas of the YPVF [*Rodman et al.*, 1996].

In a pilot field study in the winter of 1965 *Dort* [1966] recognized the potential for quantifying heat flux in Yellowstone by mapping contours of total snow depth in a small thermal area northwest of Old Faithful Geyser. Soon thereafter, *White* [1969] developed snowfall calorimetry as a rapid low-cost means of quantifying rates of total heat flow in hot spring areas. By comparing time-lapse mapped contacts between snow-covered and snow-free ground after a heavy snowfall near Old Faithful Geyser, *White* [1969] derived heat flux estimates ranging between 1 and 13 W m^{-2}. However, *White* [1969] acknowledged that with the methods available to him at the time, estimates were probably within a factor of 2 of the total conductive and convective heat flow for the area.

Conductive heat flow measurements carried out in the 1970s in Yellowstone Lake revealed that heat flow varies by more than 2 orders of magnitude spatially [*Morgan et al.*, 1977]. The southern portion of the lake, outside the caldera, is characterized by heat flow of about 0.1 W m^{-2} and the northern portion of the lake inside the Yellowstone Caldera is characterized by heat flow of 1.5–2 W m^{-2}. Locally, the heat flow can be much higher, such as east of Stevenson Island where it is $>$10 W m^2 and in the Mary Bay hydrothermal explosion crater where heat flow is up to 40 W m^{-2}. High thermal gradients in both West Thumb and Mary Bay indicate that the boiling temperature of water is reached at shallow levels ($<$300 m) suggesting shallow and laterally extensive advective flow systems [*Morgan et al.*, 1977].

Starting in the 1980s, the total heat output from the YPVF was estimated using the chloride inventory method, which assumes that all the chloride discharged by rivers draining the YPVF is derived from a single deep parent fluid estimated to have a concentration of 400 mg L^{-1} and a temperature of 340°C (enthalpy of 1594 kJ kg^{-1}) [*Fournier*, 1989]. With an average chloride discharge of ~50,000 t yr^{-1} [*Friedman and Norton*, 2007; *Hurwitz et al.*, 2007b, 2010], ~4000 L s^{-1} of parent fluid are discharged. Adiabatic decompression and cooling of the parent fluid from 340°C to 92°C (average boiling temperature in Yellowstone) would generate 53 wt % of steam with an enthalpy of 2663 kJ kg^{-1} and transport 5.6 GW of heat to the surface. Liquid water (47 wt %) with an enthalpy of 385 kJ kg^{-1} transports only 0.7 GW, and CO_2 with a flux of 45,000 t d^{-1} [*Werner and Brantley*, 2003] transports $<$ 0.2 GW, for a total heat output from Yellowstone of ~6.5 GW. If all this heat is discharged through the 2900 km^2 of the Yellowstone Caldera (although some heat is discharged outside of the caldera), it corresponds to an average heat flux of 2.2 W m^{-2}; about 25–40 times greater than that in the neighboring Rocky Mountains [*Blackwell and Richards*, 2004] and that of the average continental crust [*Jaupart and Mareschal*, 2007].

Because of the large variations and uncertainties associated with parameter values used in these heat output estimates, *Hurwitz et al.* [2012a] calculated heat output for a range of parameter values. An estimated minimum heat output of 4.0 GW corresponds to a chloride concentration of 450 mg L^{-1}, a temperature of 320°C (1462 kJ kg^{-1}), and a chloride flux of 45,000 t yr^{-1}. In contrast, an estimated maximum heat output of 8.0 GW corresponds to a chloride concentration of 350 mg L^{-1}, a temperature of 360°C (1,762 kJ kg^{-1}), and a chloride flux of 55,000 t yr^{-1}. Thus, for a set of plausible parameter values, estimates of heat output from the Yellowstone magmatic system may vary by a factor of 2. Satellite-based thermal infrared estimates account only for the radiant component of heat output from the YPVF (2 GW) [*Vaughan et al.*, 2012] and therefore are much lower than those estimated with the chloride-inventory method. Other studies that used airborne [*Jaworowski et al.*, 2006, 2010, 2013] or satellite-based methods [*Hellman and Ramsey*, 2004; *Watson et al.*, 2008; *Vaughan et al.*, 2010; *Savage et al.*, 2010] to estimate radiative heat output were either limited in their spatial coverage, or used data acquired during daytime, which introduces significant errors. The large uncertainties associated with the chloride-inventory method and the relation between radiative heat flux and total heat flux limit our ability to use heat as a tracer to constrain deep processes in Yellowstone's magmatic system.

Conceptual models of heat transport in vapor-dominated areas (Figure 16) suggest that rising steam and noncondensable gases, mainly CO_2 and H_2S, fill open fractures throughout a significant vertical extent beneath a thin low-permeability cap layer consisting mainly of clay minerals [*White et al.*, 1971; *Hochstein and*

©2014. American Geophysical Union. All Rights Reserved.

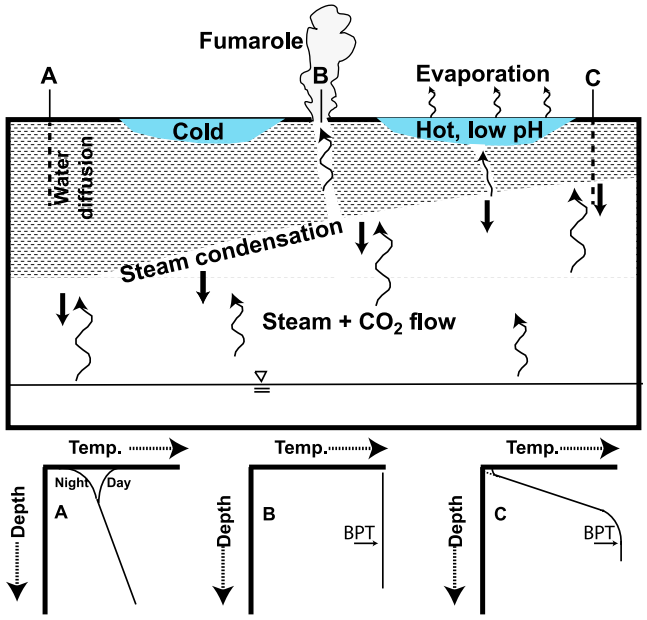

Figure 16. A schematic illustration showing modes of heat transport in vapor-dominated areas and the resulting temperature gradients [from *Hurwitz et al.*, 2012a]. In areas with a relatively thick low-permeability, clay-rich cap rock (A) temperature gradients are moderate and vary considerably in response to air temperature and solar insolation fluctuations. In areas where a fracture transects the entire cap rock and connects the vapor-dominated area with the ground surface (B), a fumarole will form with fluid discharge at boiling temperature. Areas with a thin cap rock (C) are characterized by a large temperature gradient and variations in response to air temperature and solar insolation fluctuations are small. When steam condenses into a pool (as the one on the right, top panel) it will be hot and acid. In contrast, a pool that is not connected to the vapor-dominated area will remain cold, and its waters will be neutral. Below the cap rock rising steam and noncondensable gases (curved thin lines) fill open fractures, and the vapor condensate (thick lines) descends down the fractured rocks.

Bromley, 2005; *Hurwitz et al.*, 2012a]. Heat is transferred by the rising vapor to the base of the cap layer, where the vapor condenses and the liquid descends down the fractures (heat pipe). In this conceptual model, heat transport across the low-permeability layer is dominated by conduction through the solid phase, but where the cap layer is fractured, heat discharges advectively through fumaroles or vapor condenses into pools [*Hurwitz et al.*, 2012a]. These vapor-dominated thermal areas are mostly concentrated in the eastern half of the caldera (Figure 1) where seismic tomography suggests that the silicic magma is shallower than in other parts of the caldera [*Husen et al.*, 2004; *Farrell et al.*, 2014].

Hurwitz et al. [2012a] extrapolated the average heat flux from two vapor-dominated areas in Yellowstone Caldera to the ~35 km^2 of acid sulfate areas in the YPVF (Figure 1), yielding from 1.2 GW to 3.6 GW and highlighting the large uncertainties associated with these estimates. The relatively low extrapolated values might also suggest that either the heat fluxes from the two thermal areas are not representative of the average vapor-dominated area or that the chloride inventory method does not provide a correct estimate of total heat output from the Yellowstone magmatic system. It might also suggest that a significant amount of heat is transported (without chloride) by recharging meteoric water. That is, some heat is wicked away from the plateau such that the heat does not emerge in the acid sulfate areas. A higher heat flux was estimated for Hot Spring Basin, one of the hottest basins in the YPVF, located just outside the eastern margin of the caldera (Figure 1). Based on limited measurements, the total heat output is estimated to range between 140 and 370 MW [*Werner et al.*, 2008]. The radiative heat output from the central Hot Spring Basin was estimated at 56–62 MW [*Jaworowski et al.*, 2013]. In these acid sulfate thermal areas, a link between focused thermal activity and the orientation of mapped faults surrounding the thermal areas suggests that either these faults serve as discontinuities along which the acid fluids dissolve the rocks forming permeable flow channels or that these faults are active and form the permeable pathways to the surface [*Hurwitz et al.*, 2012a].

Based on discharge measurements of water erupting at Lone Star Geyser and thermodynamic calculations, a heat output from this high-output geyser was estimated to be 1.4–1.5 MW [*Karlstrom et al.*, 2013], which is an order of magnitude greater than that estimated by other means for Old Faithful Geyser [*Rinehart*, 1980, p. 61]. Nevertheless, it is only a very small fraction of the heat output from the Yellowstone Caldera [*Hurwitz et al.*, 2012a], suggesting that even if all of the ~500 geysers in Yellowstone had the same heat output as Lone Star, their combined contribution would only constitute about 10% of the total heat output from the Yellowstone Caldera.

6.3. The State of the Magmatic System Based on Heat and Volatile Flux

The estimates of magmatic volatile discharge and heat output provide constraints on the composition and state of the underlying magmatic system. The estimated rate of CO_2 discharge is high enough to rapidly

©2014. American Geophysical Union. All Rights Reserved.

exhaust any plausible nonmagmatic source such as metasediments. CO_2 discharge rates are also significantly greater than the mass that could be dissolved in reasonable volumes of rhyolitic melt in the upper to middle crust beneath the Yellowstone Caldera [*Werner and Brantley*, 2003; *Lowenstern and Hurwitz*, 2008]. The volume of the silicic magma reservoir beneath Yellowstone is estimated at ~1.5×10^4 km^3 [*Lowenstern et al.*, 2006], and based on magmatic volatile compositions of silicate melt inclusions enclosed within quartz crystals in erupted rhyolites, Yellowstone silicic magmas appear to contain less than 500 ppm dissolved CO_2 [*Lowenstern and Hurwitz*, 2008]. At the current degassing rate, such a magma body would be entirely purged of dissolved CO_2 in less than 1000 years. Another way of looking at this mass balance problem is that the heat flow at Yellowstone is consistent with crystallization and degassing of ~0.1 km^3 rhyolitic magma per year. If the CO_2 flux came from this rhyolitic source, it would require 5.5 wt % of CO_2 to be dissolved in the melt or ~ 20 times that which can be dissolved at 400 MPa (~16 km depth) in rhyolitic liquid [*Lowenstern*, 2001].

The relative proportions of emitted volatiles are also inconsistent with extensive degassing of a silicic magma. The melt inclusions contain abundant dissolved chlorine and fluorine but scarce CO_2 and S [*Lowenstern and Hurwitz*, 2008]. Yet orders of magnitude more CO_2 is emitted through the Yellowstone hydrothermal system than chlorine, fluorine, or sulfur. In contrast, basaltic magmas generally contain lower concentrations of dissolved chlorine and fluorine, and their composition and origin at mantle pressures permit them to contain 10 to 30 times more dissolved CO_2 and sulfur than a midcrustal rhyolite [*Blank et al.*, 1993; *Papale*, 1999; *Lowenstern*, 2001]. Also, thermal considerations dictate that the volume of basaltic magma parental to the rhyolite (or those basaltic intrusions inducing crustal melting) will be at least 3 to 5 times greater than that of any derivative silicic magma [*White et al.*, 2006]. Thus, either basaltic intrusions or convection of basalt in a lower crust reservoir could provide 50 to 100 times more CO_2 than middle to upper crustal silicic magmas.

The observations and calculations summarized above imply that most of the CO_2 is derived from degassing basaltic magma that underlies the upper to middle crustal rhyolitic magma reservoir [*Lowenstern and Hurwitz*, 2008]. This inference is also supported by $^3He/^4He$ and $^3He/CO_2$ that have mantle values [*Kennedy et al.*, 1985; *Bergfeld et al.*, 2011; *Lowenstern et al.*, 2014]. If basaltic magmas provide half the CO_2 degassed at Yellowstone (the rest coming from crustal rocks), associated intrusion, cooling, crystallization, and/or large-scale convection could provide much of the observed heat flow. Assuming 1 wt % CO_2 in mantle-derived basalt [*Lowenstern and Hurwitz*, 2008], an intrusion rate of 0.3 $km^3\ yr^{-1}$ would be required to produce the observed CO_2 flux. However, this intrusion rate would generate a power output of 22 GW assuming full crystallization and further cooling of 300°C. This heat output is ~3–5 times the calculated heat output based on the Cl-enthalpy method [*Hurwitz et al.*, 2012a]. Heat output would be lower if the intruding basalt loses heat by conduction, or if it degasses during ascent with minimal cooling and crystallization.

Despite the large uncertainties in gas and heat discharge determinations, the order of magnitude estimates indicate either high intrusion rates or vigorous convection of basaltic magma that are up to 2 orders of magnitude greater than the long-term eruption rate of rhyolite in Yellowstone, 0.003 $km^3\ yr^{-1}$ [*Christiansen*, 2001]. Petrologic and seismic evidence points to a dense, high-velocity midcrust beneath the Snake River plain, consistent with emplacement and crystallization of basaltic magma throughout the 16 million year history of the Yellowstone hot spot [*Smith and Braile*, 1994; *Shervais et al.*, 2006]. Models for the generation of Yellowstone rhyolites involve crystallization and/or melting of abundant basaltic sources in the lower crust combined with 10 to 30% melting of radiogenic crust [*Hildreth et al.*, 1991]. Gas and heat released during ascent and crystallization of the basaltic magma should be able to percolate through partly molten silicic magma (mush) [*Bachmann and Bergantz*, 2006; *Parmigiani et al.*, 2011; *Huber et al.*, 2012]. The CO_2 released from the underlying basalt would be too abundant to dissolve within the overlying silicic magma and hydrothermal system, effectively saturating the crust with CO_2-rich gas (Figure 8) [*Lowenstern and Hurwitz*, 2008].

7. Geysers and Hydrothermal Explosions

Geysers are rare, with less than 1000 worldwide, of which nearly half occur in the geyser basins of Yellowstone National Park [*Rinehart*, 1980; *Bryan*, 2008]. Their rarity results from the delicate balance between water and heat supply required to generate episodic boiling events and the unique geometry of fractures and porous rocks required to focus liquid and steam into an eruptive fountain. Because of the uncommon balance between these controlling parameters, only a few geysers display relatively constant intervals

©2014. American Geophysical Union. All Rights Reserved.

between eruptions [e.g., *Hurwitz et al*., 2008, 2014]. Application of modern technology and data processing has significantly improved our understanding of the major factors that control the eruptions and their periodicity, and the relation between eruptions and the subsurface geometry of the geysers [*Hutchinson et al*., 1997; *Vandemeulebrouck et al*., 2013].

Using data acquired with a seismic array in 1992, *Kedar et al*. [1996] demonstrated that harmonic tremor at Old Faithful Geyser results from boiling and vapor-bubble cavitation in the geyser subsurface. Tremor intensity is related to conduit geometry and is controlled by the rate of occurrence of these impulsive events, which in turn is determined by the heat and mass input rate into the geyser. The absence of resonance within the water column suggests that the harmonic tremor stems from the interaction of the seismic waves with heterogeneities in the surrounding elastic medium [*Kedar et al*., 1996, 1998]. Reprocessing of the 1992 data using acoustic localization techniques depicted the spatial and temporal patterns of the seismic sources produced by boiling and cavitation in the geyser subsurface [*Vandemeulebrouck et al*., 2013]. The location of seismic sources defined a lateral reservoir on the SW side of the cone at a depth 15 m below the surface. This reservoir is activated at the beginning of each geyser eruption cycle and plays a major role in the oscillatory behavior of the water level in the conduit before each eruption.

Pressure and temperature measurements and video observations in the Old Faithful Geyser conduit [*Hutchinson et al*., 1997; *Kedar et al*., 1998] demonstrated that despite the relatively constant eruption frequency and duration, pressure and temperature time variations in the conduit result from complex recharge patterns, convection, splashing, and alternate episodes of one-phase (either steam or liquid) and two-phase flow. The conduit is a highly irregular, elongate fissure with silica sinter on the walls. It was proposed that across a constriction at a depth of 7 m, the flow is sonic, or choked (Mach 1 at 70 m/s) during the first ~30 s of eruptions [*Kieffer*, 1989]. More recently, discharge was measured with infrared and visible imaging, and particle image velocimetry (PIV) at Lone Star Geyser, 5 km to the southwest of Old Faithful. The measurements confirmed that parts of the eruptions at Lone Star are intermittently choked [*Karlstrom et al*., 2013]. Subsonic or supersonic flow downstream of the constriction largely depends on vent geometry, the sound speed of the liquid-steam mixture, and fluid overpressure upstream of the constriction.

Like geysers, historic and prehistoric hydrothermal explosion craters are located predominantly in liquid-dominated areas along the Firehole River geyser basins, in and around Yellowstone Lake, and in the southern part of the Norris-Mammoth Corridor. Numerous small sublacustrine explosion craters have also been identified within fissure zones in Yellowstone Lake by high-resolution imaging [*Johnson et al*., 2003; *Morgan et al*., 2003, 2009]. Several historic and prehistoric explosion craters and decaying geyser mounds are located within acid sulfate terrains that overlie vapor-dominated systems and currently discharge low-pH waters. Most of these explosion craters and geysers were formed before deepening of the water table and the transition from a hot water system to an acid sulfate system [*Fournier*, 1989]. Whereas geysers episodically discharge liquid water and steam into the atmosphere, hydrothermal explosions are discrete events that occur in response to a rapid reduction in confining pressure that causes water to flash to steam. The resulting two-phase mixture is highly compressible [*Grant and Sorey*, 1979], and the large pressures generated are sufficient to fracture the host rock, resulting in the ejection of steam, water, and rock [*Muffler et al*., 1971; *Browne and Lawless*, 2001; *Morgan et al*., 2009]. Thus, insights from predictable geyser eruptions may result in an improved understanding of hydrothermal explosions that have few if any premonitory signals.

Changes in geyser activity can lead to hydrothermal explosions. The small hydrothermal explosion at Porkchop Geyser in Norris Geyser Basin in September 1989 was preceded by gradual increase of inferred reservoir temperature by 60 to 70°C from 1962 through 1989, coincident with a transition from a quiescent spring with an intermittent seeping in the early 1960s, to infrequent geyser eruptions starting in 1971, perpetual spouting between 1985 and 1989, and geysering just before the explosion [*Fournier et al*., 1991]. Another documented example is a set of fractures emitting superheated steam that appeared in the Upper Geyser Basin immediately after the *M* 7.5 1959 Hebgen Lake earthquake. An explosion at this site in the spring of 1963 formed a crater with an area of 15 m^2, subsequently named Seismic Geyser [*Marler and White*, 1975].

Hydrothermal explosions are among the most significant hazards at Yellowstone [*Christiansen et al*., 2007; *Morgan et al*., 2009]. At least 20 large hydrothermal explosion craters with dimensions ranging between 100 and 2800 m in diameter, and numerous smaller craters have developed within the Yellowstone Caldera and along the Norris-Mammoth corridor over the past 16,000 years [*Morgan et al*., 2009]. Deposits from these

©2014. American Geophysical Union. All Rights Reserved.

explosions extend to distances that are greater than the diameters of their source craters. Rock fragments were ejected at least as far as 3.5 to 4 km from the Mary Bay crater rim ~13,600 years ago, and fragments from the Indian Pond explosion crater are found as far as 3 km from the vent [*Morgan et al*., 2009]. The large and quasi-circular explosion craters suggest large subsurface cavities that serve as reservoirs for pressure accumulation, such as the imaged Old Faithful reservoir [*Vandemeulebrouck et al*., 2013].

At least 26 small hydrothermal explosions have been documented in the historic record of the national park. These events include either the formation of a new crater, or significant enlargement of an existing crater by explosive excavation [*Christiansen et al*., 2007]. The largest historical hydrothermal explosions at Yellowstone occurred between 1881 and 1890 at Excelsior Geyser in the Midway Geyser Basin (Figure 1). In May 1888, blocks with a diameter of 0.3 m were ejected to more than 150 m from the crater. Excelsior erupted again for 2 days in 1985 [*Whittlesey*, 1990].

Based on the observation that the energy released by large explosions represents only a few weeks to months of the heat flow from the system, it was inferred that hydrothermal explosions should be relatively common events that do not require unusual conditions in long-lived geothermal areas [*Browne and Lawless*, 2001]. However, with the resolution of dating techniques, it appears that the large explosion craters (>1000 m in diameter) in Yellowstone were associated with periods of glacier retreat (Figure 4), decompression, and enhanced boiling, resulting in large pressure and phase changes in the hydrothermal system. If external forces do not exert a major control on hydrothermal explosions, it is estimated that an explosion creating a 100 m diameter crater occur in Yellowstone about once every 200 years [*Christiansen et al*., 2007].

8. Seasonal and Subannual Perturbation of the Hydrothermal System

Whereas enhanced hydrothermal activity and explosions were associated with glacial retreat [*Bargar and Fournier*, 1988] and likely occurred over centuries and millennia, the extreme seasonal variations and large volumes of snow melt and ice thaw in May and June result in significant modulation of hydrothermal activity [*Hurwitz et al*., 2007b, 2008, 2012b]. Statistical analysis of a 20 year seismic data set (1984–2003) revealed that earthquake occurrence in the shallow crust beneath Yellowstone Lake is correlated with the annual lake level cycles, with peak seismicity between September and October [*Christiansen et al*., 2005]. The load associated with the annual peak-to-peak water level variation is very small, ranging between 1 and 3 kPa, suggesting that the hydrothermal system underlying the lake is critically stressed.

Statistical analysis of continuous geyser-eruption-interval data collected over 4 years (2003–2006) demonstrated that eruption intervals of several geysers display an annual cycle. However, the seasonal patterns of the five studied geysers are not in phase and in some instances they are contrasting, implying that each of the geysers responds differently to the multiple processes controlling eruption intervals. The processes include evaporation, meteoric water recharge, water table elevation, and possible hydraulic interaction with the adjacent Firehole River [*Hurwitz et al*., 2008, 2012b]. It was also demonstrated that the amplitude of the seasonal eruption intervals of small-volume geysers are larger and more variable than those of geysers with larger volumes [*Hurwitz et al*., 2012b]. Geyser eruption intervals are not modulated by subannual, solid-earth tides or barometric pressures [*Rojstaczer et al*., 2003; *Hurwitz et al*., 2014]. However, eruption intervals of pool geysers are modulated by air-temperature variations and evaporation [*Hurwitz et al*., 2014].

There are abundant examples of changes in hydrothermal activity following local, regional, and global earthquakes. For example, following the *M* 7.3 1959 Hebgen Lake earthquake centered about 48 km northwest of Old Faithful, *Marler and White* [1975] wrote "By the day after the earthquake, at least 289 springs in the geyser basins of the Firehole River had erupted as geysers; of these, 160 were springs with no previous record of eruptions." The most significant changes to the eruption intervals of the iconic Old Faithful Geyser followed the August 1959, *M* 7.3 Hebgen Lake earthquake, the June 1975 *M* 6.1 Central Plateau earthquake along the Yellowstone Caldera northwest boundary, and the October 1983 *M* 6.9 Borah Peak Idaho earthquake [*Rinehart*, 1969; *Marler and White*, 1975; *Hutchinson*, 1985]. Following each of these three earthquakes, Old Faithful's annual average eruption interval gradually increased. Variations in hydrothermal activity can also occur in response to large global earthquakes thousands of kilometers away. Many studies over the past quarter of a century demonstrated that regions with an active hydrothermal system are more susceptible to seismicity that is triggered by the large amplitudes of surface waves originating from large global earthquakes [e.g., *Hill et al*., 1993; *Hill and Prejean*, 2007]. In Yellowstone, the eruption interval of several

©2014. American Geophysical Union. All Rights Reserved.

geysers changed following the 2002 *M* 7.9 Denali, Alaska, earthquake, more than 3000 km from Yellowstone, [*Husen et al*., 2004]. The most notable change was the immediate decrease of Daisy Geyser's eruption intervals from about 2 h and 50 min before the earthquake to about 1 h and 50 min about 12 h after the earthquake. The intervals then lengthened slowly and were similar to the pre-earthquake intervals after about 2 months. It was later proposed that geyser eruption intervals could vary in response to dynamic stresses induced by the surface waves that are at least 0.1 MPa [*Hurwitz et al*., 2014].

9. Suggestions for Future Research Directions

This review highlights the numerous advances made over the past quarter century in understanding Yellowstone's dynamic hydrothermal system. Reviewing these significant accomplishments also highlights some of the unresolved fundamental questions. Here we suggest some avenues for future research:

1. Multidisciplinary studies are needed to quantify the dynamic feedback between myriad tectonic, magmatic, and hydrothermal process and to establish "cause and effect" relationships. Multidisciplinary studies are also needed to link present-day hydrothermal activity with extreme climate fluctuations [e.g., *Gray et al*., 2007; *Whitlock et al*., 2012; *Krause and Whitlock*, 2013] that have shaped the YPVF since the last recession of glacial ice.
2. Develop and improve airborne and satellite-based remote sensing methods and associated software to allow for improved estimates of gas and heat flux at higher temporal and spatial resolution.
3. Add quantitative models that more accurately account for the thermodynamics of multiphase and multicomponent reactions and heat and mass transport to improve understanding of the processes controlling water and gas chemistry in the hydrothermal system.
4. Jointly invert different geophysical imaging methods (seismic, electric, and potential field) at high spatial resolution to provide a more robust characterization of the shallow subsurface in thermal basins and in the Yellowstone Caldera.
5. Better characterize and quantify the role of microbial activity in the geochemical cycle.
6. Analyze the chemical and isotopic composition of magmatic volatiles dissolved in silicate melt inclusions to constrain preeruptive dissolved volatile compositions in underlying magma.
7. Track the response of the hydrothermal system to external perturbations at multiple temporal and spatial scales to better predict the triggering and effects of hydrothermal explosions.

10. Concluding Remarks

A significant amount of information has been gathered over the past quarter of a century, mainly resulting from the application of modern technologies. The collective body of work during this period documented large changes at many different temporal and spatial scales and the coupling between physical, chemical, and biological processes. Thus, understanding of many processes operating in Yellowstone's dynamic hydrothermal system has substantially improved over the past quarter of the century since *Fournier* [1989] reviewed the state of knowledge at the time.

Answering the most fundamental question by the next generation of studies "what does the future hold for Yellowstone?" will largely depend on the ability to better resolve spatial and temporal patterns of heat and mass discharge, better characterize and quantify the spatial and temporal correlations between tectonic, magmatic, and climatic processes, and better link instrumental signals to source processes. Hopefully, addressing some of these issues will guide future research in Yellowstone and will improve current estimates of the various hazards posed by hydrothermal activity [*Christiansen et al*., 2007], provide a framework for understanding life in extreme environments, and guide the protection and preservation of the unique and diverse thermal features in Earth's first national park [*Heasler et al*., 2009].

Glossary

Ash flow tuff: deposits produced by a pyroclastic density flow. Though consolidated, welding is not required [*Neuendorf et al*., 2011].

Alteration: any change in the mineralogic composition of a rock brought about by physical or chemical means, especially by the action of hydrothermal solutions [*Neuendorf et al*., 2011].

©2014. American Geophysical Union. All Rights Reserved.

Brittle-ductile transition zone: the depth or zone at which rocks change from deforming by primarily brittle processes to deforming by primarily ductile processes. The transition depth depends upon temperature and composition of rocks [*Neuendorf et al*., 2011] as is usually thought to occur at 350°–400°C for quartz-rich rocks.

Caldera: a large, basin-shaped volcanic depression, more or less circular in form, the diameter of which is many times greater than that of any included vent or vents. It is formed by collapse during an eruption [*Neuendorf et al*., 2011].

Convection: in hydrothermal systems, the flow of waters around and through heated zones in response to thermal gradients and controlled by porosity-permeability, salinity, fluid viscosity, and allied factors [*Neuendorf et al*., 2011].

Frying pan: shallow, vigorously active bubbling or boiling hot springs, with agitation similar to the sizzling of hot grease in a frying pan.

Fumarole: a vent, usually volcanic, from which gases and vapors are emitted [*Neuendorf et al*., 2011].

Geyser: a type of hot spring that intermittently erupts jets of hot liquid water and steam [*Neuendorf et al*., 2011].

Hydrothermal: of or pertaining to hot water, to the action of hot water, or to the products of this action, such as a mineral deposit precipitated from a hot aqueous solution, with or without demonstrable association with igneous processes [*Neuendorf et al*., 2011].

Hydrothermal explosions: violent and dramatic events resulting in the rapid ejection of boiling water, steam, mud, and rock fragments from source craters that range from a few meters up to more than 2 km in diameter. Hydrothermal explosions occur where shallow interconnected reservoirs of steam and liquid with temperatures, at or near the boiling curve, underlie thermal fields. Sudden reduction in confining pressure causes fluids to flash to steam, resulting in significant expansion, rock fragmentation, and debris ejection [*Morgan et al*., 2009].

Hydrothermal system: a groundwater system that has a source (or area) of recharge, a source (or area) of discharge, and a heat source [*Neuendorf et al*., 2011].

Immiscible: the property where two substances are not capable of combining to form a homogeneous mixture. Often used in igneous and hydrothermal systems for situations where sulfide, saline, silicate, and other liquids coexist without mixing.

Magmatic volatile: an element or a compound such as H_2O or CO_2 that forms a gas at relatively low pressure and magmatic temperature. Volatiles can be dissolved in silicate melts, can occur as bubbles of exsolved gas, and can crystallize in minerals [*Wallace and Anderson*, 1999].

Mud pot: a hot spring with fine clay mud, usually having no discharge.

Oxyanion: a group of atoms consisting of three or four anions (usually oxygen) surrounding a central cation and having an overall negative charge [*Neuendorf et al*., 2011].

Rhyolite: a light-colored rock with silica (SiO_2) content greater than about 68 wt %. Sodium and potassium oxides both can reach about 5 wt %. Common mineral types include quartz, feldspar, and biotite and are often found in a glassy matrix. Rhyolite is erupted at temperatures of 700 to 850°C.

Siliceous sinter: the lightweight porous opaline variety of silica, white or nearly white, deposited as an incrustation by precipitation from the waters of geysers and hot springs. The term has been applied loosely to any deposit made by a geyser or hot spring [*Neuendorf et al*., 2011].

Travertine: biotically and/or abiotically precipitated calcium carbonate (predominantly calcite and aragonite) from spring-fed, heated, and/or ambient-temperature waters [*Neuendorf et al*., 2011].

Acknowledgments
We thank Cindy Werner for her help with revising the CO_2 flux calculations, David Shelly, Greg Waite, and Cindy Werner for providing figures and Lee Whittlesey for providing valuable historic information. Much of the work presented in this review results from work carried out by colleagues at the USGS, the Yellowstone Center for Resources, the University of Utah, and many academic and research institutes. Olivier Bachmann, Giovanni Chiodini, Bill Evans, Fabio Florindo (Journal Editor), Mark Moldwin (Journal Editor-in-Chief), Fred Murphy, and Kirk Nordstrom provided constructive reviews and comments. This study was supported by the U.S. Geological Survey Volcano Hazards Program.

References

Allen, E. T., and A. L. Day (1935), *Hot Springs of the Yellowstone National Park*, *Carnegie Inst. Washington Publ*., vol. 466, 525 pp., Carnegie Institute, Troy, Mich.

Aly, M. H., and E. S. Cochran (2011), Spatio-temporal evolution of Yellowstone deformation between 1992 and 2009 from InSAR and GPS observations, *Bull. Volcanol*., *73*, 1407–1419, doi:10.1007/s00445-011-0483-y.

Bachmann, O., and G. W. Bergantz (2006), Gas percolation in upper-crustal silicic crystal mushes as a mechanism for upward heat advection and rejuvenation of near-solidus magma bodies, *J. Volcanol. Geotherm. Res*., *149*, 85–102, doi:10.1016/j.jvolgeores.2005.06.002.

Bailey, R. C. (1990), Trapping of aqueous fluids in the deep crust, *Geophys. Res. Letters*, *17*, 1129–1132, doi:10.1029/GL017i008p01129.

Balistrieri, L., W. C. Shanks III, R. L. Cuhel, C. Aguilar, and J. V. Klump (2007), The influence of sublacustrine hydrothermal vent fluids on the geochemistry of Yellowstone Lake, in *Integrated Geoscience Studies in the Greater Yellowstone Area: Volcanic, Hydrothermal and Tectonic Processes in the Yellowstone Geoecosystem*, *U. S. Geol. Surv. Prof. Pap*., vol. 1717, edited by L. A. Morgan, pp. 170–199.

©2014. American Geophysical Union. All Rights Reserved.

Ball, J. W., D. K. Nordstrom, E. A. Jenne, and D. V. Vivit (1998), Chemical analyses of hot springs, pools, geysers, and surface waters from Yellowstone National Park, Wyoming, and vicinity, 1974-1975, *U.S. Geol. Surv. Open File Rep., 98–182*, 45 pp.

Ball, J. W., R. B. McCleskey, D. K. Nordstrom, J. M. Holloway, and P. L. Verplanck (2002), Water-chemistry data for selected springs, geysers, and streams in Yellowstone National Park, Wyoming, 1999–2000 *U.S. Geol. Surv. Open File Rep., 02-382*, 112 pp.

Ball, J. W., R. B. McCleskey, D. K. Nordstrom, and J. M. Holloway (2007), Water-chemistry data for selected springs, geysers, and streams in Yellowstone National Park, Wyoming, 2003–2005, *U.S. Geol. Surv. Open File Rep., 2006-1339*, 183 pp. [Available at http://pubs.usgs.gov/of/2006/1339/.]

Ball, J. W., R. B. McCleskey, and D. K. Nordstrom (2010), Water-chemistry data for selected springs, geysers, and streams in Yellowstone National Park, Wyoming, 2006–2008, *U.S. Geol. Surv. Open File Rep., 2010-1192*, 84 pp. [Available at http://pubs.usgs.gov/of/2010/1192/.]

Bargar, K. E., and R. O. Fournier (1988), Effects of glacial ice on subsurface temperatures of hydrothermal systems in Yellowstone National Park, Wyoming: Fluid-inclusion evidence, *Geology*, *16*, 1077–1080, doi:10.1130/0091-7613(1988)016<1077:EOGIOS>2.3.CO;2.

Barns, S. M., R. E. Fundyga, M. W. Jeffries, and N. R. Pace (1994), Remarkable archaeal diversity detected in a Yellowstone National Park hot spring environment, *Proc. Natl. Acad. Sci. U.S.A.*, *91*, 1609–1613, doi:10.1073/pnas.91.5.1609.

Bergfeld, D., J. B. Lowenstern, A. G. Hunt, W. C. P. Shanks III, and W. C. Evans (2011), Gas and isotope chemistry of thermal features in Yellowstone National Park, Wyoming, *U.S. Geol. Surv. Sci. Invest. Rep., 2011-5012*, 26 pp. [Available at http://pubs.usgs.gov/sir/2011/5012/].

Bergfeld, D., W. C. Evans, J. B. Lowenstern, and S. Hurwitz (2012), Carbon dioxide and hydrogen sulfide degassing and cryptic thermal input to Brimstone Basin, Yellowstone National Park, Wyoming, *Chem. Geol.*, *330-331*, 233–243, doi:10.1016/j.chemgeo.2012.09.001.

Bischoff, J. L., and R. J. Rosenbauer (1996), The alteration of rhyolite in CO_2 charged water at 200 and 350°C: The unreactivity of CO_2 at higher temperature, *Geochim. Cosmochim. Acta*, *60*, 3859–3867, doi:10.1016/0016-7037(96)00208-6.

Blackwell, D. D., and M. C. Richards (2004), The 2004 geothermal map of North America explanation of resources and applications, *Trans. Geotherm. Resour. Coun.*, *28*, 317–320.

Blank, C. E., S. L. Cady, and N. R. Pace (2002), Microbial composition of near-boiling silica-depositing thermal springs throughout Yellowstone National Park, *Appl. Environ. Microbiol.*, *68*, 5123–5135, doi:10.1128/AEM.68.10.5123-5135.2002.

Blank, J. G., E. M. Stolper, and M. R. Carroll (1993), Solubilities of carbon dioxide and water in rhyolitic melt at 850°C and 750 bars, *Earth Planet. Sci. Lett.*, *119*, 27–36, doi:10.1016/0012-821X(93)90004-S.

Bouligand, C., J. M. G. Glen, and R. J. Blakely (2014), Distribution of buried hydrothermal alteration deduced from high resolution magnetic surveys in Yellowstone National Park, *J. Geophys. Res. Solid Earth*, *119*, 2595–2630, doi:10.1002/2013JB010802.

Boyd, E. S., S. King, J. K. Tomberlin, D. K. Nordstrom, D. P. Krabbenhoft, T. Barkay, and G. G. Geesey (2009), Methylmercury enters an aquatic food web through acidophilic microbial mats in Yellowstone National Park, Wyoming, *Environ. Microbiol.*, *11*(4), 950–959, doi:10.1111/j.1462-2920.2008.01820.x.

Braunstein, D., and D. R. Lowe (2001), Relationship between spring and geyser activity and the deposition and morphology of high temperature (>73°C) siliceous sinter, Yellowstone National Park, Wyoming, USA, *J. Sed. Res.*, *71*, 747–763, doi:10.1306/2DC40965-0E47-11D7-8643000102C1865D.

Brock, T. D. (1978), *Thermophilic Microorganisms and Life at High Temperatures*, 465 pp, doi:10.1007/978-1-4612-6284-8, Springer-Verlag, New York.

Brock, T. D. (1985), Life at high temperatures, *Science*, *158*, 1012–1019, doi:10.1126/science.230.4722.132.

Browne, P. R. L., and J. V. Lawless (2001), Characteristics of hydrothermal eruptions, with examples from New Zealand and elsewhere, *Earth Sci. Rev.*, *52*, 299–331, doi:10.1016/S0012-8252(00)00030-1.

Bryan, T. S. (2008), *The Geysers of Yellowstone Fourth Edition*, Univ. Press of Colorado, Boulder, Colo.

Caliro, S., G. Chiodini, and A. Paonita (2014), Geochemical evidences of magma dynamics at Campi Flegrei (Italy), *Geochim. Cosmochim. Acta*, doi:10.1016/j.gca.2014.01.021.

Carroll, M. R., and J. D. Webster (1994), Solubilities of sulfur, noble gases, nitrogen, chlorine, and fluorine in magmas, *Rev. Mineral. Geochem.*, *30*, 231–279.

Chafetz, H. S., and S. A. Guidry (2003), Deposition and diagenesis of Mammoth Hot Springs travertine, Yellowstone National Park, Wyoming, USA, *Canad. J. Earth Sci.*, *40*, 1515–1529, doi:10.1139/e03-051.

Chaffee, M. A., W. C. Shanks III, R. O. Rye, C. C. Shwartz, M. G. Adams, R. R. Carlson, and S. R. Podruzny (2007), Applications of trace-element and stable-isotope geochemistry to wildlife issues, Yellowstone National Park and vicinity, in *Integrated Geoscience Studies in the Greater Yellowstone Area: Volcanic, Hydrothermal and Tectonic Processes in the Yellowstone Geoecosystem*, *U. S. Geol. Surv. Prof. Pap.*, vol. 1717, edited by L. A. Morgan, pp. 300–334.

Chang, W.-L., R. B. Smith, C. Wicks, J. M. Farrell, and C. M. Puskas (2007), Accelerated uplift and magmatic intrusion of the Yellowstone Caldera, 2004 to 2006, *Science*, *318*, 952–956, doi:10.1126/science.1146842.

Chang, W.-L., R. B. Smith, J. M. Farrell, and C. M. Puskas (2010), An extraordinary episode of Yellowstone Caldera uplift, 2004–2010, from GPS and InSAR observations, *Geophys. Res. Lett.*, *37*, L23302, doi:10.1029/2010GL045451.

Channing, A., and I. B. Butler (2007), Cryogenic opal-A deposition from Yellowstone hot springs, *Earth Planet. Sci. Lett.*, *257*, 121–131, doi:10.1016/j.epsl.2007.02.026.

Chiodini, G., and L. Marini (1998), Hydrothermal gas equilibria: The H_2O–H_2–CO_2–CO–CH_4 system, *Geochim. Cosmochim. Acta*, *62*, 2673–2687, doi:10.1016/S0016-7037(98)00181-1.

Chiodini, G., M. Todesco, S. Caliro, C. Del Gaudio, G. Macedonio, and M. Russo (2003), Magma degassing as a trigger of bradyseismic events: The case of Phlegrean Fields (Italy), *Geophys. Res. Lett.*, *30*(8), 1434, doi:10.1029/2002GL016790.

Chiodini, G., S. Caliro, P. De Martino, R. Avino, and F. Gherardi (2012a), Early signals of new volcanic unrest at Campi Flegrei caldera? Insights from geochemical data and physical simulations, *Geology*, *40*, 943–946, doi:10.1130/G33251.1.

Chiodini, G., S. Caliro, J. B. Lowenstern, W. C. Evans, D. Bergfeld, F. Tassi, and D. Tedesco (2012b), Insights from fumarole gas geochemistry on the origin of hydrothermal fluids on the Yellowstone Plateau, *Geochim. Cosmochim. Acta*, *89*, 265–278, doi:10.1016/j.gca.2012.04.051.

Christiansen, L. B., S. Hurwitz, M. O. Saar, S. E. Ingebritsen, and P. A. Hsieh (2005), Seasonal seismicity at western United States volcanic centers, *Earth Planet. Sci. Lett.*, *240*, 307–321, doi:10.1016/j.epsl.2005.09.012.

Christiansen, R. L. (2001), The Quaternary and Pliocene Yellowstone Plateau volcanic field of Wyoming, Idaho, and Montana, *U.S. Geol. Surv. Prof. Pap.*, *729-G*, 145 pp.

Christiansen, R. L., J. B. Lowenstern, R. B. Smith, H. Heasler, L. A. Morgan, M. Nathenson, L. G. Mastin, L. J. P. Muffler, and J. E. Robinson (2007), Preliminary assessment of volcanic and hydrothermal hazards in Yellowstone National Park and vicinity, *U.S. Geol. Surve. Open File Rep., 2007-1071*, 94 pp. [Available at http://pubs.usgs.gov/of/2007/1071/.]

Chu, R., D. V. Helmberger, D. Sun, J. M. Jackson, and L. Zhu (2010), Mushy magma beneath Yellowstone, *Geophys. Res. Lett.*, *37*, L01306, doi:10.1029/2009GL041656.

 ©2014. American Geophysical Union. All Rights Reserved.

Clifton, C. G., C. C. Walters, and B. R. T. Simoneit (1990), Hydrothermal petroleums from Yellowstone National Park, Wyoming, U.S.A, *Appl. Geochem.*, *5*, 169–191, doi:10.1016/0883-2927(90)90047-9.

Clingenpeel, S., et al. (2011), Yellowstone Lake: high-energy geochemistry and rich bacterial diversity, *Environ. Microbiol.*, doi:10.1111/j.1462-2920.2011.02466.x.

Clor, L. E., R. B. McCleskey, M. A. Huebner, J. B. Lowenstern, H. P. Heasler, D. L. Mahony, T. Moloney, and W. C. Evans (2012), *Water Chemistry and Electrical Conductivity Database for Rivers in Yellowstone National Park, Wyoming*, *U.S. Geol. Surv. Data Series* 632, 18 pp. [Available at http://pubs.usgs.gov/ds/632/.]

Cox, A., E. L. Shock, and J. R. Havig (2011), The transition to microbial photosynthesis in hot spring ecosystems, *Chem. Geol.*, *280*, 344–351, doi:10.1016/j.chemgeo.2010.11.022.

Cox, S. F. (2005), Coupling between deformation, fluid pressures and fluid flow in ore-producing hydrothermal environments, edited by J. W. Hedenquist et al., *Econ. Geol.* pp. 39–75.

Craig, H., G. Boato, and D. E. White (1956), Isotope geochemistry of thermal waters: National Academy of Sciences, *Nat. Res. Council Pub.*, *19*, 29–39.

Cuhel, R. L., C. Aguilar, P. D. Anderson, J. S. Maki, R. W. Paddock, C. C. Remsen, J. V. Klump, and D. Lovalvo (2002), Underwater domains in Yellowstone Lake: Hydrothermal vent geochemistry and bacterial chemosynthesis, in *Yellowstone Lake: Hotbed of Chaos or Reservoir of Resilience. Yellowstone National Park*, proceedings of the 6th Biennial Scientific Conference, edited by R. J. Anderson and D. Harmon, pp. 27–53, Yellowstone Center for Resources and the George Wright Society, Yellowstone National Park, WY.

D'Imperio, S., C. R. Lehr, H. Oduro, G. Druschel, M. Kuhl, and T. R. McDermott (2008), Relative importance of H_2 and H_2S as energy sources for primary production in geothermal springs, *Appl. Environ. Microb.*, *74*, 5802–5808, doi:10.1128/AEM.00852-08.

Deng, Y., D. K. Nordstrom, and R. B. McCleskey (2011), Fluoride geochemistry of thermal waters in Yellowstone National Park: I. Aqueous fluoride speciation, *Geochim. Cosmochim. Acta*, *75*, 4476–4489, doi:10.1016/j.gca.2011.05.028.

Dingwell, D. B. (1997), The brittle–ductile transition in high-level granitic magmas: Material constraints, *J. Petrol.*, *38*, 1635–1644, doi:10.1093/petroj/38.12.1635.

Dobson, P. F., T. J. Kneafsey, J. Hulen, and A. Simmons (2003), Porosity, permeability, and fluid flow in the Yellowstone geothermal system, Wyoming, *J. Volcanol. Geotherm. Res.*, *123*, 313–324, doi:10.1016/S0377-0273(03)00039-8.

Donahoe-Christiansen, J., S. D'Imperio, C. R. Jackson, W. P. Inskeep, and T. R. McDermott (2004), Arsenite-oxidizing *Hydrogenobaculum* strain isolated from an acid-sulfate-chloride geothermal spring in Yellowstone National Park, *Appl. Environ. Microbiol.*, *70*, 1865–1868, doi:10.1128/AEM.70.3.1865-1868.2004.

Dort, W. (1966), Rapid reconnaissance of heat-flow patterns in snow-covered thermal areas, *J. Geophys. Res.*, *71*, 4439–4440, doi:10.1029/JZ071i018p04439.

Dzurisin, D., and K. M. Yamashita (1987), Vertical surface displacements at Yellowstone Caldera, Wyoming, 1976–1986, *J. Geophys. Res.*, *92*, 13,753–13,766, doi:10.1029/JB092iB13p13753.

Dzurisin, D., J. C. Savage, and R. O. Fournier (1990), Recent crustal subsidence at Yellowstone Caldera, Wyoming, *Bull. Volcanol.*, *52*, 247–270, doi:10.1007/BF00304098.

Dzurisin, D., C. J. Wicks Jr., and W. Thatcher (1999), Renewed uplift at the Yellowstone Caldera measured by leveling surveys and satellite radar interferometry, *Bull. Volcanol.*, *61*, 349–355, doi:10.1007/s004450050277.

Dzurisin, D., C. W. Wicks Jr., and M. P. Poland (2012), History of surface displacements at the Yellowstone Caldera, Wyoming, from leveling surveys and InSAR observations, 1923–2008, *U.S. Geol. Surv. Prof. Pap. 1788*, 68 pp. [Available at http://pubs.usgs.gov/pp/1788/.]

Ellis, A. J., and W. A. J. Mahon (1964), Natural hydrothermal systems and experimental hot water/rock interactions, *Geochim. Cosmochim. Acta*, *28*, 1323–1357, doi:10.1016/0016-7037(64)90132-2.

Ellis, A. J., and W. A. J. Mahon (1977), *Chemistry and Geothermal Systems*, 392 pp., Academic Press, New York.

Evans, B., J. T. Fredrich, and T. F. Wong (1990), The brittle-ductile transition in rocks: Recent experimental and theoretical progress, in *The Brittle-Ductile Transition in Rocks*, *Geophys. Monogr. Ser.*, vol. 56, edited by A. G. Duba et al., pp. 1–20, AGU, Washington, D. C., doi:10.1029/GM056p0001.

Evans, W. C., D. Bergfeld, M. C. van Soest, M. A. Huebner, J. Fitzpatrick, and K. M. Revesz (2006), Geochemistry of low-temperature springs northwest of Yellowstone Caldera: Seeking the link between seismicity, deformation, and fluid flow, *J. Volcanol. Geotherm. Res.*, *154*, 169–180, doi:10.1016/j.jvolgeores.2006.01.001.

Evans, W. C., D. Bergfeld, J. P. McGeehin, J. C. King, and H. Heasler (2010), Tree-ring ^{14}C links seismic swarm to CO_2 spike at Yellowstone, USA, *Geology*, *38*, 1075–1078, doi:10.1130/G31345.1.

Farrell, J., S. Husen, and R. B. Smith (2009), Earthquake swarm and b-value characterization of the Yellowstone volcano-tectonic system, *J. Volcanol. Geotherm. Res.*, *188*, 260–276, doi:10.1016/j.jvolgeores.2009.08.008.

Farrell, J., R. B. Smith, T. Taira, W.-L. Chang, and C. M. Puskas (2010), Dynamics and rapid migration of the energetic 2008–2009 Yellowstone Lake earthquake swarm, *Geophys. Res. Lett.*, *37*, L19305, doi:10.1029/2010GL044605.

Farrell, J., R. B. Smith, S. Husen, and T. Diehl (2014), Tomography from twenty-six years of seismicity reveals the spatial extent of the Yellowstone crustal magma reservoir extends well beyond the Yellowstone Caldera, *Geophys. Res. Lett.*, *41*, 3068–3073, doi:10.1002/2014GL059588.

Finn, C. A., and L. A. Morgan (2002), High-resolution aeromagnetic mapping of volcanic terrain, Yellowstone National Park, *J. Volcanol. Geotherm. Res.*, *115*, 207–231, doi:10.1016/S0377-0273(01)00317-1.

Foley, D. (2006), Dating Castle Geyser: Preliminary results and broad speculations on the geologic development of geysers and hydrothermal systems in Yellowstone National Park, Wyoming, USA, *GRC Transactions*, *30*, 413–417.

Fouke, B. W. (2011), Hot-spring systems geobiology: Abiotic and biotic influences on travertine formation at Mammoth Hot Springs, Yellowstone National Park, USA, *Sedimentology*, *58*, 170–219, doi:10.1111/j.1365-3091.2010.01209.x.

Fouke, B. W., J. D. Farmer, D. J. Des Marais, L. Pratt, N. C. Sturchio, P. C. Burns, and M. K. Discipulo (2000), Depositional facies and aqueous-solid geochemistry of travertine-depositing hot springs (Angel Terrace, Mammoth Hot Springs, Yellowstone National Park, USA), *J. Sediment. Res.*, *70*, 565–585, doi:10.1306/2DC40929-0E47-11D7-8643000102C1865D.

Fournier, R. O. (1979), Geochemical and hydrologic considerations and the use of enthalpy-chloride diagrams in the prediction of underground conditions in hot-spring systems, *J. Volcanol. Geotherm. Res.*, *5*, 1–16, doi:10.1016/0377-0273(79)90029-5.

Fournier, R. O. (1981), Application of water geochemistry to geothermal exploration and reservoir engineering, in *Geothermal Systems: Principles and Case Histories*, edited by L. Ryback and L. J. P. Muffler, pp. 109–143, John Wiley, New York.

Fournier, R. O. (1985), The behavior of silica in hydrothermal solutions, in *Geology and Geochemistry of Epithermal Systems*, *Rev. Econ. Geol.*, vol. 2, edited by B. R. Berger and P. M. Bethke, pp. 45–61, Society of Economic Geologists.

Fournier, R. O. (1989), Geochemistry and dynamics of the Yellowstone National Park hydrothermal system, *Ann. Rev. Earth Planet. Sci.*, *17*, 13–53, doi:10.1146/annurev.ea.17.050189.000305.

 ©2014. American Geophysical Union. All Rights Reserved.

Fournier, R. O. (1991), The transition from hydrostatic to greater than hydrostatic fluid pressure in presently active continental hydrothermal systems in crystalline rock, *Geophys. Res. Lett.*, *18*, 9555–958, doi:10.1029/91GL00966.

Fournier, R. O. (1999), Hydrothermal processes related to movement of fluid from plastic into brittle rock in the magmatic-epithermal environment, *Econ. Geol.*, *94*, 1193–1211, doi:10.2113/gsecongeo.94.8.1193.

Fournier, R. O. (2004), Yellowstone Caldera inflation-deflation and hydrothermal Cl flux revisited, in *Proceedings of the Eleventh International Symposium on Water-Rock Interaction*, edited by R. B. Wanty and R. R. Seal II, pp. 53–58, A.A. Balkema, New York.

Fournier, R. O., and R. Potter (1982), An equation correlating the solubility of quartz in water from 25° to 900°C at pressures up to 10,000 bars, *Geochim. Cosmochim. Acta*, *46*, 1969–1973, doi:10.1016/0016-7037(82)90135-1.

Fournier, R. O., D. E. White, and A. H. Truesdell (1976), Convective heat flow in Yellowstone National Park, in *Proceedings of the Second U.N. Symposium on the Development and Use of Geothermal Resources*, pp. 731–739, U.S. Energy Res. and Dev. Admin., Washington, D. C.

Fournier, R. O., J. M. Thompson, C. G. Cunningham, and R. A. Hutchinson (1991), Conditions leading to a recent small hydrothermal explosion at Yellowstone National Park, *Geol. Soc. Amer. Bull.*, *103*, 1114–1120, doi:10.1130/0016-7606(1991)103<1114:CLTARS>2.3.CO;2.

Fournier, R. O., J. M. Thompson, and R. A. Hutchinson (1992), The geochemistry of hot spring waters at Norris Geyser Basin, Yellowstone National Park, USA, in *Proceedings of the Seventh International Symposium on Water-Rock Interaction*, edited by Y. K. Kharaka and A. S. Maest, pp. 1289–1292, Balkema, New York.

Fournier, R. O., B. M. Kennedy, M. Aoki, and J. M. Thompson (1994), Correlation of gold in siliceous sinters with ^{3}He ^{4}He in hot spring waters of Yellowstone National Park, *Geochim. Cosmochim. Acta*, *58*, 5401–5419, doi:10.1016/0016-7037(94)90238-0.

Fournier, R. O., U. Weltman, D. Counce, L. D. White, and C. J. Janik (2002), Results of weekly chemical and isotopic monitoring of selected springs in Norris Geyser Basin, Yellowstone National Park during June–September, 1995, *U.S. Geol. Surv. Open File Rep., 02-344*. [Available at http://pubs.er.usgs.gov/publication/ofr02344.]

Friedman, I., and D. R. Norton (1990), Anomalous chloride flux discharges from Yellowstone National Park, *J. Volcanol. Geotherm. Res.*, *42*, 225–234, doi:10.1016/0377-0273(90)90001-V.

Friedman, I., and D. R. Norton (2007), Is Yellowstone losing its steam? Chloride flux out of Yellowstone National Park, in *Integrated Geoscience Studies in the Greater Yellowstone Area: Volcanic, Hydrothermal and Tectonic Processes in the Yellowstone Geoecosystem*, *U. S. Geol. Surv. Prof. Pap., 1717*, edited by L. A. Morgan, pp. 275–297.

Gaillardet, J., B. Dupré, P. Louvat, and C. J. Allègre (1999), Global silicate weathering and CO_2 consumption rates deduced from the chemistry of large rivers, *Chem. Geol.*, *159*, 3–30, doi:10.1016/S0009-2541(99)00031-5.

Gansecki, C. A., G. A. Mahood, and M. O. McWilliams (1996), $^{40}Ar/^{39}Ar$ geochronology of rhyolites erupted following collapse of the Yellowstone Caldera, Yellowstone Plateau volcanic field: Implications for crustal contamination, *Earth Planet. Sci. Lett.*, *142*, 91–107, doi:10.1016/0012-821X(96)00088-X.

Gardner, W. P., D. D. Susong, D. K. Solomon, and H. P. Heasler (2010a), Using noble gases measured in spring discharge to trace hydrothermal processes in the Norris Geyser Basin, Yellowstone National Park, U.S.A., *J. Volcanol. Geotherm. Res.*, *198*, 394–404, doi:10.1016/j.jvolgeores.2010.09.020.

Gardner, W. P., D. D. Susong, D. K. Solomon, and H. P. Heasler (2010b), Snowmelt hydrograph interpretation: Revealing watershed scale hydrologic characteristics of the Yellowstone volcanic plateau, *J. Hydrol.*, *383*, 209–222, doi:10.1016/j.jvolgeores.2010.09.020.

Gardner, W. P., D. D. Susong, D. K. Solomon, and H. P. Heasler (2011), A multitracer approach for characterizing interactions between shallow groundwater and the hydrothermal system in the Norris Geyser Basin area, Yellowstone National Park, *Geochem. Geophys. Geosys.*, *12*, Q08005, doi:10.1029/2010GC003353.

Gemery-Hill, P., W. C. P. Shanks III, L. S. Balistrieri, and G. K. Lee (2007), Geochemical Data for selected rivers, lake waters, hydrothermal vents and sub-aerial geysers in Yellowstone National Park, Wyoming, and vicinity, 1996–2004, in *Integrated Geoscience Studies in the Greater Yellowstone Area: Volcanic, Hydrothermal and Tectonic Processes in the Yellowstone Geoecosystem*, *U. S. Geol. Surv. Prof. Pap., 1717*, edited by L. A. Morgan, pp. 365–426.

Gibson, M. L., and N. W. Hinman (2013), Mixing of hydrothermal water and groundwater near hot springs, Yellowstone National Park (USA): Hydrology and geochemistry, *Hydrogeol. J.*, *21*, 919–933, doi:10.1007/s10040-013-0965-4.

Giggenbach, W. F. (1988), Geothermal solute equilibria. Derivation of Na-K-Mg-Ca geoindicators, *Geochim. Cosmochim. Acta*, *52*, 2749–2765.

Giggenbach, W. F. (1997), The origin and evolution of fluids in magmatic-hydrothermal systems, in *Geochemistry of Hydrothermal Ore Deposits 3rd Edition*, edited by H. L. Barnes, pp. 737–796, John Wiley, New York.

Gooch, F. A., and J. E. Whitfield (1888), Analyses of waters of the Yellowstone National Park, with an account of the methods of analysis employed, *U.S. Geol. Surv. Bull. 47*. 84 pp.

Grant, M. A., and M. L. Sorey (1979), The compressibility and hydraulic diffusivity of a water steam flow, *Water Resour. Res.*, *15*, 684–686, doi:10.1029/WR015i003p00684.

Gray, S. T., L. J. Graumlich, and J. L. Betancourt (2007), Annual precipitation in the Yellowstone National Park region since AD 1173, *Quarter. Res.*, *68*, 18–27, doi:10.1016/j.yqres.2007.02.002.

Guidry, S. A., and H. S. Chafetz (2002), Factors governing subaqueous siliceous sinter precipitation in hot springs: Examples from Yellowstone National Park, USA, *Sedimentology*, *49*, 1253–1267, doi:10.1046/j.1365-3091.2002.00494.x.

Guidry, S. A., and H. S. Chafetz (2003), Anatomy of siliceous hot springs: Examples from Yellowstone National Park, Wyoming, USA, *Sed. Geol.*, *157*, 71–106, doi:10.1016/S0037-0738(02)00195-1.

Hall, B. D., M. L. Olson, A. P. Rutter, R. R. Frontiera, D. P. Krabbenhoft, D. S. Gross, M. Yuen, T. M. Rudolph, and J. J. Schauer (2006), Atmospheric mercury speciation in Yellowstone National Park, *Sci. Total Environ.*, *367*, 354–366, doi:10.1016/j.scitotenv.2005.12.007.

Hamamura, N., R. E. Macur, S. Korf, G. Ackerman, W. P. Taylor, M. Kozubal, A.-L. Reysenbach, and W. P. Inskeep (2009), Linking microbial oxidation of arsenic with detection and phylogenetic analysis of arsenite oxidase genes in diverse geothermal environments, *Environ. Microbiol.*, *11*, 421–431, doi:10.1111/j.1462-2920.2008.01781.x.

Hamilton, T. L., R. K. Lange, E. S. Boyd, and J. W. Peters (2011), Biological nitrogen fixation in acidic high-temperature geothermal springs in Yellowstone National Park, Wyoming, *Environ. Microbiol.*, *13*, 2204–2215, doi:10.1111/j.1462-2920.2011.02475.x.

Hamilton, T. L., K. Vogl, D. A. Bryant, E. S. Boyd, and J. W. Peters (2012), Environmental constraints defining the distribution, composition, and evolution of chlorophototrophs in thermal features of Yellowstone National Park, *Geobiology*, *10*, 236–249, doi:10.1111/j.1472-4669.2011.00296.x.

Havig, J. R., J. Raymond, D. A. R. Meyer-Dombard, N. Zolotova, and E. L. Shock (2011), Merging isotopes and community genomics in a siliceous sinter-depositing hot spring, *J. Geophys. Res.*, *116*, G01005, doi:10.1029/2010JG001415.

Hayden, V. F. (1883), A report of progress of the exploration in Wyoming and Idaho for the year 1878. *U.S. Geology and Geography Survey of the Territories*, *12th Annual Report*, *part II*, p. 503.

Hearn, E. H., B. M. Kennedy, and A. H. Truesdell (1990), Coupled variations in helium isotopes and fluid chemistry: Shoshone Geyser Basin, Yellowstone National Park, *Geochim. Cosmochim. Acta*, *54*, 3103–3113, doi:10.1016/0016-7037(90)90126-6.

 ©2014. American Geophysical Union. All Rights Reserved.

Heasler, H. P., C. Jaworowski, and D. Foley (2009), Geothermal systems and monitoring hydrothermal features, in *Geological Monitoring*, edited by R. Young and L. Norby, pp. 105–140, Special Paper of the Geol. Soc. Am., doi:10.1130/2009.monitoring(05).

Hellman, M. J., and M. S. Ramsey (2004), Analysis of hot springs and associated deposits in Yellowstone National Park using ASTER and AVIRIS remote sensing, *J. Volcanol. Geotherm. Res.*, *135*, 195–219, doi:10.1016/j.jvolgeores.2003.12.012.

Hildreth, W., A. N. Halliday, and R. L. Christiansen (1991), Isotopic and chemical evidence concerning the genesis and contamination of basaltic and rhyolitic magma beneath the Yellowstone Plateau volcanic field, *J. Petrol.*, *32*, 63–138, doi:10.1093/petrology/32.1.63.

Hill, D. P. (1977), A model for earthquake swarms, *J. Geophys. Res.*, *82*, 1347–1352, doi:10.1029/JB082i008p01347.

Hill, D. P., and S. G. Prejean (2007), Dynamic triggering, in *Treatise on Geophysics*, vol. 4, edited by G. Schubert, pp. 257–291, doi:10.1016/B978-044452748-6.00070-5.

Hill, D. P., et al. (1993), Seismicity in the western United States remotely triggered by the M 7.4 Landers, California, earthquake of June 28, 1992, *Science*, *260*, 1617–1623, doi:10.1126/science.260.5114.1617.

Hinman, N. W., and R. F. Lindstrom (1996), Seasonal changes in silica deposition in hot spring systems, *Chem. Geol.*, *132*, 237–246, doi:10.1016/S0009-2541(96)00060-5.

Hirth, G., and J. Tullis (1994), The brittle-plastic transition in experimentally deformed quartz aggregates, *J. Geophys. Res.*, *99*, 11,731–11,747, doi:10.1029/93JB02873.

Hochstein, M. P., and C. J. Bromley (2005), Measurement of heat flux from steaming ground, *Geothermics*, *34*, 133–160, doi:10.1016/j.geothermics.2004.04.002.

Holloway, J. M., D. K. Nordstrom, J. K. Böhlke, R. B. McCleskey, and J. W. Ball (2011), Ammonium in thermal waters of Yellowstone National Park: Processes affecting speciation and isotope fractionation, *Geochim. Cosmochim. Acta*, *75*, 4611–4636, doi:10.1016/j.gca.2011.05.036.

Honda, S., and L. J. P. Muffler (1970), Hydrothermal alteration in core from research drill hole Y-1, Upper Geyser Basin, Yellowstone National Park, Wyoming, *Amer. Mineral.*, *55*, 1714–1737.

Huber, C., O. Bachmann, J.-L. Vigneresse, J. Dufek, and A. Parmigiani (2012), A physical model for metal extraction and transport in shallow magmatic systems, *Geochem. Geophys. Geosyst.*, *13*, Q08003, doi:10.1029/2012GC004042.

Hurwitz, S., L. B. Christiansen, and P. A. Hsieh (2007a), Hydrothermal fluid flow and Deformation in large calderas: Inferences from numerical simulations, *J. Geophys. Res.*, *112*, B02206, doi:10.1029/2006JB004689.

Hurwitz, S., J. B. Lowenstern, and H. Heasler (2007b), Spatial and temporal geochemical trends in the hydrothermal system of Yellowstone National Park: Inferences from river solute fluxes, *J. Volcanol. Geotherm. Res.*, *162*, 149–171, doi:10.1016/j.jvolgeores.2007.01.003.

Hurwitz, S., S. Eagan, H. Heasler, and J. B. Lowenstern (2007c), *River Chemistry and Solute Flux in Yellowstone National Park*, *U.S. Geol. Surv. Dig. Data Series* 278. [Available at http://pubs.usgs.gov/ds/2007/278/.]

Hurwitz, S., A. Kumar, R. Taylor, and H. Heasler (2008), Climate-induced variations of geyser periodicity in Yellowstone National Park, USA, *Geology*, *36*, 451–454, doi:10.1130/G24723A.1.

Hurwitz, S., W. C. Evans, and J. B. Lowenstern (2010), River solute fluxes reflecting active hydrothermal chemical weathering of the Yellowstone Plateau volcanic field, USA, *Chem. Geol.*, *276*, 331–343, doi:10.1016/j.chemgeo.2010.07.001.

Hurwitz, S., R. N. Harris, C. A. Werner, and F. Murphy (2012a), Heat flow in vapor dominated areas of the Yellowstone Plateau volcanic field: Implications for the thermal budget of the Yellowstone Caldera, *J. Geophys. Res.*, *117*, B10207, doi:10.1029/2012JB009463.

Hurwitz, S., A. G. Hunt, and W. C. Evans (2012b), Temporal variations of geyser water chemistry in the Upper Geyser Basin, Yellowstone National Park, USA, *Geochem. Geophys. Geosys.*, *13*, Q12005, doi:10.1029/2012GC004388.

Hurwitz, S., R. A. Sohn, K. Luttrell, and M. Manga (2014), Triggering and modulation of geyser eruptions in Yellowstone National Park by earthquakes, Earth tides, and weather, *J. Geophys. Res. Solid Earth*, *119*, 1718–1737, doi:10.1002/2013JB010803.

Husen, S., R. B. Smith, and G. P. Waite (2004), Evidence for gas and magmatic sources beneath the Yellowstone volcanic field from seismic tomographic imaging, *J. Volcanol. Geotherm. Res.*, *131*, 397–410, doi:10.1016/S0377-0273(03)00416-5.

Hutchinson, R. A. (1985), Hydrothermal changes in the Upper Geyser Basin, Yellowstone National Park, after the 1983 Borah Peak, Idaho, earthquake, *U.S. Geol. Surv. Open File Rep.*, *(85–290)*, 612–624.

Hutchinson, R. A., J. A. Westphal, and S. W. Kieffer (1997), In situ observations of Old Faithful Geyser, *Geology*, *25*, 875–878, doi:10.1130/0091-7613(1997)025<0875:ISOOOF>2.3.CO;2.

Hutnak, M., S. Hurwitz, S. E. Ingebritsen, and P. A. Hsieh (2009), Numerical models of caldera deformation: Effects of multi-phase and multi-component hydrothermal fluid flow, *J. Geophys. Res.*, *114*, B04411, doi:10.1029/2008JB006151.

Ikeuchi, K., N. Doi, Y. Sakagawa, H. Kamenosono, and T. Uchida (1998), High-temperature measurements in well WD-1a and the thermal structure of the Kakkonda geothermal system, Japan, *Geothermics*, *27*, 591–607, doi:10.1016/S0375-6505(98)00035-2.

Ingebritsen, S. E., and C. E. Manning (2010), Permeability of the continental crust: Dynamic variations inferred from seismicity and metamorphism, *Geofluids*, *10*, 193–205, doi:10.1111/j.1468-8123.2010.00278.x.

Ingebritsen, S. E., D. L. Galloway, E. M. Colvard, M. L. Sorey, and R. H. Mariner (2001), Time-variation of hydrothermal discharge at selected sites in the western United States: Implications for monitoring, *J. Volcanol. Geotherm. Res.*, *111*, 1–23, doi:10.1016/S0377-0273(01)00207-4.

Inskeep, W. P., R. E. Macur, G. Harrison, B. C. Bostick, and S. Fendorf (2004), Biomineralization of As(V)-hydrous ferric oxyhydroxide in microbial mats of an acid-sulfate-chloride geothermal spring, Yellowstone National Park, *Geochim. Cosmochim. Acta*, *68*, 3141–3155, doi:10.1016/j.gca.2003.09.020.

Inskeep, W. P., G. G. Ackerman, W. P. Taylor, M. Kozubal, S. Korf, and R. E. Macur (2005), On the energetics of chemolithotrophy in nonequilibrium systems: Case studies of geothermal springs in Yellowstone National Park, *Geobiology*, *3*, 297–317, doi:10.1111/j.1472-4669.2006.00059.x.

Inskeep, W. P., R. E. Macur, N. Hamamura, T. P. Warelow, S. A. Ward, and J. M. Santini (2007), Detection, diversity and expression of aerobic bacterial arsenite oxidase genes, *Environ. Microbiol.*, *9*, 934–943, doi:10.1111/j.1462-2920.2006.01215.x.

Jaupart, C., and J.-C. Mareschal (2007), Heat flow and thermal structure of the lithosphere, in *Treatise on Geophysics*, vol. 6, edited by G. Schubert, pp. 217–252, Elsevier, Oxford.

Jaworowski, C., H. P. Heasler, C. C. Hardy, and L. P. Queen (2006), Control of hydrothermal fluids by natural fractures at Norris Geyser Basin, *Yellowstone Sci.*, *14*, 13–23.

Jaworowski, C., H. Heasler, C. M. U. Neale, and S. Sivarajan (2010), Using thermal infrared imagery and LiDAR in Yellowstone Geyser Basins, *Yellowstone Sci.*, *18*, 8–19.

Jaworowski, C., H. Heasler, C. Neale, S. Saravanan, and A. Masih (2013), Temporal and seasonal variations of the Hot Spring Basin hydrothermal system, Yellowstone National Park, USA, *Remote Sens.*, *5*, 6587–6610, doi:10.3390/rs5126587.

Johnson, S. Y., W. J. Stephenson, L. A. Morgan, W. C. Shanks, and K. L. Pierce (2003), Hydrothermal and tectonic activity in northern Yellowstone Lake, Wyoming, *Bull. Geol. Soc. Amer.*, *115*, 954–971, doi:10.1130/B25111.1.

Jones, B., and R. W. Renaut (2011), Hot springs and geysers, in *Encyclopedia of Geobiology*, edited by J. Reitner and V. Thiel, pp. 447–451, Springer, New York.

 ©2014. American Geophysical Union. All Rights Reserved.

Kan, J., S. R. Clingenpeel, R. Macur, W. P. Inskeep, D. Lavalvo, J. Varley, K. Nealson, and T. R. McDermott (2011), Archaea in Yellowstone Lake, *Inter. Soc. Microb. Ecol. J.*, *5*, 1784–1795, doi:10.1038/ismej.2011.56.

Karlstrom, L., S. Hurwitz, R. A. Sohn, J. Vandemeulebrouck, F. Murphy, M. L. Rudolph, M. J. S. Johnston, M. Manga, and R. B. McCleskey (2013), Eruptions at Lone Star Geyser, Yellowstone National Park, USA, Part 1: Energetics and eruption dynamics, *J. Geophys. Res. Solid Earth*, *118*, 1–15, doi:10.1002/jgrb.50251.

Kedar, S., B. Sturtevant, and H. Kanamori (1996), The origin of harmonic tremor at Old Faithful Geyser, *Nature*, *379*, 708–711, doi:10.1038/379708a0.

Kedar, S., H. Kanamori, and B. Sturtevant (1998), Bubble collapse as the source of tremor at Old Faithful Geyser, *J. Geophys. Res.*, *103*, 24,283–224,299, doi:10.1029/98JB01824.

Keith, T. E. C., and L. J. P. Muffler (1978), Minerals produced during cooling and hydrothermal alteration of ash flow tuff from Yellowstone drill hole Y-5, *J. Volcanol. Geotherm. Res.*, *3*, 373–402, doi:10.1016/0377-0273(78)90044-6.

Keith, T. E. C., D. E. White, and M. H. Beeson (1978), Hydrothermal alteration and self-sealing in Y-7 and Y-8 drill holes in northern part of Upper Geyser Basin, Yellowstone National Park, Wyoming, *U.S. Geol. Surv. Prof. Pap., 1054-A*, 26 pp, [Available at http://pubs.er.usgs.gov/publication/pp1054A.]

Kelbert, A., G. D. Egbert, and C. deGroot-Hedlin (2012), Crust and upper mantle electrical conductivity beneath the Yellowstone hotspot track, *Geology*, *40*, 447–450, doi:10.1130/G32655.1.

Kennedy, B. M., M. A. Lynch, J. H. Reynolds, and S. P. Smith (1985), Intensive sampling of noble gases in fluids at Yellowstone: I. Early overview of the data; regional patterns, *Geochim. Cosmochim. Acta*, *49*, 1251–1261, doi:10.1016/0016-7037(85)90014-6.

Kharaka, Y. K., M. L. Sorey, and J. J. Thordsen (2000), Large-scale hydrothermal fluid discharges in the Norris-Mammoth corridor, Yellowstone National Park, USA, *J. Geochem. Explor.*, *69-70*, 201–205, doi:10.1016/S0375-6742(00)00025-X.

Kharaka, Y. K., J. J. Thordsen, and L. D. White (2002), *Isotope and chemical compositions of meteoric and thermal waters and snow from the greater Yellowstone National Park Region*, *U.S. Geol. Surv. Open File Rep. 02-194*, 75 pp. [Available at http://pubs.er.usgs.gov/publication/ofr02194.]

Kieffer, S. W. (1989), Geologic nozzles, *Rev. Geophys.*, *27*, 3–38, doi:10.1029/RG027i001p00003.

King, S. A., S. Behnke, K. Slack, D. P. Krabbenhoft, D. K. Nordstrom, M. D. Burr, and R. G. Striegl (2006), Mercury in water and biomass of microbial communities in hot springs of Yellowstone National Park, USA, *Appl. Geochem.*, *21*, 1868–1879, doi:10.1016/j.apgeochem.2006.08.004.

Klump, J. V., C. C. Remsen, D. Lovalvo, P. D. Anderson, R. L. Cuhel, M. Kaplinski, J. L. Kaster, J. S. Maki, and R. W. Paddock (1995), 20,000 leagues under Yellowstone Lake: Strangeness and beauty in the hidden deeps, *Yellowstone Sci.*, *3*, 10–14.

Knickerbocker, C., D. K. Nordstrom, and G. Southam (2000), The role of "blebbing" in overcoming the hydrophobic barrier during biooxidation of elemental sulfur by Thiobacillus thiooxidans, *Chem. Geol.*, *169*, 425–433, doi:10.1016/S0009-2541(00)00221-7.

Krause, T. R., and C. Whitlock (2013), Climate and vegetation change during the late-glacial/early Holocene transition inferred from multiple proxy records from Blacktail Pond, Yellowstone National Park, USA, *Quarter. Res.*, *79*, 391–402, doi:10.1016/j.yqres.2013.01.00.

Lalonde, S. V., L. A. Amskold, L. A. Warren, and K. O. Konhauser (2007), Surface chemical reactivity and metal adsorptive properties of natural cyanobacterial mats from an alkaline hydrothermal spring, Yellowstone National Park, *Chem. Geo.*, *243*, 36–52, doi:10.1016/j.chemgeo.2007.05.016.

Lanphere, M. A., D. E. Champion, R. L. Christiansen, G. A. Izett, and J. D. Obradovich (2002), Revised ages for tuffs of the Yellowstone Plateau volcanic field: Assignment of the Huckleberry Ridge Tuff to a new geomagnetic polarity event, *Geol Soc Amer Bull.*, *114*, 559–568, doi:10.1130/0016-7606(2002)114<0559:RAFTOT>2.0.CO;2.

Leeman, W. P., and V. B. Sisson (1996), Geochemistry of boron and its implications for crustal and mantle processes, in *Boron Mineralogy, Petrology and Geochemistry*, *Rev. Mineral.*, vol. 33, edited by E. S. Grew and L. M. Anovitz, pp. 645–707, Mineral. Soc. Am.

Leeman, W. P., B. R. Doe, and J. Whelan (1977), Radiogenic and stable isotope studies of hot-spring deposits in Yellowstone National Park and their genetic implications, *Geochem. J.*, *11*, 65–74.

Lewis, A. J., M. R. Palmer, N. C. Sturchio, and A. J. Kemp (1997), The rare earth element geochemistry of acid-sulphate and acid-sulphatechloride geothermal systems from Yellowstone National Park, *Geochim. Cosmochim. Acta*, *61*, 695–706, doi:10.1016/S0016-7037(96)00384-5.

Lewis, A. J., A. Komninou, B. W. D. Yardley, and M. R. Palmer (1998), Rare earth element speciation in geothermal fluids from Yellowstone National Park, Wyoming, USA, *Geochim. Cosmochim. Acta*, *62*, 657–663, doi:10.1016/S0016-7037(97)00367-0.

Livo, K. E., F. A. Kruse, R. N. Clark, R. F. Kokaly, and W. C. P. Shanks III (2007), Hydrothermally altered rock and hot-spring deposits at Yellowstone National Park—Characterized using airborne visible- and infrared-spectroscopy data, in *Integrated Geoscience Studies in the Greater Yellowstone Area: Volcanic, Hydrothermal and Tectonic Processes in the Yellowstone Geoecosystem*, *U. S. Geol. Surv. Prof. Pap. 1717*, edited by L. A. Morgan, pp. 491–507.

Locke, W. W., and G. A. Meyer (1994), A 12,000 year record of vertical deformation across the Yellowstone Caldera margin: The shorelines of Yellowstone Lake, *J. Geophys. Res.*, *99*(B10), 20,079–20,094, doi:10.1029/94JB00243.

Lorenson, T. D., K. A. Kvenvolden, B. R. Simoneit, and R. N. Leif (1991), Composition of gas seeps in northwestern Wyoming, *U.S. Geol. Surv. Open File Rep., 91- 121*, p. 35.

Lovalvo, D., S. R. Clingenpeel, S. Mcginnis, R. E. Macur, J. D. Varley, W. P. Inskeep, J. Glime, K. Nealson, and T. R. Mcdermott (2010), A geothermal-linked biological oasis in Yellowstone Lake, Yellowstone National Park, Wyoming, *Geobiology*, *8*, 327–336.

Love, J. D., and J. M. Good (1970), Hydrocarbons in thermal areas, northwestern Wyoming, *U.S. Geol. Surv. Prof. Pap, 644-B*, 23 pp.

Lowe, D. R., and D. Braunstein (2003), Microstructure of high-temperature (>73°C) siliceous sinter deposited around hot springs and geysers, Yellowstone National Park: The role of biological and abiological processes in sedimentation, *Canad. J. Earth Sci.*, *40*, 1611–1642, doi:10.1139/e03-066.

Lowenstern, J. B. (2001), Carbon dioxide in magmas and implications for hydrothermal systems, *Mineral. Depos.*, *36*, 490–502, doi:10.1007/s001260100185.

Lowenstern, J. B., and S. Hurwitz (2008), Monitoring a supervolcano in repose: Heat and volatile flux at the Yellowstone Caldera, *Elements*, *4*, 35–40, doi:10.2113/GSELEMENTS.4.1.35.

Lowenstern, J. B., R. B. Smith, and D. P. Hill (2006), Monitoring super-volcanoes: Geophysical and geochemical signals at Yellowstone and other large caldera systems, *Phil. Transac. Royal Soc.*, *364*, 2055–2072.

Lowenstern, J. B., D. Bergfeld, W. C. Evans, and S. Hurwitz (2012), Generation and evolution of hydrothermal fluids at Yellowstone: Insights from the Heart Lake Geyser Basin, *Geochem. Geophys. Geosys.*, *13*, Q01017, doi:10.1029/2011GC003835.

Lowenstern, J. B., W. C. Evans, D. Bergfeld, and A. G. Hunt (2014), Prodigious degassing of a billion years of accumulated radiogenic helium at Yellowstone, *Nature*, *506*, 355–358.

Lü, Y., S. Ni, J. Xie, Y. Xia, X. Zeng, and B. Liu (2013), Crustal S-wave velocity structure of the Yellowstone region using a seismic ambient noise method, *Earthq. Sci.*, *26*, 283–291, doi:10.1007/s11589-013-0016-1.

©2014. American Geophysical Union. All Rights Reserved.

Luttrell, K., D. Mencin, O. Francis, and S. Hurwitz (2013), Constraints on the upper crustal magma reservoir beneath Yellowstone Caldera inferred from Lake-Seiche induced strain observations, *Geophys. Res. Lett.*, *40*, 501–506, doi:10.1002/grl.50155.

Macur, R. E., Z. J. Jay, W. P. Taylor, M. A. Kozubal, B. D. Kocar, and W. P. Inskeep (2013), Microbial community structure and sulfur biogeochemistry in mildly-acidic sulfidic geothermal springs in Yellowstone National Park, *Geobiology*, *11*, 86–99, doi:10.1111/gbi.12015.

Mader, H. M., E. W. Llewellin, and S. P. Müller (2013), The rheology of two-phase magmas: A review and analysis, *J. Volcanol. Geotherm. Res.*, *257*, 135–158, doi:10.1016/j.jvolgeores.2013.02.014.

Manga, M., I. Beresnev, E. E. Brodsky, J. E. Elkhoury, D. Elsworth, S. Ingebritsen, D. C. Mays, and C.-Y. Wang (2012), Changes in permeability by transient stresses: Field observations, experiments and mechanisms, *Rev. Geophys.*, *50*, RG2004, doi:10.1029/2011RG000382.

Marler, G. D. (1956), How old is Old Faithful Geyser [Wyoming]?, *Amer. J. Sci.*, *254*, 615–622, doi:10.2475/ajs.254.10.615.

Marler, G. D., and D. E. White (1975), Seismic geyser and its bearing on the origin and evolution of geysers and hot springs of Yellowstone National Park, *Geol. Soc. Amer. Bull.*, *86*, 749–759, doi:10.1130/0016-7606(1975)86<749:SGAIBO>2.0.CO;2.

McCleskey, R. B., J. W. Ball, D. K. Nordstrom, J. M. Holloway, and H. E. Taylor (2005), Water-chemistry data for selected springs, geysers, and streams in Yellowstone National Park Wyoming, 2001–2002, *U.S. Geol. Surv. Open File Rep., 2004-1316*, 94 pp. [Available at http://pubs.usgs.gov/of/2004/1316/.]

McCleskey, R. B., D. K. Nordstrom, D. D. Susong, J. W. Ball, and J. M. Holloway (2010a), Source and fate of inorganic solutes in the Gibbon River, Yellowstone National Park, Wyoming, USA. I. Low-flow discharge and major solute chemistry, *J. Volcanol. Geotherm. Res.*, *193*, 189–202, doi:10.1016/j.jvolgeores.2010.03.014.

McCleskey, R. B., D. K. Nordstrom, D. D. Susong, J. W. Ball, and H. E. Taylor (2010b), Source and fate of inorganic solutes in the Gibbon River, Yellowstone National Park, Wyoming, USA. II. Trace element chemistry, *J. Volcanol. Geotherm. Res.*, *196*, 139–155, doi:10.1016/j.jvolgeores.2010.05.004.

McCleskey, R. B., L. E. Clor, J. B. Lowenstern, W. C. Evans, D. K. Nordstrom, H. Heasler, and M. A. Huebner (2012), Solute and geothermal flux monitoring using electrical conductivity in the Madison, Firehole, and Gibbon Rivers, Yellowstone National Park, *Appl. Geochem.*, *27*, 2370–2381, doi:10.1016/j.apgeochem.2012.07.019.

Meertens, C. M., and R. B. Smith (1991), Crustal deformation of the Yellowstone Caldera from first GPS measurements: 1987–1989, *Geophys. Res. Lett.*, *18*, 1763–1766, doi:10.1029/91GL01470.

Meyer-Dombard, D. R., E. L. Shock, and J. P. Amend (2005), Archaeal and bacterial communities in geochemically diverse hot springs of Yellowstone National Park, USA, *Geobiology*, *3*, 211–227, doi:10.1111/j.1472-4669.2005.00052.x.

Miller, D. S., and R. B. Smith (1999), P and S velocity structure of the Yellowstone volcanic field from local earthquake and controlled source tomography, *J. Geophys. Res.*, *104*, 15,105–15,121, doi:10.1029/1998JB900095.

Morgan, L. A., and W. C. Shanks (2005), Influences of rhyolitic lava flows on hydrothermal processes in Yellowstone Lake and on the Yellowstone Plateau, in *Geothermal Biology and Geochemistry in Yellowstone National Park*, edited by W. P. Inskeep and T. R. McDermott, pp. 31–52, Montana State Univ. Thermal Biology Institute, Bozeman, Mont.

Morgan, L. A., et al. (2003), Exploration and discovery in Yellowstone Lake: Results from high-resolution sonar imaging, seismic reflection profiling, and submersible studies, *J. Volcanol. Geotherm. Res.*, *122*, 221–242, doi:10.1016/S0377-0273(02)00503-6.

Morgan, L. A., et al. (2007), The floor of Yellowstone Lake is anything but quiet—New discoveries from high-resolution sonar imaging, seismic-reflection profiling, and submersible studies, in *Integrated Geoscience Studies in the Greater Yellowstone Area: Volcanic, Hydrothermal and Tectonic Processes in the Yellowstone Geoecosystem*, *U. S. Geol. Surv. Prof. Pap. 1717*, 205-234, edited by L. A. Morgan.

Morgan, L. A., W. C. P. Shanks III, and K. L. Pierce (2009), Hydrothermal processes above the Yellowstone magma chamber: Large hydrothermal systems and large hydrothermal explosions, *Special Paper of the Geol. Soc. Amer.*, *459*, 1–95.

Morgan, P., D. D. Blackwell, R. E. Spafford, and R. B. Smith (1977), Heat flow measurements in Yellowstone Lake and the thermal structure of the Yellowstone Caldera, *J. Geophys. Res.*, *82*(26), 379–3732, doi:10.1029/JB082i026p03719.

Muffler, L. J. P., D. E. White, and A. H. Truesdell (1971), Hydrothermal explosion craters in Yellowstone National Park, *Geol. Soc. Amer. Bull.*, *82*, 723–740, doi:10.1130/0016-7606(1971)82[723:HECIYN]2.0.CO;2.

Neuendorf, K. K. E., J. P. Mehl Jr., and J. A. Jackson (Eds) (2011), *Glossary of Geology*, American Geosciences Institute, Alexandria, VA.

Newhall, C. G., and D. Dzurisin (1988), Historical unrest at large calderas of the world, *U.S. Geol. Surv. Bul., 1855*, 1108 pp. [Available at http://pubs.er.usgs.gov/publication/b1855.]

Nimick, D. A., J. N. Moore, C. E. Dalby, and M. W. Savka (1998), The fate of geothermal arsenic in the Madison and Missouri Rivers, Montana and Wyoming, *Water Resour. Res.*, *34*, 3051–3067, doi:10.1029/98WR01704.

Nimick, D. A., R. R. Caldwell, D. R. Skaar, and T. M. Selch (2013), Fate of geothermal mercury from Yellowstone National Park in the Madison and Missouri Rivers, USA, *Sci. Total Environ.*, *443*, 40–54, doi:10.1016/j.scitotenv.2012.10.080.

Nordstorm, K. D., and R. B. McCleskey (2012), As, Sb, Mo, V, W, and Se oxyanions in Yellowstone's thermal waters, *Mineral. Mag.*, *76*, 2172.

Nordstrom, D. K., and E. A. Jenne (1977), Fluorite solubility equilibria in selected geothermal waters, *Geochim. Cosmochim. Acta*, *41*, 175–188, doi:10.1016/0016-7037(77)90224-1.

Nordstrom, D. K., J. W. Ball, and R. B. McCleskey (2005), Ground water to surface water—Chemistry of thermal outflows in Yellowstone National Park, in *Geothermal Biology and Geochemistry in Yellowstone National Park*, edited by W. Inskeep and T. R. McDermott, pp. 73–94, Thermal Biology Institute, Montana State University, Bozeman, MT.

Nordstrom, D. K., R. B. McCleskey, and J. W. Ball (2009), Sulfur geochemistry of hydrothermal waters in Yellowstone National Park: IV Acid-sulfate waters, *Appl. Geochem.*, *24*, 191–207, doi:10.1016/j.apgeochem.2008.11.019.

Norton, D. R., and I. Friedman (1985), Chloride flux out of Yellowstone National Park, *J. Volcanol. Geotherm. Res.*, *26*, 231–250, doi:10.1016/0377-0273(85)90058-7.

Obrebski, M., R. M. Allen, F. Pollitz, and S. H. Hung (2011), Lithosphere-asthenosphere interaction beneath the western United States from the joint inversion of body-wave traveltimes and surface-wave phase velocities, *Geophys. J. Inter.*, *185*, 1003–1021, doi:10.1111/j.1365-246X.2011.04990.x.

Palmer, M. R., and N. C. Sturchio (1990), The boron isotope systematics of the Yellowstone National Park (Wyoming) hydrothermal system: A reconnaissance, *Geochim. Cosmochim. Acta*, *54*, 2811–2815.

Papale, P. (1999), Modeling of the solubility of a two-component $H_2O + CO_2$ fluid in silicate liquids, *Amer. Mineral.*, *84*, 477–492.

Parmigiani, A., C. Huber, B. Chopard, and O. Bachmann (2011), Pore-scale mass and reactant transport in multiphase porous media flows, *J. Fluid Mechan.*, *686*, 40–76, doi:10.1017/jfm.2011.268.

Parry, W. T., and J. R. Bowman (1990), Chemical and stable isotopic models for Boundary Creek warm springs, southwestern Yellowstone National Park, Wyoming, *J. Volcanol. Geotherm. Res.*, *43*, 133–157, doi:10.1016/0377-0273(90)90049-L.

Pearson, F. J., Jr., and A. H. Truesdell (1978), Tritium in the waters of Yellowstone National Park, U.S. Geol. Surv., Open-File Rep., 78-701, pp. 327–329.

©2014. American Geophysical Union. All Rights Reserved.

Pelton, J. R., and R. B. Smith (1979), Recent crustal uplift in Yellowstone National Park, *Science*, *206*, 1179–1182, doi:10.1126/science.188.4190.787.

Pierce, K. L., and L. A. Morgan (1992), The track of the Yellowstone hotspot: Volcanism, faulting, and uplift, in *Regional Geology of eastern Idaho and western Wyoming*, *Geol. Soc. Amer. Mem*., vol. 179, edited by P. K. Link, M. A. Kuntz, and L. B. Platt, Special Paper of the Geol. Soc. Am. pp. 1–53.

Pierce, K. L., and L. A. Morgan (2009), Is the track of the Yellowstone hotspot driven by a deep mantle plume?—Review of volcanism, faulting, and uplift in light of new data, *J. Volcanol. Geotherm. Res.*, *188*, 1–25, doi:10.1016/j.jvolgeores.2009.07.009.

Pierce, K. L., K. D. Adams, and N. C. Sturchio (1991), Geologic setting of the Corwin Springs known geothermal resources area Mammoth Hot Springs area in and adjacent to Yellowstone National Park, in *Effects of Potential Geothermal Development in the Corwin Springs Known Geothermal Resources Area, Montana, on the Thermal Features of Yellowstone National Park*, *U.S. Geol. Surv. Water Resour. Invest. Rep., 91-4052*, edited by M. L. Sorey, pp. I–37.

Pierce, K. L., K. P. Cannon, G. A. Meyer, M. J. Trebesch, and R. Watts (2002), Post-glacial inflation-deflation cycles, tilting and faulting in the Yellowstone Caldera based on Yellowstone Lake shorelines, *U.S. Geol. Surv. Open File Rep*., *02-0142*, 61 pp. [Available at http://pubs.usgs.gov/of/2002/ofr-02-0142/.]

Planer-Friedrich, B., and B. J. Merkel (2006), Volatile metals and metalloids in hydrothermal gases, *Environ. Sci. Tech.*, *40*, 3181–3187, doi:10.1021/es051476r.

Planer-Friedrich, B., C. Lehr, J. Matschullat, B. J. Merkel, D. K. Nordstrom, and M. W. Sandstrom (2006), Speciation of volatile arsenic at geothermal features in Yellowstone National Park, *Geochim. Cosmochim. Acta*, *70*, 2480–2491, doi:10.1016/j.gca.2006.02.019.

Planer-Friedrich, B., J. London, R. B. Mccleskey, D. K. Nordstrom, and D. Wallschläger (2007), Thioarsenates in geothermal waters of Yellowstone National Park: Determination, preservation, and geochemical importance, *Environ. Sci. Tech.*, *41*, 5245–5251, doi:10.1021/es070273v.

Puskas, C. M., R. B. Smith, C. M. Meertens, and W.-L. Chang (2007), Crustal deformation of the Yellowstone-Snake River Plain volcano-tectonic system: Campaign and continuous GPS observations, 1987–2004, *J. Geophys. Res.*, *112*, B03401, doi:10.1029/2006JB004325.

Reyes, A. G., and E. J. Trompetter (2012), Hydrothermal water-rock interaction and the redistribution of Li, B and Cl in the Taupo Volcanic Zone, New Zealand, *Chem. Geol.*, *314*, 96–112, doi:10.1016/j.chemgeo.2012.05.002.

Reysenbach, A.-L., M. A. Ehringer, and K. Hershberger (2000), Microbial diversity at 83°C in Calcite Springs Yellowstone National Park, reveals a novel deeply rooted bacterial lineage and another member of the Korarchaeota, *Extremophiles*, *4*, 61–67.

Rice, G., K. Stedman, J. Snyder, B. Wiedenheft, D. Willits, S. Brumfield, T. McDermott, and M. J. Young (2001), Viruses from extreme thermal environments, *Proc. Natl. Acad. Sci. U. S. A.*, *98*, 13,341–13,345, doi:10.1073/pnas.231170198.

Richardson, C. K., and H. D. Holland (1979a), Fluorite deposition in hydrothermal systems, *Geochim. Cosmochim. Acta*, *43*, 1327–1335, doi:10.1016/0016-7037(79)90122-4.

Richardson, C. K., and H. D. Holland (1979b), The solubility of fluorite in hydrothermal solutions, an experimental study, *Geochim. Cosmochim. Acta*, *43*, 1313–1325, doi:10.1016/0016-7037(79)90121-2.

Rinaldi, A. P., M. Todesco, and M. Bonafede (2010), Hydrothermal instability and ground displacement at the Campi Flegrei Caldera, *Phys. Earth Planet. Inter.*, *178*, 155–161, doi:10.1016/j.pepi.2009.09.005.

Rinehart, J. S. (1969), Old Faithful geyser performance 1870 to 1966, *Bull. Volcanol.*, *33*, 153–163.

Rinehart, J. S. (1980), *Geysers and Geothermal Energy*, Springer–Verlag, New York.

Rodman, A., H. Shovic, and D. Thoma (1996), *Soils of Yellowstone National Park*, Yellowstone Center for Resources, Mammoth Hot Springs, Wyo, p. 324.

Rojstaczer, S., D. L. Galloway, S. E. Ingebritsen, and D. M. Rubin (2003), Variability in geyser eruptive timing and its causes; Yellowstone National Park, *Geophys. Res. Lett.*, *30*(18), 1953, doi:10.1029/2003GL017853.

Rye, R. O., and A. H. Truesdell (2007), The question of recharge to the deep thermal reservoir underlying the geysers and hot springs of Yellowstone National Park, in *Integrated Geoscience Studies in the Greater Yellowstone Area: Volcanic, Hydrothermal and Tectonic Processes in the Yellowstone Geoecosystem*, edited by L. A. Morgan, *U. S. Geol. Surv. Prof. Pap., 1717*, pp. 205–234.

Savage, S., R. Lawrence, S. Custer, J. Jewett, S. Powell, and J. Shaw (2010), Review of alternative methods for estimating terrestrial emittance and geothermal heat flux for Yellowstone National Park using Landsat imagery, *GISci. Remote Sens.*, *47*, 460–479, doi:10.2747/1548-1603.47.4.460.

Savov, I. P., W. P. Leeman, C.-T. A. Lee, and S. B. Shirey (2009), Boron isotopic variations in NW USA rhyolites: Yellowstone, Snake River Plain, eastern Oregon, *J. Volcanol. Geotherm. Res.*, *188*, 162–172, doi:10.1016/j.jvolgeores.2009.03.008.

Schiffman, P., R. A. Zierenberg, A. K. Mortensen, G. O. Fridleifsson, and W. A. Elders (2012), High temperature metamorphism in the conductive boundary layer adjacent to a rhyolite intrusion in the Krafla geothermal system, Iceland, *Geothermics*, *49*, 42–48, doi:10.1016/j.geothermics.2012.11.002.

Shanks, W. C. P., III, L. A. Morgan, L. Balistrieri, and J. C. Alt (2005), Hydrothermal vent fluids, siliceous hydrothermal deposits, and hydrothermally altered sediments in Yellowstone Lake, in *Geothermal Biology and Geochemistry in Yellowstone National Park*, edited by W. P. Inskeep and T. R. McDermot, pp. 53–72, Thermal Biology Institute, Montana State University, Bozeman MT.

Shanks, W. C., III, J. C. Alt, and L. A. Morgan (2007), Geochemistry of sublacustrine hydrothermal deposits in Yellowstone Lake—Hydrothermal reactions, stable isotope systematics, sinter deposition, and spire growth, in *Integrated Geoscience Studies in the Greater Yellowstone Area: Volcanic, Hydrothermal and Tectonic Processes in the Yellowstone Geoecosystem*, *U. S. Geol. Surv. Prof. Pap.*, edited by L. A. Morgan, pp. 205–234.

Sharp, Z. D., J. D. Barnes, A. J. Brearley, M. Chaussidon, T. P. Fischer, and V. S. Kamenetsky (2007), Chlorine isotope homogeneity of the mantle, crust and carbonaceous chondrites, *Nature*, *446*, 1062–1065, doi:10.1038/nature05748.

Sharp, Z. D., J. D. Barnes, T. P. Fischer, and M. Halick (2010), An experimental determination of chlorine isotope fractionation in acid systems and applications to volcanic fumaroles, *Geochim. Cosmochim. Acta*, *74*, 264–273, doi:10.1016/j.gca.2009.09.032.

Shaw, D. M., and N. C. Sturchio (1992), Boron-lithium relationships in rhyolites and associated thermal waters of young silicic calderas, with comments on incompatible element behavior, *Geochim. Cosmochim. Acta*, *56*, 3723–3731, doi:10.1016/0016-7037(92)90165-F.

Shelly, D. R., D. P. Hill, F. Massin, J. Farrell, R. B. Smith, and T. A. Taira (2013), A fluid-driven earthquake swarm on the margin of the Yellowstone Caldera, *J. Geophys. Res. Solid Earth*, *118*, 4872–4886, doi:10.1002/jgrb.50362.

Sherman, L. S., J. D. Blum, D. K. Nordstrom, R. B. McCleskey, T. Barkay, and C. Vetriani (2009), Mercury isotopic composition of hydrothermal systems in the Yellowstone Plateau volcanic field and Guaymas Basin sea-floor rift, *Earth Planet. Sci. Lett.*, *279*, 86–96, doi:10.1016/j.epsl.2008.12.032.

Shervais, J. W., S. K. Vetter, and B. B. Hanan (2006), Layered mafic sill complex beneath the eastern Snake River Plain: Evidence from cyclic geochemical variations in basalt, *Geology*, *34*, 365–368, doi:10.1130/G22226.1.

Shock, E. L., M. Holland, D. Meyer-Dombard, J. P. Amend, G. R. Osburn, and T. P. Fischer (2010), Quantifying inorganic sources of geochemical energy in hydrothermal ecosystems, Yellowstone National Park, USA, *Geochim. Cosmochim. Acta*, *74*, 4005–4043, doi:10.1016/j.gca.2009.08.036.

 ©2014. American Geophysical Union. All Rights Reserved.

Shock, E. L., P. Canovas, Z. Yang, G. Boyer, K. Johnson, K. Robinson, K. Fecteau, T. Windman, and A. Cox (2013), Thermodynamics of organic transformations in hydrothermal fluids, *Rev. Mineral. Geochem.*, *76*, 311–350, doi:10.2138/rmg.2013.76.9.

Sibson, R. H. (1987), Earthquake rupturing as a mineralizing agent in hydrothermal systems, *Geology*, *15*, 701–704, doi:10.1130/0091-7613(1987)15<701:ERAAMA>2.0.CO;2.

Sibson, R. H. (1996), Structural permeability of fluid-driven fault-fracture meshes, *J. Struct. Geol.*, *18*, 1031–1042, doi:10.1016/0191-8141(96)00032-6.

Simpson, F. (2001), Fluid trapping at the brittle-ductile transition re-examined, *Geofluids*, *1*, 123–136, doi:10.1046/j.1468-8123.2001.00011.x.

Smith, R. B., and L. W. Braile (1994), The Yellowstone hotspot, *J. Volcanol. Geotherm. Res.*, *61*, 121–129, 135–187, doi:10.1016/0377-0273(94)90002-7.

Smith, R. B., M. Jordan, B. Steinberger, C. M. Puskas, J. Farrell, G. P. Waite, S. Husen, W.-L. Chang, and R. O'Connell (2009), Geodynamics of the Yellowstone hotspot and mantle plume: Seismic and GPS imaging, kinematics, and mantle flow, *J. Volcanol. Geotherm. Res.*, *188*, 26–56, doi:10.1016/j.jvolgeores.2009.08.020.

Sorey, M.L. and E. M. Colvard (1997), Hydrologic investigations in the Mammoth Corridor, Yellowstone National Park and vicinity, *U.S.A., Geotherm.*, *26*, 221–249.

Spear, J. R., J. J. Walker, T. M. McCollom, and N. R. Pace (2005), Hydrogen and bioenergetics in the Yellowstone geothermal ecosystem, *Proc. Natl. Acad. Sci. U. S. A.*, *102*, 2555–2560, doi:10.1073/pnas.0409574102.

Sturchio, N. C. (1990), Radium isotopes, alkaline earth diagenesis, and age determination of travertine from Mammoth Hot Springs, Wyoming, USA, *Appl. Geochem.*, *5*, 631–640, doi:10.1016/0883-2927(90)90061-9.

Sturchio, N. C., and L. H. Chan (2003), Lithium isotope geochemistry of the Yellowstone hydrothermal system, in *Volcanic, Geothermal, and Ore-forming Fluids: Rulers and Witnesses of Processes Within the Earth*, edited by S. F. Simmons and I. Graham, 171 pp., Society of Economic Geologists, 180.

Sturchio, N. C., K. L. Pierce, M. T. Murrell, and M. L. Sorey (1994), Uranium-series ages of travertines and timing of the last glaciation in the northern Yellowstone area, Wyoming-Montana, *Quarter. Res.*, *4*, 265–277, doi:10.1006/qres.1994.1030.

Symonds, R. B., T. M. Gerlach, and M. H. Reed (2001), Magmatic gas scrubbing: Implications for volcano monitoring, *J. Volcanol. Geotherm. Res.*, *108*, 303–341, doi:10.1016/S0377-0273(00)00292-4.

Takacs-Vesbach, C., K. Mitchell, O. Jackson-Weaver, and A.-L. Reysenbach (2008), Volcanic calderas delineate biogeographic provinces among Yellowstone thermophiles, *Environ. Microbiol.*, *10*, 1681–1689, doi:10.1111/j.1462-2920.2008.01584.x.

Thompson, J. M., and J. M. DeMonge (1996), Chemical analyses of hot springs, pools, and geysers from Yellowstone National Park, Wyoming, and vicinity, 1980–1993, *U. S. Geol. Surv. Open-File Rep. 96-0068*, 66 pp. [Available at http://pubs.er.usgs.gov/publication/ofr9668.]

Todesco, M. (2009), Signals from the Campi Flegrei hydrothermal system: Role of a "magmatic" source of fluids, *J. Geophys. Res.*, *114*, B05201, doi:10.1029/2008JB006134.

Truesdell, A.H. and R.O. Fournier (1976), Conditions in the deeper parts of hot spring systems of Yellowstone National Park, Wyoming, *U.S. Geol. Surv. Open File Rep.*, 76–428, 29 pp.

Truesdell, A. H., M. Nathenson, and R. O. Rye (1977), The effects of subsurface boiling and dilution on the isotopic compositions of Yellowstone thermal waters, *J. Geophys. Res.*, *82*(26), 3694–3704, doi:10.1029/JB082i026p03694.

Vandemeulebrouck, J., P. Roux, and E. Cros (2013), The plumbing of Old Faithful Geyser revealed by hydrothermal tremor, *Geophys. Res. Lett.*, *40*, 1989–1993, doi:10.1002/grl.50422.

Vasco, D. W., C. M. Puskas, R. B. Smith, and C. M. Meertens (2007), Crustal deformation and source models of the Yellowstone volcanic field from geodetic data, *J. Geophys. Res.*, *112*, B07402, doi:10.1029/2006JB004641.

Vaughan, R. G., L. P. Keszthelyi, A. G. Davies, D. J. Schneider, C. Jaworowski, and H. Heasler (2010), Exploring the limits of identifying sub-pixel thermal features using ASTER TIR data, *J. Volcanol. Geotherm. Res.*, *189*, 225–237, doi:10.1016/j.jvolgeores.2009.11.010.

Vaughan, R. G., L. P. Kestay, J. B. Lowenstern, C. Jaworowski, and H. P. Heasler (2012), Use of ASTER and MODIS thermal infrared data to quantify heat flow and hydrothermal change at Yellowstone National Park, *J. Volcanol. Geotherm. Res.*, *233–234*, 72–89, doi:10.1016/j.jvolgeores.2012.04.022.

Vitale, M. V., W. P. Gardner, and N. W. Hinman (2008), Surface water-groundwater interaction and chemistry in a mineral-armored hydrothermal outflow channel, Yellowstone National Park, USA, *Hydrogeol. J.*, *16*, 1381–1393, doi:10.1007/s10040-008-0344-8.

Wagner, L. S., M. J. Fouch, D. E. James, and S. Hanson-Hedgecock (2012), Crust and upper mantle structure beneath the Pacific Northwest from joint inversions of ambient noise and earthquake data, *Geochem., Geophys., Geosys.*, *13*, Q0AN03, doi:10.1029/2012GC04353.

Waite, G. P., and R. B. Smith (2002), Seismic evidence for fluid migration accompanying subsidence of the Yellowstone Caldera, *J. Geophys. Res.*, *107*(B9), 2177, doi:10.1029/2001JB000586.

Waite, G. P., and R. B. Smith (2004), Seismotectonics and stress field of the Yellowstone volcanic plateau from earthquake first motions and other indicators, *J. Geophys. Res.*, *109*, B02301, doi:10.1029/2003JB002675.

Walker, J. J., J. R. Spear, and N. R. Pace (2005), Geobiology of a microbiol endolithic community in the Yellowstone geothermal environment, *Nature*, *434*, 1011–1014, doi:10.1038/nature03447.

Wallace, P., and A. T. Anderson (1999), Volatiles in magmas, in *Encyclopedia of Volcanoes*, edited by H. Sigurdsson et al., pp. 149–170, Academic Press, San Diego.

Walter, M. R., J. Bauld, and T. D. Brock (1972), Siliceous algal and bacterial stromatolites in hot spring and geyser effluents of Yellowstone National Park, *Science*, *178*, 402–405, doi:10.1126/science.178.4059.402.

Watson, F. G. R., R. E. Lockwood, W. B. Newman, T. N. Anderson, and R. A. Garrott (2008), Development and comparison of Landsat radiometric and snowpack model inversion techniques for estimating geothermal heat flux, *Remote Sens. Environ.*, *112*, 471–481.

Werner, C., and S. Brantley (2003), CO_2 emissions from the Yellowstone volcanic system, *Geochem. Geophys. Geosyst.*, *4*, 1061, doi:10.1029/2002GC000473.

Werner, C., S. L. Brantley, and K. Boomer (2000), CO_2 emissions related to the Yellowstone volcanic system 2. Statistical sampling, total degassing, and transport mechanisms, *J. Geophys. Res.*, *105*(B5), 10,831–10,846, doi:10.1029/1999JB900331.

Werner, C., S. Hurwitz, W. C. Evans, J. B. Lowenstern, D. Bergfeld, H. Heasler, C. Jaworowski, and A. Hunt (2008), Volatile emissions and gas geochemistry of Hot Spring Basin, Yellowstone National Park, USA, *J. Volcanol. Geotherm. Res.*, *178*, 751–762, doi:10.1016/j.jvolgeores.2008.09.016.

White, D. E. (1969), Rapid heat-flow surveying of geothermal areas, utilizing individual snowfalls as calorimeters, *J. Geophys. Res.*, *74*(22), 5191–5201, doi:10.1029/JB074i022p05191.

White, D. E., L. J. P. Muffler, and A. H. Truesdell (1971), Vapor-dominated hydrothermal systems compared with hot-water systems, *Econ. Geol.*, *66*, 75–97, doi:10.2113/gsecongeo.66.1.75.

White, D. E., R. O. Fournier, L. J. P. Muffler, and A. H. Trusdell (1975), Physical results of research drilling in thermal areas of Yellowstone National Park, Wyoming, *U.S. Geol. Surv. Prof. Pap.*, *892*, 70 p.

©2014. American Geophysical Union. All Rights Reserved.

White, S. M., J. A. Crisp, and F. J. Spera (2006), Long term volumetric eruption rates and magma budgets, *Geochem. Geophys. Geosyst.*, *7*, Q03010, doi:10.1029/2005GC001002.

Whitlock, C., W. E. Dean, S. C. Fritz, L. R. Stevens, J. R. Stone, M. J. Power, J. R. Rosenbaum, K. L. Pierce, and B. B. Bracht-Flyr (2012), Holocene seasonal variability inferred from multiple proxy records from Crevice Lake, Yellowstone National Park, USA, *Palaeogeogr. Palaeoclimatol. Palaeoecol.*, *331-332*, 90–103, doi:10.1016/j.palaeo.2012.03.001.

Whittlesey, L. (1990), Monarch of all these mighty wonders: Tourists and Yellowstone's Excelsior Geyser, 1881–1890, *Mag. West Hist.*, *4*, 2–15.

Wicks, C. W., W. Thatcher, and D. Dzurisin (1998), Migration of fluids beneath Yellowstone Caldera inferred from satellite radar interferometry, *Science*, *282*, 458–462, doi:10.1126/science.282.5388.458.

Wicks, C. W., W. Thatcher, D. Dzurisin, and J. Svarc (2006), Uplift, thermal unrest and magma intrusion at Yellowstone Caldera, *Nature*, *440*, 72–75, doi:10.1038/nature04507.

Xu, Y., M. A. A. Schoonen, D. K. Nordstrom, K. M. Cunningham, and J. W. Ball (1998), Sulfur geochemistry of hydrothermal waters in Yellowstone National Park: I. The origin of thiosulfate in hot spring waters, *Geochim. Cosmochim. Acta*, *62*, 3729–3743, doi:10.1016/S0016-7037(98)00269-5.

Xu, Y., M. A. A. Schoonen, D. K. Nordstrom, K. M. Cunningham, and J. W. Ball (2000), Sulfur geochemistry of hydrothermal waters in Yellowstone National Park, Wyoming, USA. II. Formation and decomposition of thiosulfate and polythionate in Cinder Pool, *J. Volcanol. Geotherm. Res.*, *97*, 407–423, doi:10.1016/S0377-0273(99)00173-0.

Yang, T., S. Lyons, C. Aguilar, R. Cuhel, and A. Teske (2011), Microbial communities and chemosynthesis in Yellowstone Lake sublacustrine hydrothermal vent waters, *Front. Microbiol.*, *2*, 130, doi:10.3389/fmicb.2011.00130.

Yokochi, R., N. C. Sturchio, R. Purtschert, W. Jiang, Z.-T. Lu, P. Mueller, G.-M. Yang, B. M. Kennedy, and Y. Kharaka (2013), Noble gas radionucleides in Yellowstone geothermal gas emissions: A reconnaissance, *Chem. Geol.*, *339*, 43–51, doi:10.1016/j.chemgeo.2012.09.037.

Yokochi, R., N. C. Sturchio, R. Purtschert, W. Jiang, Z.-T. Lu, P. Mueller, G.-M. Yang, B. M. Kennedy, and Y. Kharaka (2014), Corrigendum to "Noble gas radionuclides in Yellowstone geothermal gas emissions: A reconnaissance", *Chem. Geol.*, *339*, 43–51, doi:10.1016/j.chemgeo.2014.02.004.

Zhang, M., M. Y. Hobbs, S. K. Frape, D. K. Nordstrom, J. W. Ball, and R. B. McCleskey (2004), Stable chlorine isotope composition of goethermal waters from Yellowstone National Park, in *Proceedings of the Eleventh International Symposium on Water-Rock Interaction*, edited by R. B. Wanty and R. R. Seal II, pp. 233–236, A.A. Balkema, New York.

©2014. American Geophysical Union. All Rights Reserved.